Perturbative QCD studies of multijet structures in electron-positron annihilation

Yanos Michopoulos

PERTURBATIVE QCD STUDIES OF MULTIJET STRUCTURES IN ELECTRON-POSITRON ANNIHILATION

Yanos Michopoulos
Department of Physics
University of Durham

A thesis submitted in the University of Durham
for the Degree of Doctor of Philosophy
September 1987

ABSTRACT

To investigate the effect in perturbative QCD of multigluon emissions on the transverse momentum distributions of multijet final states in electron-positron annihilation, we use a simplified model based on the approximation that gluons are emitted independently.

As a guide to these multigluon emissions, we study the two-gluon contribution in some detail and calculate the Q_T-distribution for four-jet events in e^+e^- annihilation, using suitable jet-defining cuts, needed both theoretically, to regularize the soft- and collinear-gluon singularities, as well as experimentally, to group the final-state particles into distinct jets. To ascertain the accuracy of our approximate model, we compare our results with the exact ones, obtained by a Monte Carlo generation of events using the full matrix elements. We find that, for realistic values of the cuts, there is a significant kinematic region of agreement.

This agreement and the validity of our model are further elaborated by taking its Abelian QCD limit, calculating distributions in other event shape variables and studying the jet broadening phenomenon. The applicability of our model is also delineated by finding it to be in remarkable structural and numerical agreement with the more exact algorithm of Altarelli *et al.*

Finally, to investigate the effect of higher order and virtual graphs corrections to low order tree-level results, we use our model to calculate the $O(\alpha_s^2)$ Q_T-distribution for three-jet events in e^+e^- annihilation with virtual contributions included. We study the dependence of these corrections on the resolution parameters used to perform the (analytic) cancellation of infrared and collinear singularities between real and virtual graphs and discuss their physical consequences.

DECLARATION

I declare that no material contained in this thesis has previously been submitted for a degree in this or any other university.

The research described in the following sections has been carried out in collaboration with Nick Brown and Mike Pennington and has been published as Durham University preprints:

(i) Sections IV.3.1 and Appendix B have been published in:
'Parisi Multijet Shape Variables in e^+e^- Annihilation
in terms of Partonic Energy-Momentum Fractions'.
(to be submitted to Journal of Physics G)

(ii) Sections III.5 and IV.4 have been published in:
'Perturbative QCD Algorithms for Transverse
Momentum Distributions in e^+e^- Annihilation '.
(submitted to Nuclear Physics)

ACKNOWLEDGEMENTS

There is a number of people whom I wish to thank for their direct or indirect contributions towards the completion of this thesis:

I am indebted to my supervisor Mike Pennington for his continuous support and encouragement, invaluable assistance and true friendship during the three years of my research studies. I would also like to thank him for his constructive suggestions in improving the form of this thesis, and his patience whilst reading the manuscript and correcting my numerous mistakes, both scientific and literary.

My thanks to past and present members of the High Energy Physics group of the Physics Department: Peter Collins, Stuart Grayson, Alan Martin, Chris Maxwell, Cho Ng, James Stirling, Anthony Allan, Nigel Glover, Neil Spiers, Anthony Worrall, King-Lun Au, Martin Carter, Tony Peacock, Ahmed Bawa, Peter Harriman, Mohammed Hussein, Jenny Nicholls and David Pentney and especially my room-mates Simon Webb, Nick Brown and Mohammed Nobary for providing a friendly and stimulating enviroment in which to work. The last three should also be commended for a continuous supply of caffeine. A mention too, of Ed Witten for his letter of encouragement.

In particular, I would like to thank Nick Brown for his helpful comments, jokes, discussions and a most enjoyable collaboration. Also Mike Whalley for giving up his time and teaching me all I needed to know about computing.

Sincere thanks to the following individuals:

Efharis, for much love and helping me make it through the many cold nights in the non-Mediterranean resorts of North East England. She has shown great patience with me, especially whilst I was writing this thesis, as I have not always been easy to live with. Σ' $\epsilon\upsilon\chi\alpha\rho\iota\sigma\tau\omega$ $\alpha\gamma\alpha\pi\eta$ $\mu\upsilon$.

Spiros, who first suggested the whole idea of postgraduate research and gave much good advice and friendship to a naive younsgter fresh from his first studies.

Aris and my cousins Kostas, Eleni and Thodoris, who supplied this expatriate with postcards, newspapers, magazines and much love from his beloved homeland.

Last, but most important of all, I wish to express my gratitude to my family, my parents and my sister, for both their moral and financial support, and for having always believed in me. Without them, I doubt whether this work would have ever been started, let alone completed; so it is to them that I dedicate this thesis.

Princeton University

Department of Physics: Joseph Henry Laboratories
Jadwin Hall
Post Office Box 708
Princeton, New Jersey 08544

Dear Messrs. Webb, Brown, and
Tsikopoulos,

Best wishes for success
in all your endeavors!

Sincerely,
Edward Witten

Telephone: 609 452-4400 Telex: 499-3512

TABLE OF CONTENTS

The use of Quantum Chromodynamics (Q C D) in treating the hadronic world has become an overwhelming trend in Particle Physics....Perhaps it is for the first time in the history of physics that a theory which is neither precisely defined nor proved to have the right to exist as a consistent theory has become so popular.

DOKSHITZER, DYAKONOV and TROYAN [1979]

CHAPTER I : INTRODUCTION

I.1 THE ROAD TO Q C D

The formulation of QCD as the theory of strong interactions is the result of both theoretical as well as experimental developments in the last two or three decades. The theoretical strand of these developments incorporates the quark model of hadron structure, with a class of quantum field theories known as gauge theories [ref.I.1].

I.1.A THE QUARK MODEL

I.1.A.1 The $SU(3)_F$ Classification of Hadrons

In the early 60's, experiments in High Energy Physics (H E P) were performed using very sophisticated machines designed to accelerate particles to sufficient energies such that, when they collided with other matter, they were able to create new particles. These machines, combined with improved means of detecting particles, enabled hundreds of new particles to be discovered.

As the number of the newly discovered particles was increasing dramatically with time, it became less and less reasonable to suppose that all these particles were elementary. Instead, particles were grouped into families with similar properties. In fact, in 1962, Gell-Mann, and independently, Ne'eman made use of conservation laws, symmetry principles and group theory to propose a classification scheme known as the 'Eightfold Way' [ref.I.2].

Their starting point was the property of charge independence of the strong nuclear force. The fact that particles (such as the proton and the neutron) with almost equal masses but quite different electric charges are indistinguishable in a world where strong force is the only interaction, can be described in an elegant mathematical way, by introducing the concept of isospin. By regarding the proton and the neutron as the isospin-up and isospin-down components respectively, of a single nucleon, the strong interaction's indifference to neutron-ness and proton-ness, can be expressed as the invariance of strong interactions to rotations in the isospin space. The group of rotations which achieves these rotations is the Special Unitary group of transformations of dimension 2, called SU(2) which acts on the 2-dimensional space defined by the proton and the neutron, redefining them as a mixture of the original two. Schematically:

$$G^{SU(2)}\begin{pmatrix} p \\ n \end{pmatrix} \longrightarrow \begin{pmatrix} p' \\ n' \end{pmatrix}$$

leaving the free-nucleon Lagrangian invariant:

$$L_0 \quad = \quad \bar{\psi}\,(i\gamma^\mu \partial_\mu - m)\,\psi \qquad , \qquad \psi = \begin{pmatrix} p \\ n \end{pmatrix} \qquad \text{I.1.A.1}$$

But isospin is not the only quantum number respected by strong interactions. Strangeness, a quantum number assigned to each of the then discovered 'strange' particles (such as the Λ's and the K's), is also conserved in strong interactions, as strange particles can only be produced in pairs (associated production).

When conservation of strangeness is added to that of isospin as a property of strong interactions, it is clear that the strongly interacting particles (hadrons) are governed by a bigger symmetry group. It turns out that SU(3) is the appropriate group whose representations exactly fit the quantum number structure of the observed light hadrons. Light mesons occur only in SU(3) singlets and octets, whereas light baryons are restricted to singlets, octets and decuplets (fig.1.1.1).

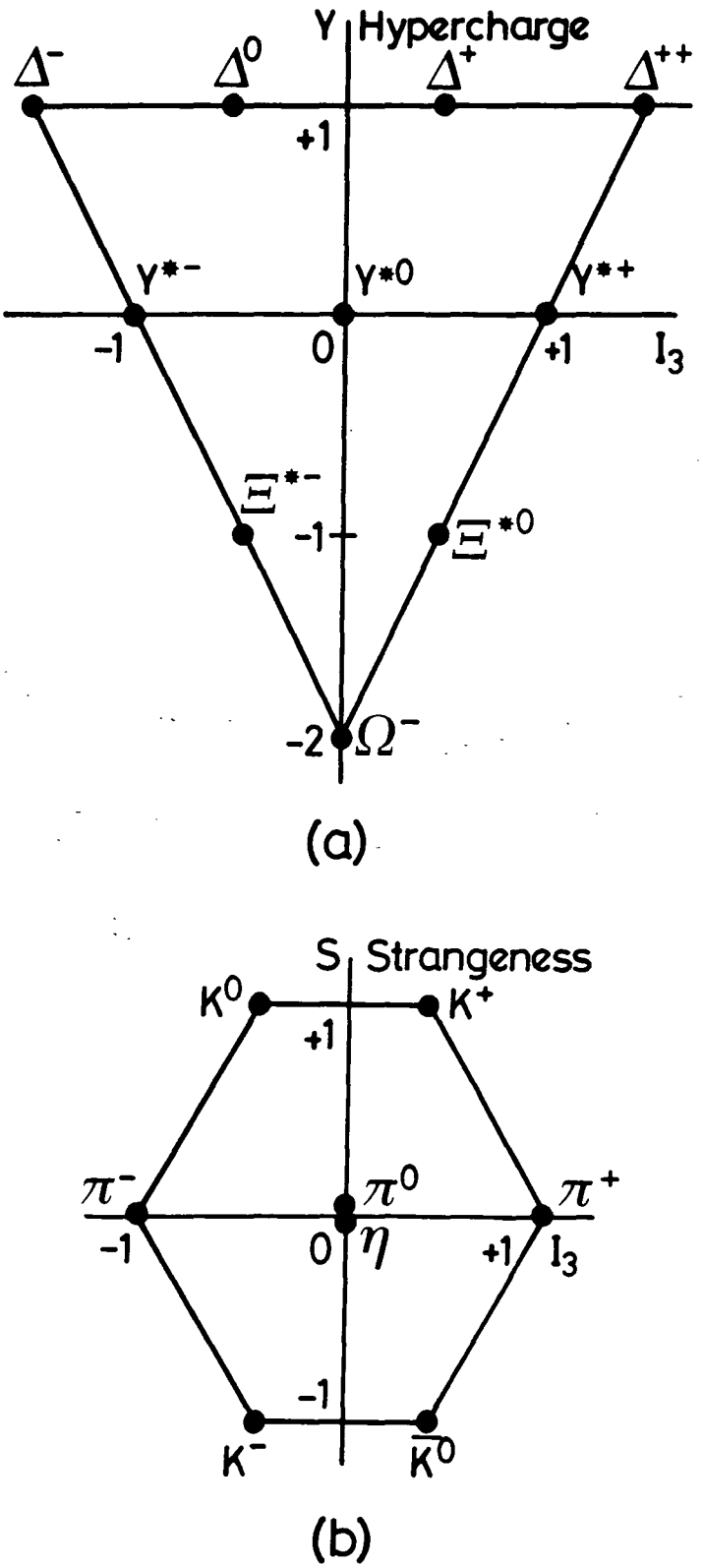

Figure I.1.1 $SU(3)_F$ classification of Hadrons

a] The decuplet of the spin-3/2 baryons

b] The octet of spin-0 mesons

Having found the correct symmetry group, a major problem remained: Why the mesons filled some multiplets, the baryons fitted others, but other multiplets had no particles? In other words, a more dynamical explanation of the observed hadron structure was needed to understand how the representations of SU(3) which were occupied by particles could be chosen from amongst all those mathematically possible.

I.1.A.2 The Genesis of Quarks

In 1964, Gell-Mann and Zweig (independently) proposed an understanding of the SU(3) classification of hadrons by introducing the concept of 'quarks' [ref. I.2,3]. As they pointed out, the observed patterns can be understood in terms of the hypothesis that hadrons are composite structures, built from an elementary triplet of spin-1/2 quarks, corresponding to the fundamental representation of SU(3). The combinations of quarks which give the occupied hadronic representations of SU(3) are a quark-antiquark pair for the meson multiplets and three quarks for the baryon multiplets. This is expressed mathematically by combining the representations of the group:

$$\mathbf{q} \otimes \mathbf{q} \otimes \mathbf{q} \equiv \mathbf{3} \otimes \mathbf{3} \otimes \mathbf{3} \rightarrow \mathbf{1} \oplus \mathbf{8} \oplus \mathbf{8} \oplus \mathbf{10}$$

$$\mathbf{q} \otimes \bar{\mathbf{q}} \equiv \mathbf{3} \otimes \mathbf{3}^{*} \rightarrow \mathbf{1} \oplus \mathbf{8}$$

The quark constituents of the baryon decuplet and of the meson octet are illustrated in figure I.1.2.

I.1.A.3 Properties of Quarks

There are several interesting consequences of the above scheme. We first note that, if three quarks are to make up each baryon with baryon number 1, then the quarks themselves must have baryon number 1/3. Then, using formulae relating charge to isospin and baryon number, we can see that quarks must have fractional charges. Moreover, to ensure that the baryons generated are fermions and the mesons bosons, it is necessary to assign the quarks spin 1/2.

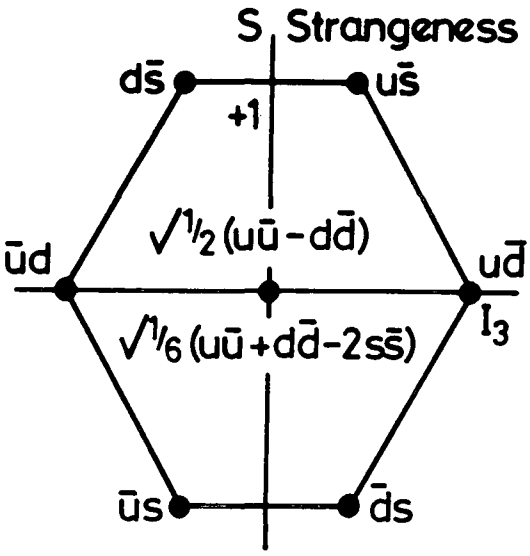

(a)

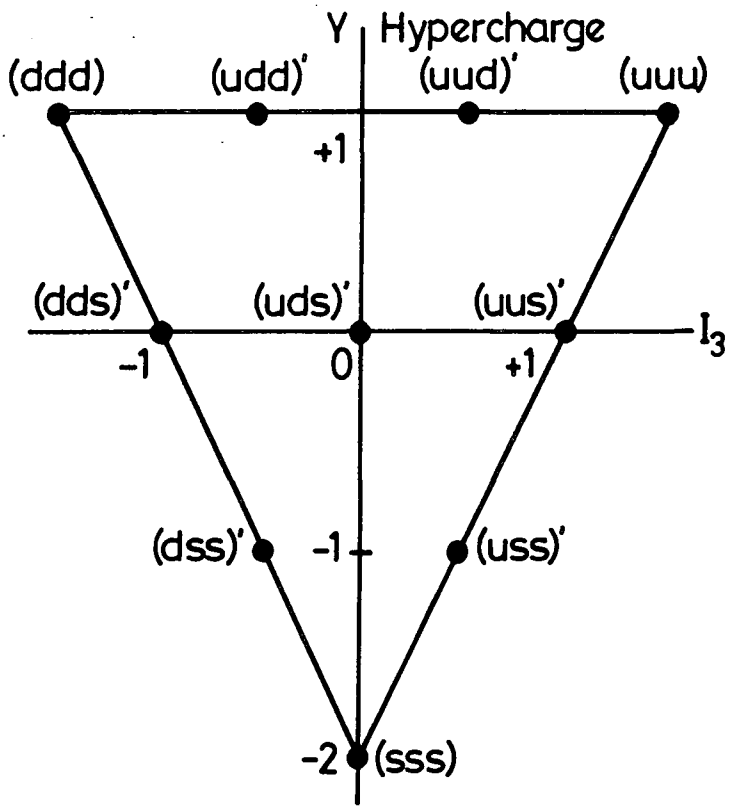

(b)

Figure I.1.2 Quark content of Hadrons

a] The meson octet

b] The baryon decuplet

A summary of the quark properties is shown in the following Table:

Quark	q	Spin	Charge	I	I_3	S	B
Up	u	1/2	+2/3	1/2	+1/2	0	1/3
Down	d	1/2	-1/3	1/2	-1/2	0	1/3
Strange	s	1/2	-1/3	0	0	-1	1/3

It should be emphasized that in this Quark Model quarks are regarded as 'entities' rather than particles. In other words, we do not have to assume their existence as observed particles to enjoy the successes of SU(3) of so-called flavour. However, there was more to the idea of quarks than just mathematical rules for constructing hadrons, and that was revealed by a series of classic experiments on Deep Inelastic lepton Scattering (DIS), as described in the next section.

I.1.A.4 Bjorken Scaling and the Parton Model in D I S

In this class of experiments, a high momentum probe, usually a photon, strikes a nucleon (fig.I.1.3) and, provided its momentum is high enough so that its wavelength will be smaller than the size of the nucleon, probes its structure, thus providing dynamical evidence for the existence of quarks [ref.I.4].

The main measurement of the experiment is the variation of the cross-section with energy lost by the lepton during the collision and with the angle through which the incident lepton is scattered. The energy lost by the lepton ν is simply the difference between its incident and final energy:

$$\nu = E_i - E_f$$

The angle through which the lepton is scattered is related to the square of the momentum transferred by the photon q^2 from the lepton to the nucleon, by the formula:

$$q^2 = 2E_iE_f(1 - \cos\theta)$$

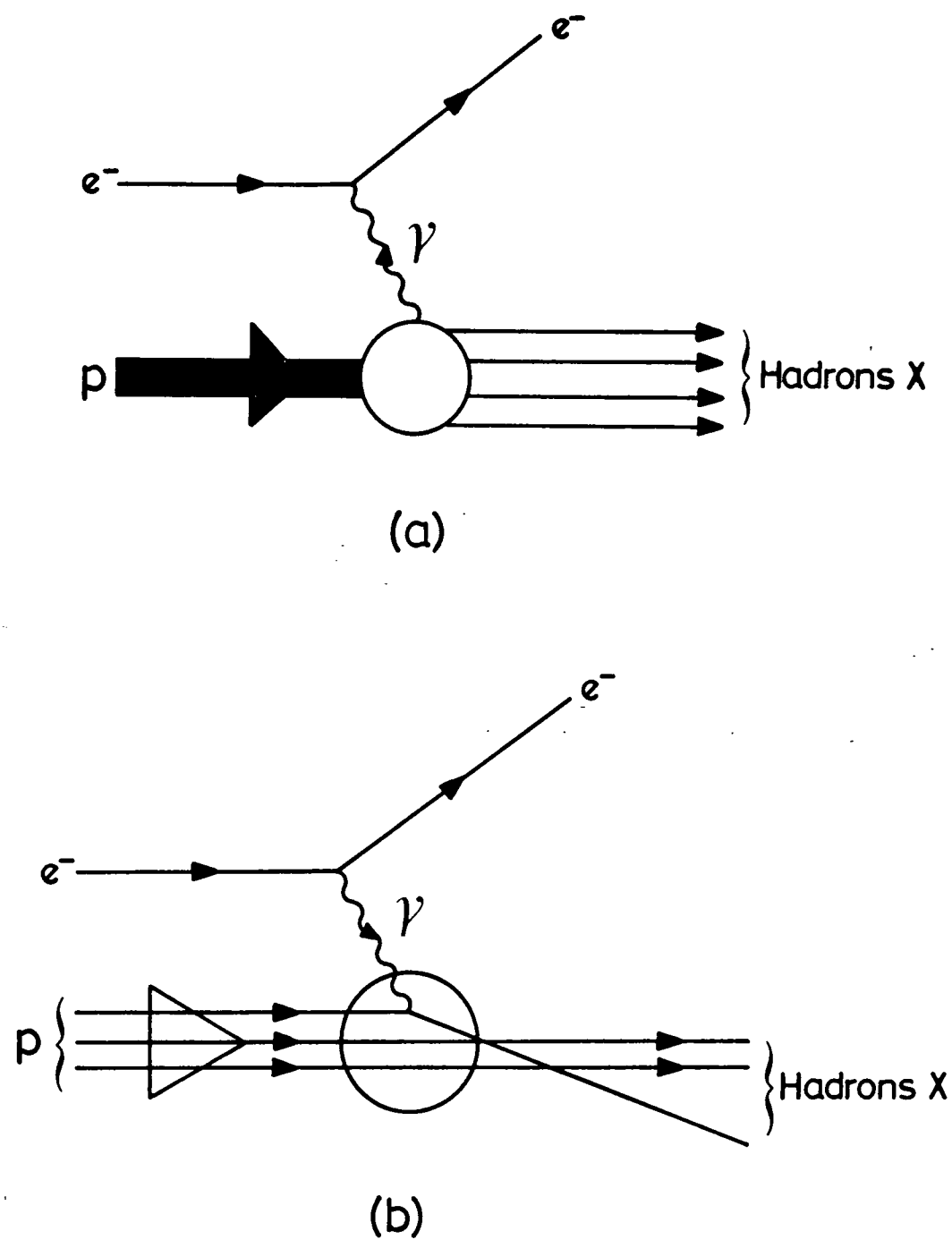

Figure I.1.3 Deep Inelastic Scattering

a] Inelastic electron-proton scattering via single photon exchange :

$e^- p \rightarrow e^- X$

b] Quark-Parton model description of Deep Inelastic Scattering

Two ideas in particular played an important role in the development of the experiments and our understanding of them. The two ideas, both put forward in 1969, are those of scaling and of the parton model [ref.I.4].

(i) *Scaling* is the name given to a phenomenon of the cross-section, first predicted by J.Bjorken. The prediction is that, when the momentum carried by the probe becomes very large, then the dedendence of the cross-section on parameters such as the energy ν and the momentum squared q^2 becomes very simple.

(ii) *The Parton Model* was first put forward by R.Feynman as a simple explanation of Bjorken scaling. He assumed that the struck nucleon is made of smaller constituents, the partons, and visualized DIS as a process where the incoming lepton emits a photon which interacts with one of these 'free' partons (inside the hadron).

In other words, the scaling behaviour of the cross-section was interpretted as an indication of scattering off point-like partons, which turned out to be identified with the quarks of the quark model, as they were found to have identical properties (spin 1/2, fractional charges etc).

The Quark-Parton Model was further elaborated when it was realized that the cloud of quarks-partons inside hadrons had two components. One contained the minimum number of quarks required to construct the SU(3) quantum numbers of the hadron, whereas the second comprised a $q\bar{q}$ sea, an SU(3) singlet cloud contained an indefinite number of quark-antiquark pairs. Furthermore, momentum conservation rules when applied to DIS results suggested that quarks carry only about half of the total proton momemtum. The other half was thought to be carried by neutral 'gluons', particles that were responsible for glueing quarks together to form hadrons. (If hadrons were a simple composite of non-interacting quarks, then they would fall appart!) Therefore, we can schematically say:

$$\text{Partons} \quad = \quad \text{Quarks} \quad + \quad \text{Gluons}$$

I.1.A.5 Evaluation of the Quark-Parton Model

During the 60's the Quark Model enjoyed a number of successes. It not only provided a classification scheme for hadrons and generated the spectrum of masses for particles with the same quantum numbers, but also predicted relations between cross-sections for the interactions of particles from different multiplets. Later, the Quark-Parton Model provided a straightforward and intutively appealing explanation of scaling in Deep Inelastic Scattering experiments.

However, the naive quark model was unable to provide answers to very fundamental questions, such as:

a) Why are quarks not seen as physical particles?

b) Why do they seem to form only certain combinations?

c) What is the nature of the forces they experience?

Questions like these could not be answered until a consistent dynamical theory of strong interactions between quarks and gluons was constructed.

I.1.B GAUGE FIELD THEORIES

I.1.B.1 The Idea of Gauge Invariance

In the last section, we reviewed the establishment of the quark model as a picture of the hadronic world. Through a process of modelling or analogy, hadrons are now seen as quark composites, just as nuclei were seen as composites of neutrons and protons, and atoms as composites of nuclei and electrons.

A similar conceptual process governed the development of the gauge theories of quark interactions, as these were explicitly modelled upon the already established theory of electromagnetic interactions, known as QED, the foundations of which were laid down by Maxwell in 1864 in his equations that unified electric and magnetic interactions [ref.I.5]. The electromagnetic potential that one is led to introduce in order to generate fields that comply with Maxwell's equations, is not uniquely defined. The freedom to choose many potentials that describe the same electromagnetic fields has come to be called 'gauge invariance'. It has also been seen that this invariance can be phrased in terms of a continuous symmetry of the Lagrangian, which leads, through Noether's theorem, to the conservation of electric charge.

Although it is clearly possible to regard gauge invariance as simply an outcome of Maxwell's unification, a greater importance could be attached to the symmetry itself, when we investigate the degree to which Maxwell's equations might be seen to follow from the symmetry.

I.1.B.2 Phase Invariance in Quantum Mechanics

Suppose that we knew the Schroedinger equation, but not the laws of electrodynamics. Would it be possible to derive Maxwell's equations from a gauge principle? The answer is yes and let us see why: [ref.I.6]

A quantum-mechanical state is decribed by a complex Schroedinger wave function $\psi(x)$. Quantum mechanical observables involve inner products of the form:

$$\langle A \rangle \quad = \quad \int \psi^* A \psi$$

which are unchanged under a global phase rotation:

$$\psi(x) \quad \rightarrow \quad \psi'(x) \quad = \quad e^{i\theta}\psi(x)$$

The requirement that under a local change of phase:

$$\psi(x) \quad \rightarrow \quad \psi'(x) \quad = \quad e^{i\theta(x)}\psi(x)$$

physical quantities should be invariant can be satsfied, but at the price of introducing an interaction that must be electrodynamics.

I.1.B.3 Non Abelian Gauge Theories

In other words, electromagnetism posesses a local gauge invariance such that, when we impose that local symmetry on a free-particle Lagrangian, it is possible to construct the theory of electrodynamics. Recall that the free-nucleon Lagrangian (eq.I.1.1) has an invariance under global isospin rotations (see §I.1.A.1). In analogy with electromagnetism, we may ask whether we can turn the global SU(2) invariance of the free field theory into a mathematically consistent local SU(2) invariance. If so, what are the physical consequences?

Yang and Mills were the first to construct such a non-Abelian theory, in complete analogy with the Abelian case. The interaction term in this case couples the gauge fields to the conserved isospin current of the nucleons [ref.I.7].

Despite the similarities between Abelian and non-Abelian Gauge Theories, there are important differences too. Yang-Mills theory has a richer structure. In additon to the gauge field propagator, it contains three- and four-gauge boson vertices shown in fig.I.1.4. As a consequence of gauge invariance, there is only one coupling strength. One single constant g couples all matter fields to the gauge bosons and self-couples the last.

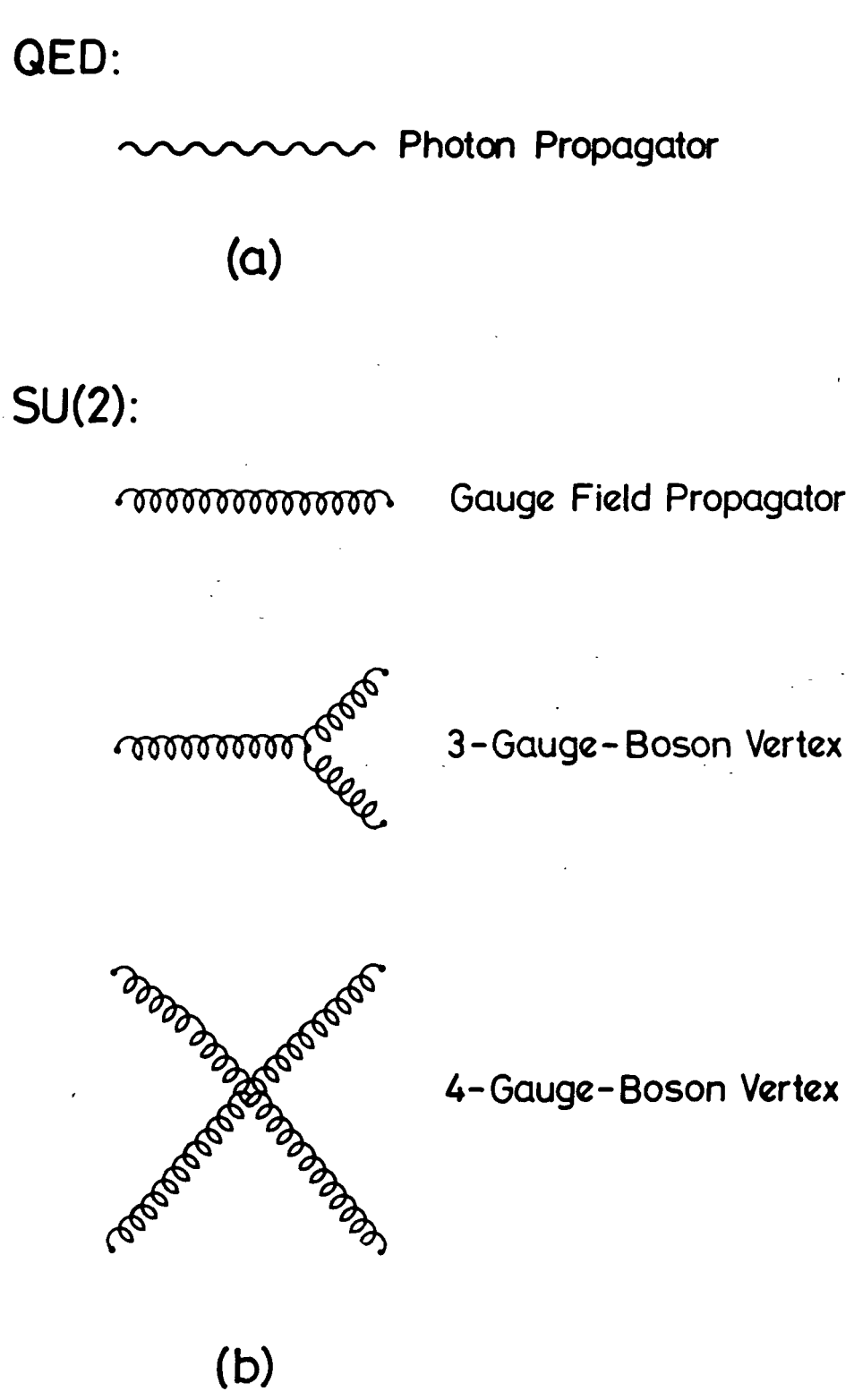

Figure I.1.4 Feynman Rules for Gauge Theories

a] The photon propagator in Quantum Electrodynamics

b] Gauge boson propagator and self-interactions in Yang-Mills theory.

In the next section we shall see that, as a result of these extra gauge boson self-couplings, non-Abelian Gauge Theories have a very interesting property known as Asymptotic Freeedom.

I.1.B.4 From Scaling to Asymptotic Freedom

In section I.1.A.4 we emphasized the importance of the scaling phenomenon observed in Deep Inelastic Scattering experiments and its straightforward explanation in terms of the naive quark-parton model. In this section we review the field theoretical approach to scaling and we sketch the argument that gauge field theories are the only interacting field theories capable of underwriting the phenomenological successes of the quark-parton model and hence giving an explanation of scaling. [The only other theories which reproduced the required 'scaling behaviour' were the free-field theories. That free-field theories displayed such behaviour was no surprise; the parton model could itself be regarded as a free-field theory since the partons did not interact with one another].

Renormalization Group Equation

It is a general feature of field theories that their predictions change in going from one momentum scale to another in a way which is governed by the so-called Renormalization Group Equation (RGE) [ref.I.8]. This equation enables such scale transformations to be understood in terms of changes in an effective coupling constant, g, of the underlying field theory, the behaviour of g being determined by a mathematical function $\beta(g)$. In general, the precise form of this function is unknown, but for small values of g it can be calculated using conventional perturbative techniques. When RGE was applied to Gauge Theories a remarkable and unique property emerged which became known as Asymptotic Freedom [ref.I.9].

It was found that when $\beta(g)$ is computed perturbatively in non-Abelian Gauge Theories its form is such that at higher and higher momenta the effective coupling constant g becomes smaller and smaller, tending asymptotically to zero. In other words, at high momenta, a non-Abelian Gauge Theory behaves more and more like a free, non-interacting field theory: a non-Abelian Gauge Theory is Asymptotically Free. The above discovery increased the hopes for a realistic and calculable field theory of strong interactions. Non-Abelian Gauge Field Theories (NAGFT) were a serious candidate for the job.

I.1.B.5 SU(3) of Colour

Once Asymptotic Freedom had been discovered, two questions remained to be decided in the construction of a realistic candidate gauge theory of strong interactions:

(i) What were the fundamental fields which appeared in the Lagrangian of the theory and

(ii) Under what symmetry group was the L invariant.

An obvious conjecture, given that gauge theory reproduced the predictions of the quark-parton model, was that the fundamental fields were quark fields. In a gauge theory, the quark fields would interact with one another via the exchange of gauge vector fields; and an equally obvious conjecture was that the gauge vector bosons were the enigmatic gluons, already put to use in parton-model phenomenology.

On the other hand, the choice of group was not so obvious. As there was increasing evidence that $SU(3)_F$ could not be the basis of a successful theory of the hadronic interactions, we had to look for a property that really distinguishes quarks from leptons. The clue came from the fact that , unlike leptons, quarks cannot be seen as free particles.

The confinement of the quarks was thought to be the effect of a new quantum number called 'colour'. Each quark flavour was assumed to come in three colours, but the colour of quarks is permanently hidden from us because all the allowed quark structures (observed hadrons) are colourless, colour singlets. Since then, several pieces of evidence have been arrayed in favour of the hypothesis that quarks are colour triplets [ref.I.10]. These include the resolution of the spin-statistics problem for baryons, the magnitude of the cross-section for electron-positron annihilation into hadrons, the branching ratios for τ-decay, the π^0 lifetime, and the requirement of anomaly cancellation in the standard model of weak and electromagnetic interaction. The known leptons, in contrast, are all colourless states. The distinction suggested the possibility that colour was the appropriate change of strong interactions and supported the attempts to formulate a dynamical theory based on local colour-symmetry, a coloured gauge theory.

I.B.1.6 Formulation of Q C D

The construction of an SU(3) colour gauge theory for the interactions of colour triplet quarks followed the general procedure introduced for non-Abelian gauge theories by Yang and Mills and is schematically described below: [ref.I.11]

1. A wavefunction ψ describes the propagation of a quark
2. The Lagrangian $L(\psi_1, \psi_2)$ describes the wavefunction of two quarks in interaction
3. Gauge invariance demands that the Lagrangian must be invariant under the redefinition of the quarks' colour code:

$$G^{SU(3)_c}\,\psi \rightarrow \psi' \quad , \quad G^{SU(3)_c}\,L(\psi_1, \psi_2) \rightarrow L(\psi_1', \psi_2')$$

4. This gauge invariance may be required to hold locally:

$$G^{SU(3)_c(x)}\,\psi \rightarrow \psi' \quad , \quad G^{SU(3)_c(x)}\,L(\psi_1, \psi_2) \not\rightarrow L(\psi_1{}', \psi_2{}')$$

5. The Lagrangian can remain invariant under this local group only if a new, self-interacting gauge field is introduced:

$$G^{SU(3)_c(x)}\, L(\psi_1, \psi_2, A) \rightarrow L(\psi_1{}', \psi_2{}', A')$$

6. The quanta of the colour gauge field, the gluons, mediate the strong force between the quarks and also between themselves

   The QCD Lagangian has the standard form:

$$L \quad = \quad \bar{\psi}(i\gamma^{\mu} D_{mu} - m)\psi - 1/2\mathrm{Tr}(G_{\mu\nu} G^{\mu\nu})$$

where the colour triplet quark spinor is given by:

$$\psi \quad = \quad \begin{pmatrix} q_{red} \\ q_{blue} \\ q_{green} \end{pmatrix}$$

and the covariant derivative is:

$$D_{\mu} \quad = \quad \partial_{\mu} + igB_{\mu}$$

B_{μ} represents the coloured gauge fields (gluons) which mediate the strong force between coloured quarks and $G_{\mu\nu}$ is the gluon field strength tensor:

$$G_{\mu\nu} \quad = \quad \partial_{\nu} B_{\mu} - \partial_{\mu} B_{\nu} + ig[B_{\nu}, B_{\mu}]$$

Knowing the QCD Lagrangian, interactions between quarks can be studied in a very simplified fashion and used to verify that coloured singlets enjoy a preferred status (so that the QCD spectrum displays the systematics that inspired the invention of the theory).

The above statement, shown to be true by calculations of the 'interaction-energies' for two body- systems (composed of quark-quark and quark-antiquark), demonstrated that the colour singlet $q\bar{q}$ is the most attractive of all the two-body channels (for instance, the one gluon contribution for $q\bar{q}$ is attractive for the colour singlets but repulsive for the colour octet), whereas similar calculations for three quark systems confirmed that the colour singlet qqq is the most energetically favoured state.

I.1.B.7 QCD in Practice

If QCD is indeed the correct theory of the strong interactions it must describe an enormous range of phenomena, from the spectrum of light-hadrons to DIS.

Recall thet field theoretic predictions change when going from one momentum scale to another and these transformations can be understood in terms of changes in the effective coupling g of the theory. The RGE ensures that a change in the momentum scale from μ to Q is compensated by corresponding changes in the coupling and the fields, in such a way that all bare Green functions are independent of the change; so that:

$$g(Q^2) \quad = \quad g(\mu^2) - \frac{\beta_0}{32\pi^2} g(\mu^2)^2 \ln Q^2/\mu^2 + O(g^5 \ln^2 Q^2/\mu^2) + \ldots$$

The running of the coupling is governed by the equation:

$$\beta\Big(g(\mu^2)\Big) \quad = \quad \mu \frac{\partial g(\mu^2)}{\partial \mu} \tag{1}$$

where the β-function is calculated perturbatively in QCD:

$$\beta\Big(g(\mu^2)\Big) \quad = \quad -\frac{g(\mu^2)^3}{16\pi^2}\beta_0 \tag{2}$$

Solving (1) and (2) and defining $\alpha_s = g^2/4\pi$ as the strong interaction coupling constant, we obtain:

$$\alpha_s(Q^2) \quad = \quad \frac{4\pi}{\beta_0 \ln Q^2/\Lambda^2_{QCD}}$$

where: Q^2 : momentum scale

$\beta_0 \quad = \quad 11 - 2n_f/3$

n_f : number of quark flavours

Λ_{QCD} : integration constant (the scale of strong interactions)

Therefore, at sufficiently high momenta (that is, short distances) $\alpha_s(Q^2) \ll 1$ so that perturbation theory is applicable and QCD is a calculable theory of strong interactions. Although the property of Asymptotic Freedom by no means justifies all the hypotheses of the quark-parton model, it does make it plausible that at very short distances (i.e. when examined by very high-Q^2 probes) quarks may behave nearly as free particles within hadrons. Applications of QCD perturbation theory include calculations in $e^+e^- \rightarrow$ hadrons, (see next section), lepton-hadron (DIS) and hadron-hadron (collider) physics.

At the other end of the spectrum, as we consider smaller and smaller momentum scales (that is larger and larger distances) the effective coupling becomes larger and larger, so that the perturbative expansion breaks down and non-perturbative techniques are needed to understand the low energy hadronic world. It is generally believed (but not yet proved) that, as a consequence of the continuous growing of the coupling, colour is 'confined' and all coloured particles - quarks and gluons - interact so strongly with one another that only colourless combinations - hadrons - can exist in isolation [ref.I.12].

The proof of confinement has been seen as one of the most important problems in theoretical physics despite the fact that several new theoretical traditions - the 1/N expansion [ref.I.13], monopoles [ref.I.14], instantons [ref.I.15], and lattice gauge theories [ref.I.16] - have been put forward by QCD theorists. Experimentally, the confinement hypothesis has been tested by (so far unsuccessful) searches for free quarks or for signatures of unconfined colour. Sensitive negative searches for quarks continue to be interesting and the definitive observation of free quarks would certainly be revolutionary !

I.2 JETS IN e^+e^- ANNIHILATION

I.2.1 Introduction

Although technologically extremely complex and sophisticated, experiments in HEP are in principle rather simple. As indicated in figure I.2.1, one takes a beam of particles and fires it at a target. Interactions take place within the target (some of the beam particles are deflected or 'scattered'; often additional particles are produced) and the particles that emerge are registered in detectors of various kinds.

An interesting development of recent years has been the transitition from fixed-target accelerators (of the type described above) to collider machines where particle-antiparticle beams collide head-on. Of the latter type are electron-positron colliders which display a number of attractive features (summarized below) that have made e^+e^- collisions the most fruitful class of experiments in recent years [ref.I.17].

(i) Because the electron and the positron are antiparticles, they often annihilate into a 'vacuum' state of pure energy . All the quantum numbers of the initial particles cancel and the energy resulting from the annihilation is free to create new particle-antiparticle pairs (an e^+e^- pair or a $q\bar{q}$ pair for instance). In this way e^+e^- are ideal reactions in which to look for new particles.

(ii) e^+e^- annihilation is also potentially rich in energy with which to create new particles. This is because, being antiparticles, the electron and the positron have exactly the same mass. So that, if they collide head-on with equal and opposite momentum, all the energy is free to create particles. This is in contrast to accelerating electrons into a fixed target where momentum conservation requires that much of the energy be used in accelerating the electron up to the energy for particle creation.

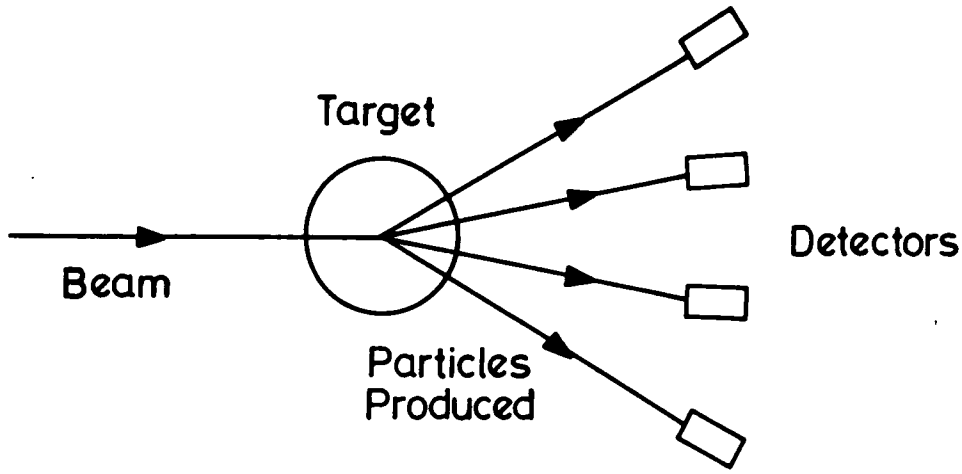

Figure I.2.1 Layout of a HEP experimemt

Collider	Location	Start	c.m.s Energy (GeV)
SPEAR	Stanford,USA	1973	2.4-8.4
DORIS	DESY,Hamburg, W.Germany	1974	3.0-10.5 (12)
PETRA	DESY,Hamburg	1978	10-37 (45)
CESR	Cornell, USA	1979	8-16
PEP	Stanford,USA	1980	10-30
LEP	CERN,Geneva, Switzerland	1988	44-260

Table I.2.1 Important e^+e^- collider machines of the recent past and the near future

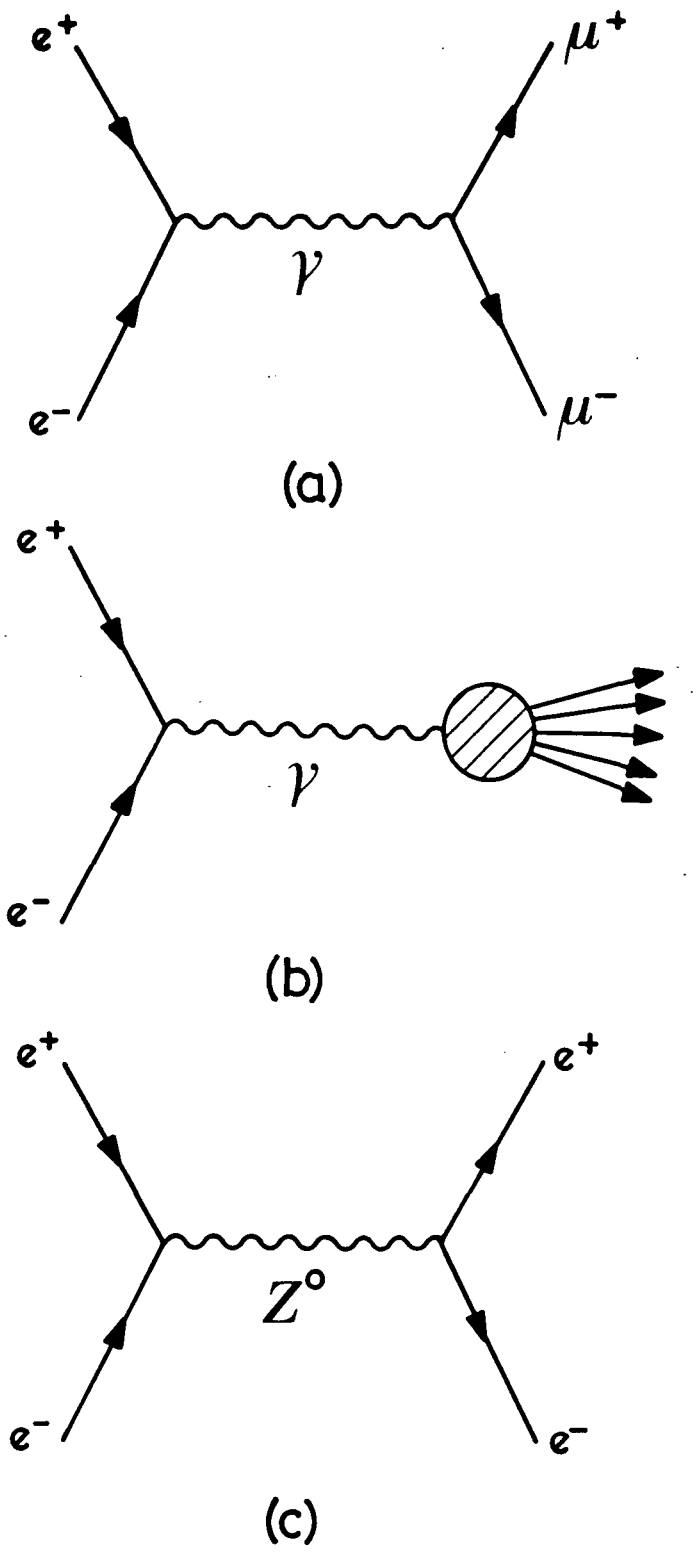

Figure I.2.2 Basic processes in e^+e^- annihilation

a] Muon pair production (Electromagetic Interaction)

b] Hadron production (Strong Interaction)

c] Annihilation into Z^0 (Weak Interaction)

(iii) Another benefit of head-on collisions with stationary centre-of-mass is that the angular distribution of the created particles can be measured directly and any significant asymmetries detected that much more easily.

(iv) Because of the pointlike nature of the colliding particles, e^+e^- reactions are very clean with no debris from the initial state. This is in contrast to proton-antiproton collisions in which quark-antiquark annihilation or quark-gluon scattering take place in the presence of spectator quarks and leptons.

(v) Finally, e^+e^- experiments provide an ideal framework in which to study particle interactions as they allow all three fundamental interactions relevant at fermi distance scales to occur. These manifest themselves in the possibilities illustrated in figure I.2.2.

I.2.2 Hadron Formation in e^+e^- annihilation

An important class of e^+e^- collisions is those in which hadrons emerge in the final state and which indicate that the strong interaction is involved somewhere. Hadron production in e^+e^- annihilation has been seen as a two-stage process. Since the electron and the positron are antiparticles, they can cancel one another out to form a single virtual photon (multiphoton processes being strongly suppressed by powers of α_{QED}). This virtual photon then converts into a quark-antiquark ($q\bar{q}$) pair. The process $e^+e^- \rightarrow q\bar{q}$ is very similar to the (pure electromagnetic) process $e^+e^- \rightarrow \mu^+\mu^-$ (the only difference being that the charges of the quarks are only some fraction of that of the muons), and can be described in familiar QED terms. Shortly after its formation the $q\bar{q}$ pair rearranges itself into a shower of hadrons in a process that involves the creation of more $q\bar{q}$ (fig.I.2.3), but which is not fully understood as it is related to the confinement mechanism of quarks inside hadrons (fig.I.2.3).

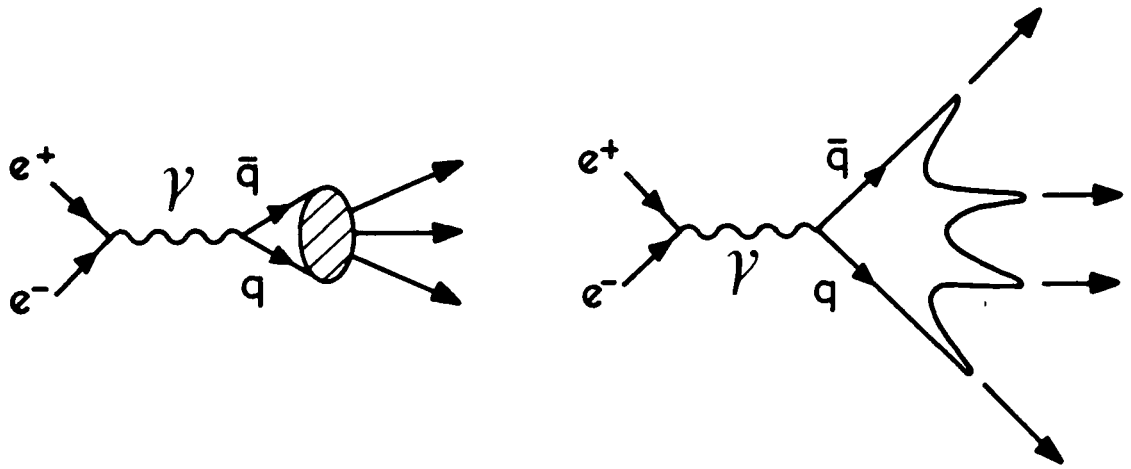

Figure I.2.3 The transformation of the $q\bar{q}$ pair into observed hadrons involves the creation of more $q\bar{q}$ pairs

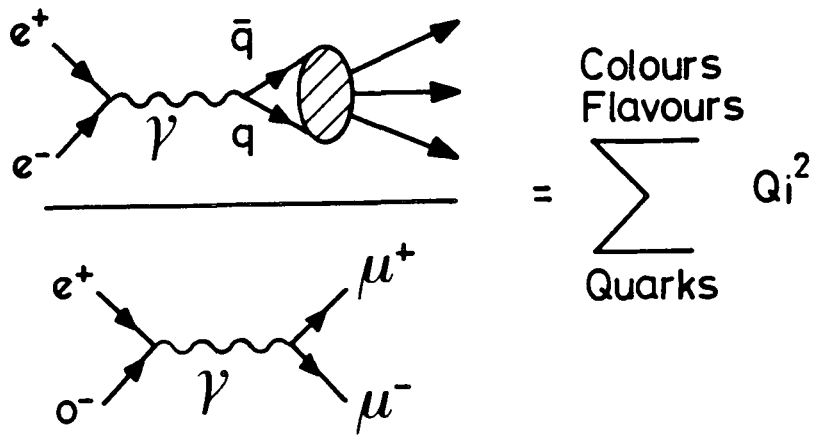

Figure I.2.4 The value of the ratio R is equal to the sum of the squares of the quark charges

The ratio R of the cross-section for $e^+e^- \rightarrow$ hadrons to that for $e^+e^- \rightarrow \mu^+\mu^-$ (measured as the energy of the collision varies) has been seen as one of the most significant quantities in particle physics in the last decade. Its significance is that it compares a reaction we understand very well (muon-pair production) with a class of reactions we wish to understand (hadron production) thus providing a very useful guide to our thinking about the unknown.

In fact, the ratio R was involved in one of the most revolutionary discoveries in HEP: the discovery of the J/psi particle in November 1974, which proved the existence of a fourth flavour of quark , charm c. To see how R is a directly observable quark-counting opportunity which provides a measure of the number of quarks and their properties, let us recall its value in the simple three-flavour quark model: u (charge +2/3e) d(-1/3e) and s(-1/3e) [fig.I.2.4]:

R was then predicted to be:

$$R_{uds} = (\frac{2}{3})^2 + (-\frac{1}{3})^2 + (-\frac{1}{3})^2 = \frac{2}{3}$$

If we now take into account that each flavour of quarks comes in three different colours (see §I.1.B.5) then the predicted value of R at low energy (few GeV) is R=2. This prediction agreed reasonably well with the value measured experimentally in the resonance region during the early 70's, and it gave support to the idea of coloured quarks.

In November 1974, two experimental groups (at SLAC and Brookhaven) reported independently and (almost) simultaneously the discovery of a new resonance (particle) at 3GeV, the J/psi particle. In the SLAC e^+e^- experiment R was seen to have an almost δ-function spike at the ψ mass with a background of roughly 2 below 3GeV and rising to about 3 (above 5GeV) ; in contradiction with the above predicted value. After a brief period of speculation the correct interpretation of the J/psi emerged. What had happened was that the increasing energy of the e^+e^- collision had become sufficiently large to create a new flavour $q\bar{q}$ pair.

This new flavour, called charm, had been already predicted by Glashow, Iliopoulos and Maiani in order to explain the behaviour of hadrons in the Glashow-Weinberg-Salam theory of the weak force and understand the absence of Strangeness-changing neutral currents. The discovery of the c-quark emphasized the ability of e^+e^- -annihilation experiments to produce new particles and marked the beginning of further developments, theoretical as well as experimental, in the late 70's, during which:

The existing set of four leptons (e, ν_e, μ, ν_μ) was augmented by the discoveries of the heavy lepton tau (τ) and of the b-quark and the presumption of the associated tau-neutrino (ν_τ) and the t-quark.

The resulting six-lepton and six-quark ontology has the aesthetically pleasing property of grouping the leptons and the quarks in three generations (see Table I.2.2) and, if blended with the developing gauge theoretical orthodoxy (described in the last section), provides a complete and consistent framework for the study of the microworld, known as the Standard Model [ref.I.18].

Elementary Particles

Generation (Family)	1	2	3	Charge
Quarks	u	c	t	2/3
	d	s	b	-1/3
Leptons	e^-	μ^-	τ^-	-1
	ν_e	ν_μ	ν_τ	0

Fundamental Forces

Interaction	Theory	Gauge group	Mediator	Strength
Strong	QCD	$SU(3)_c$	Gluons	~ 1
Electromagnetic	QED	U(1)	Photon	1/137
Weak	GWS	SU(2)	$W^\pm, Z^0$	10^{-5}
Gravity	General Relativity	Superstrings ?	Graviton	10^{-38}

Table I.2.2 The 'Standard Model' in Theoretical High Energy Physics: Elementary Particles and Fundamental Interactions

I.2.3 Jets and Fragmentation Models

If 'psichology' was the most fashionable experimental field in the 70's, this decade has seen the study of jets to emerge as the most significant testing ground for QCD as a theory of strong interactions.

As already mentioned, the quark-antiquark pair produced in e^+e^- annihilation somehow 'dresses' itself to form normal hadrons. The hadrons produced this way seemed to favour an interesting configuration: sprays of particles (jets) all travelling in the general direction of the parent quark (or antiquark) and having only a small component of momentum transverse to that direction. In other words, quarks converted to 'jets' and the hadrons produced showed a two-jet structure (fig. I.2.5).

The claim that jet studies can be very informative about the quarks and their properties can be seen from the following example: As these jets preserved the directions of motion of the outgoing quarks, which in turn depended upon their spins, measurements of the jet angular distributions indicated the spin of the quarks. The $1+\cos^2\theta$ behaviour, where θ is the angle between the incoming beam axis and the outgoing jet, confirmed that quarks are indeed spin 1/2 objects.

More detailed QCD tests became possible when it was realized that three-jet as well as two-jet events were visible in e^+e^- annihilation [ref.I.19]. It was argued that in QCD three-jet events would arise when either of the outgoing quark and antiquark emitted a 'hard' gluon, a gluon carrying a large momentum transverse to that of the emitting quark, which would form its own separate jet [fig.I.2.5b] In QCD, the rate of emission of gluons from quarks and antiquarks is controlled by the effective quark-gluon coupling, α_s, so that measurements of the ratio of three- to two-jet events provided quantitative estimates of the size of α_s [ref.I.17,19], comparable with those determined from scaling violations in DIS.

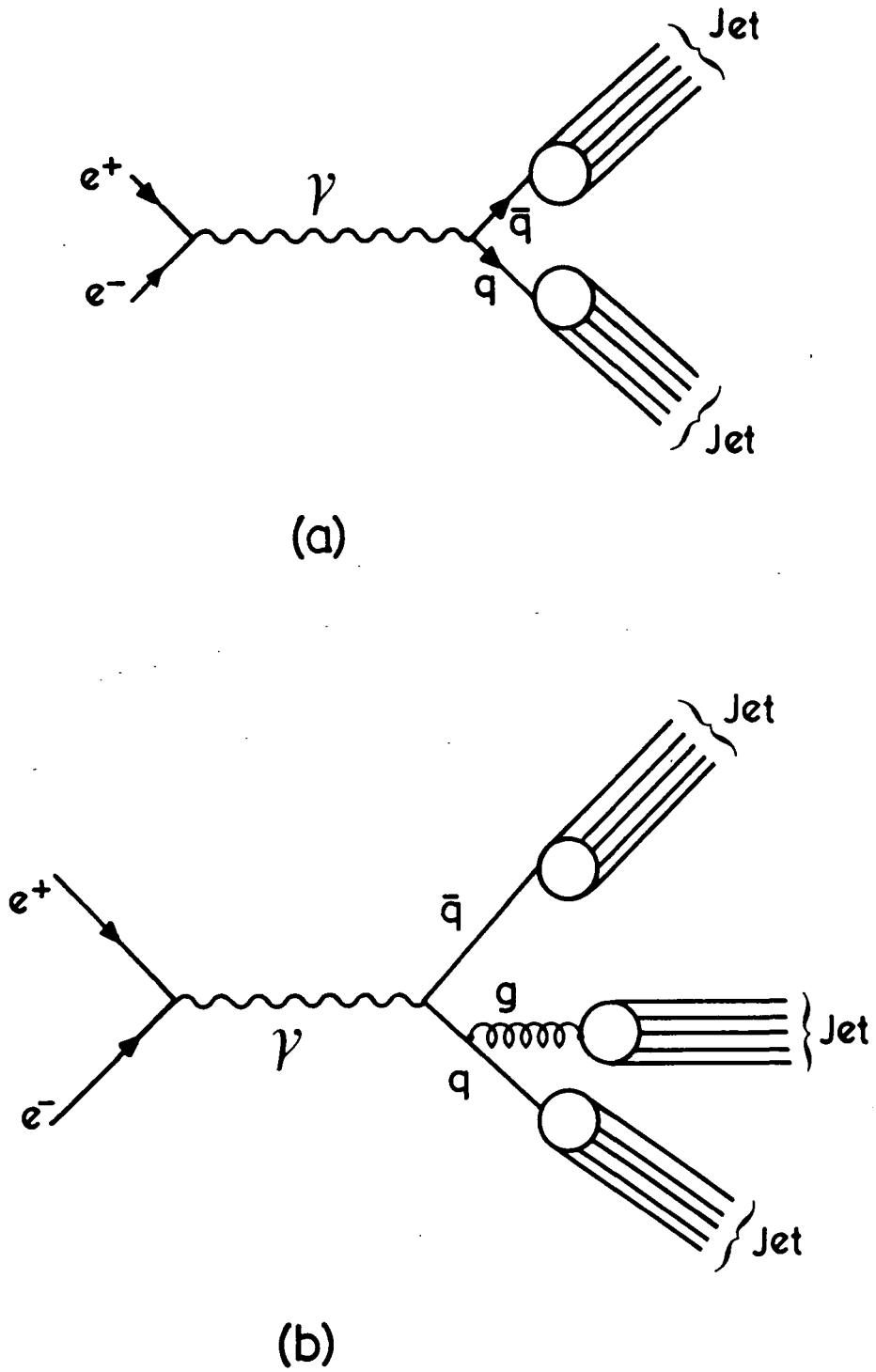

Figure I.2.5 Jet production in electron-positron annihilation

a] Parton model description of a two-jet event in e^+e^- annihilation

b] Three-jet production in perturbative QCD

Ever since, studies of multijet configurations in hard processes (such as the e^+e^- annihilation) have continued to be one of the most fruitful tests of the structure of perturbative QCD [ref.I.17,19]. They have supported our belief that QCD **is** the theory of strong interactions, despite the many theoretical questions that remain unanswered. For instance, the 'dressing' mechanism that converts the 'coloured' quarks and gluons into 'colourless' hadrons, apparently related to the confinement problem, is still not very well understood, requiring the use of certain 'fragmentation models', which have been implemented in Monte Carlo simulation programs. These models have enjoyed many phenomenological successes in describing the properties of the observed hadronic jets and can be generally divided into three major classes [ref.I.20]:

1. Independent Fragmentation Models, originally proposed by Feynman and Field and recently improved and generalized, in which the outgoing partons fragment independently of what else emerges from the reaction.

2. String Models, due to the Lund group of Andersson *et.al.*, in which quarks and gluons are pictured to be confined via a string-like structure and the jet formation is due to the progressive breaking of the string.

3. QCD-Shower Models, of Webber *et. al.*, in which a perturbative QCD radiation of gluons in the initial stage of the reaction is followed by a production of pair of resonances in a (non-perturbative) quark-gluon fusion.

I.3 OUTLINE OF THIS THESIS

Having given the background, we outline here the topics of this thesis. These are organized as follows:

Chapter II serves as an introduction to tranverse momentum distributions in 'semi-hard' processes, their description in terms of perturbative QCD and the theoretical uncertainties that are involved in such calculations. As a working example, we look at the production of multijets in electron-positron annihilation in some more detail and we set up a simple model for quick and reliable calculations of multigluon cross-sections in $e^+e^- \rightarrow q\bar{q} + (ng)$. The model is based on the approximation that the gluons are emitted independently (apart from transverse momentum conservation) and is particularly useful for calculating transverse momentum distributions in the multijet case.

In chapter III, we calculate the four-jet cross-section in e^+e^- annihilation as the first application of this model and compare its predictions with the exact fixed order result obtained using a Monte Carlo generation of events, according to the full matrix elements. The comparison of the two results helps to identify the kinematic region in which the model is most likely to be reliable, and determine the choice of the various parameters involved for maximal agreement.

In chapter IV, we explore the possibility of using our model in other calculations which are not very different from the one described in the previous chapter. Comparisons of our results with the full ones will serve as a measure of the potential of our model to be used as a tool to study the structure of multijet final states in some more detail, thus providing us with some answers to the main theoretical questions formulated in chapter II.

These studies are detailed in chapter V, where we investigate the importance of higher order corrections to low order tree calculations. In particular, the dependence of these corrections on the values of the 'jet-defining cuts', which are necessary to regularize infrared and collinear singularities between higher order real and virtual graphs as well as to group the final-state particles into hadronic jets, is studied in the case of a three-jet event in e^+e^- annihilation.

Finally, a summary of this thesis, the overall conclusions of our studies, a critical overview of the present status of the Standard Model and some hints of the sort of new Physics we expect to see in the near and remote future, are all the subject of the concluding chapter VI.

It should be noted that, a brief introduction and a summarizing paragraph are included at the beginning and the end, respectively, of each chapter. Also note that, for reasons of simplicity, equations, figures and references are separately numbered in idividual chapters. A list of all the references can be found at the end of the thesis.

CHAPTER II TRANSVERSE MOMENTUM DISTRIBUTIONS

II.1 INTRODUCTION.

One of the characteristic features of a field theory with a dimensionless coupling constant is a large value of transverse momenta of final state particles in hard processes. The experimental observation of these high Q_T phenomena has served as a decisive test of the applicability of perturbative QCD to short distance physics .

A list of such hard processes that have been studied in detail include :

a) The annihilation of an electron-positron pair into jets which are at a relative transverse momentum Q_T to each other (fig.II.1.1) [ref. II.1].

b) The production of a lepton pair with mass Q^2 and relative transverse momentum Q_T in hadron collisions (the Drell- Yan process $A + B \rightarrow l_1 + l_2 + X$, where X is often specified by the number of hadronic jets produced) (fig.II.1.2 and 3) [ref.II.2].

c) The production of multijets at the collider : $p\bar{p} \rightarrow$ jets (fig.II.1.4) [ref.II.3].

In perturbative QCD , all these high Q_T-processes are understood to be the result of gluons being emitted off quarks and antiquarks to balance the relative Q_T of the fermions (fig.II.1c,2c).

Let us consider the first case as a typical example :

To lowest order in perturbative QCD , this process is described by the decay of the virtual photon of mass Q produced by the annihilation of the electron-positron pair into a quark-antiquark pair . The hadronisation of this parton pair gives rise to two back-to-back jets. However, to next order, the quark and the antiquark can emit a gluon which, upon fragmentation, produces an additional jet. The two original jets are now at a relative transverse momentum.

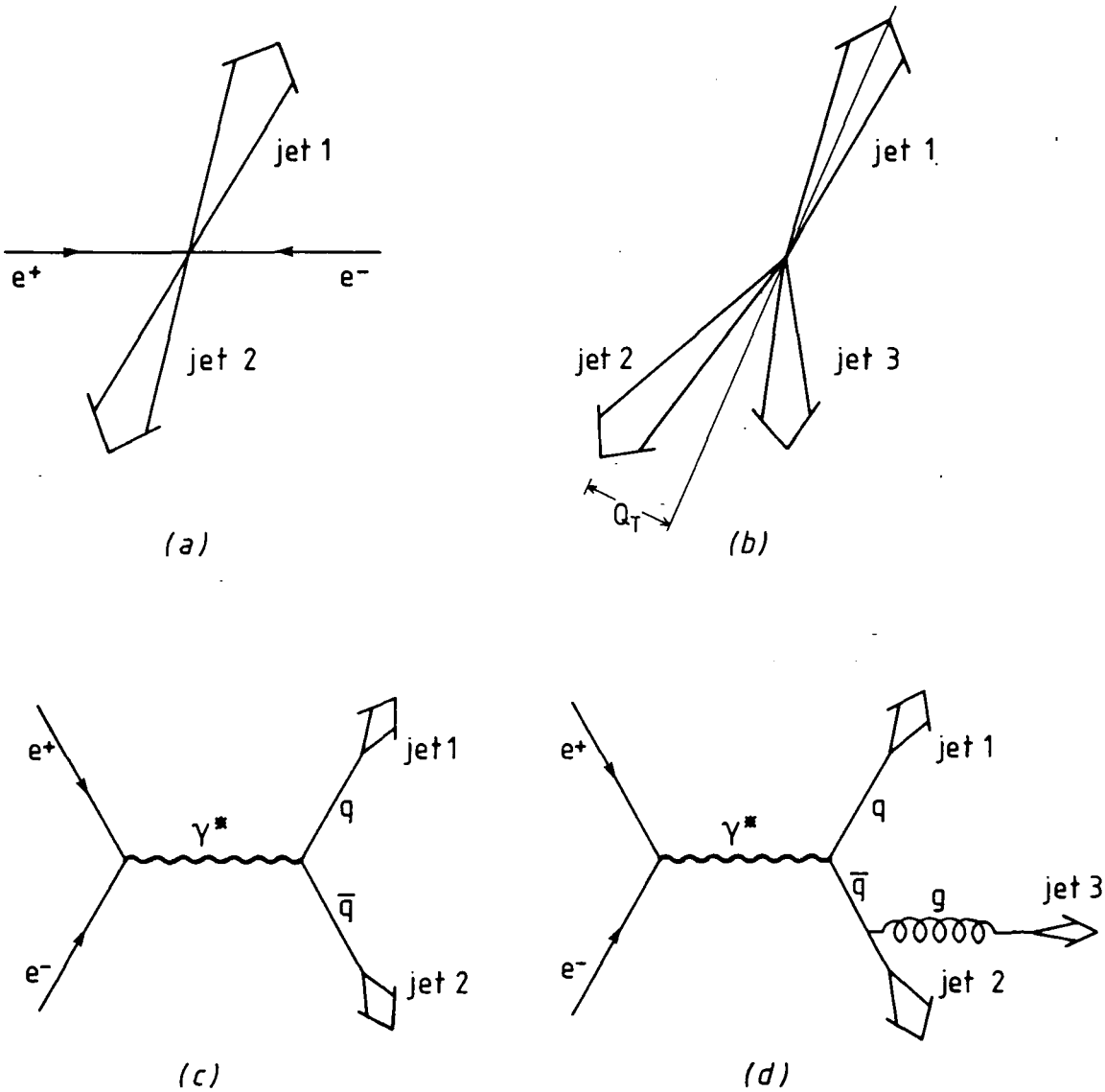

Figure II.1.1 Jets in e^+e^- annihilation.

1a] Two back-to-back jets

1b] Jets at a relative transverse momentum Q_T

1c] Parton model description of $e^+e^- \rightarrow$jets

1d] Gluon emission to balance the relative Q_T of the final state jets

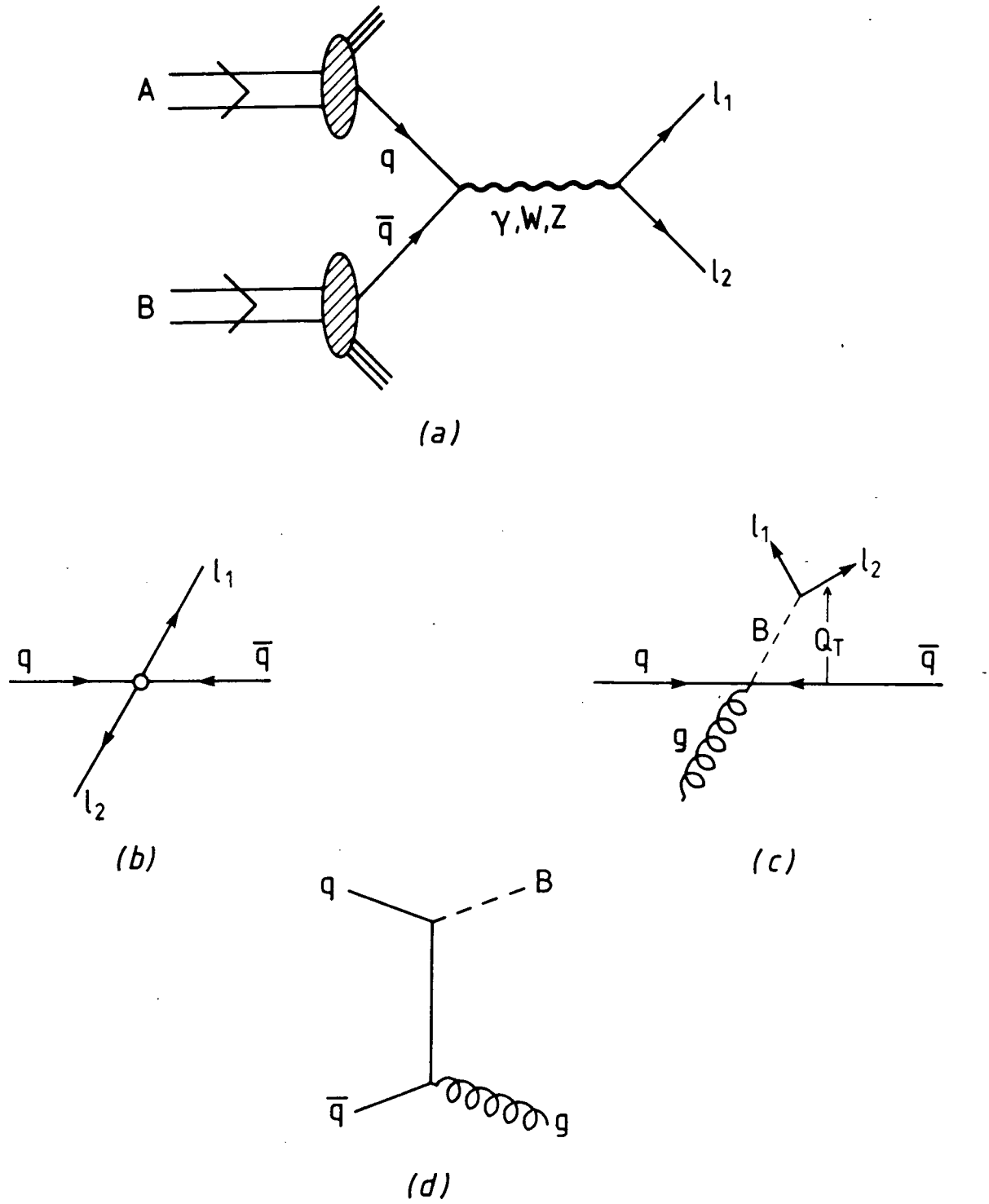

Figure II.1.2 The Drell-Yan process.

2a] Lepton pair production in hadron collisions $A + B \rightarrow l_1 + l_2 + X$

2b] Parton model description (Boson at rest)

2c] Boson (lepton pair) with Q_T. Gluon emitted to balance it

2d] Typical Feynman diagram for $q\bar{q} \rightarrow Bg$,where $B = \gamma, W, Z$

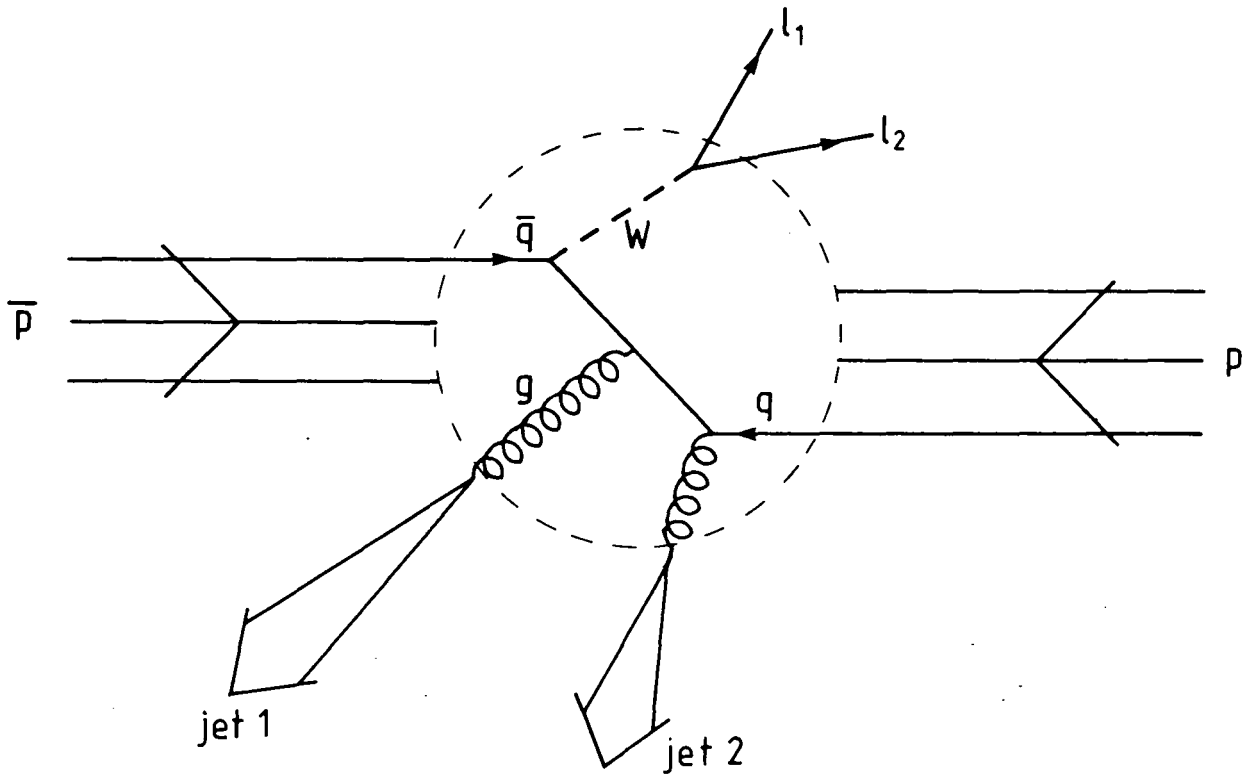

Figure II.1.3 $p\bar{p} \rightarrow W^{\pm}, Z^{0}+$ jets

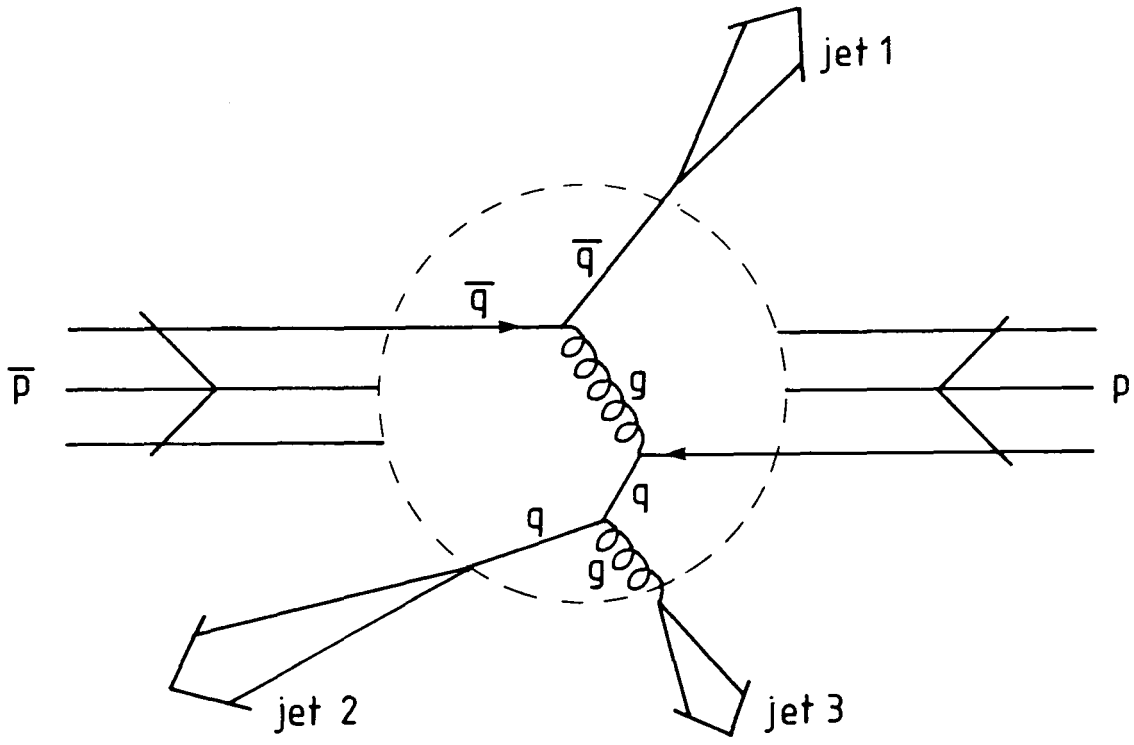

Figure II.1.4 $p\bar{p} \rightarrow$ jets

II.1.1 The aim of this work

The study of all the above processes enables us to investigate the structure of perturbative QCD as a theory with massless vector gluons. In fact, order by order in a perturbative analysis, gluon emissions give rise to terms of the form [ref.II.4]:

$$\frac{1}{Q_T^2}\,\alpha_s^n(Q_T^2)\ln^m(\frac{Q^2}{Q_T^2}) \qquad , \qquad m \leq 2n-1$$

Now, the high energy scales reached by present and future accelerators leads us to distinguish between two large, but distinct, kinematic regimes:

(i) $Q_T \sim Q$

At large transverse momentum, the coupling constant $\alpha_s(Q_T)$ is small and the logarithms are under control, so that the perturbative expansion is rapidly convergent. The property of Asymptotic Freedom ensures the dominance of the emission of a single, hard gluon, making the $O(\alpha_s)$ result a reliable approximation.

(ii) $\Lambda_{QCD} << Q_T << Q$

As Q_T becomes smaller, such that $\Lambda << Q_T << Q$, the coupling constant $\alpha_s(Q_T)$ increases and the logarithms become dangerously large so that the simple perturbative expansion breaks down. Multigluon emission becomes increasingly more important, forcing a consideration of all orders in α_s.

One of the major theoretical advances of recent years has been the development of techniques to sum these large logarithms to all orders, thus extending the range of applicability of perturbative QCD. Such resummation was first attempted by Dokshitzer, Dyakinov and Troyan (DDT) [ref.II.5], who showed how the leading double logarithms (DLLA) to each order exponentiate, allowing a simple resummation that produces the Sudakov form-factor suppression of small Q_T processes. Their approach was further improved when subleading contributions were also taken into account by an exact treatment of transverse momentum conservation. Resummation and exponentiation of non-leading terms was theoretically proposed by Parisi and Petronzio [ref. II.6] and phenomenologically elaborated by Halzen, Martin and Scott [ref. II.7].

Subsequently Collins and Soper [ref .II.8] systematised the summation of non-dominant logarithms to all orders in α_s and analysed the origin and form of exponentiating and non-exponentiating terms, thus providing a consistent framework for studing transverse momentum distributions in perturbative QCD.

More recently, Altarelli *et.al.* [ref.II.9] re-examined the Q_T- distribution of the vector boson produced at the collider, taking into account both kinematic regions mentioned above. Their final formulation not only sums the multigluon emissions to DLLA at small Q_T, but at large Q_T reproduces the $O(\alpha_s)$ perturbative result coming from one-gluon emission (fig.II.1.5).

In contrast with these developments, Ellis *et.al.* [ref.II.10] have used a simple tree-level approach to compare the one- and two-jet cross-sections for hadrons accompanying the W-boson in $p\bar{p}$ collisions as a function of the transverse momentum Q_T of the W. Surprisingly enough, they found that the magnitude of the $O(\alpha_s^2)$ two-jet rate is comparable to the $O(\alpha_s)$ one-jet rate for sizeable Q_T of the W (fig.II.1.6). At first sight their result seems to disagree with that of Altarelli *et.al.*. This leads us to ask the following question:

Wherein lies the difference between the tree-level approximation to a fixed order in α_s and the all orders summation of some specific logarithms?

Before answering this question, an important remark should be made. Recall that to order $O(\alpha_s^2)$ the two gluon result is exact, but to this same order there will be virtual and collinear corrections to the tree-level result. Therefore, another question (apparently related to the previous one) can be asked:

Can these corrections be so appreciable that they ensure the $O(\alpha_s)$ result dominates at large Q_T, as Altarelli et.al. believe?

The aim of this work is to shed some light on these differences using a simply calculable model, which has virtual corrections included. It is based on the approximation in which the gluons are emitted independently. For simplicity, we only consider the production of jets at relative Q_T in e^+e^- annihilation, as a less convoluted problem, than that of W, Z production at hadron colliders.

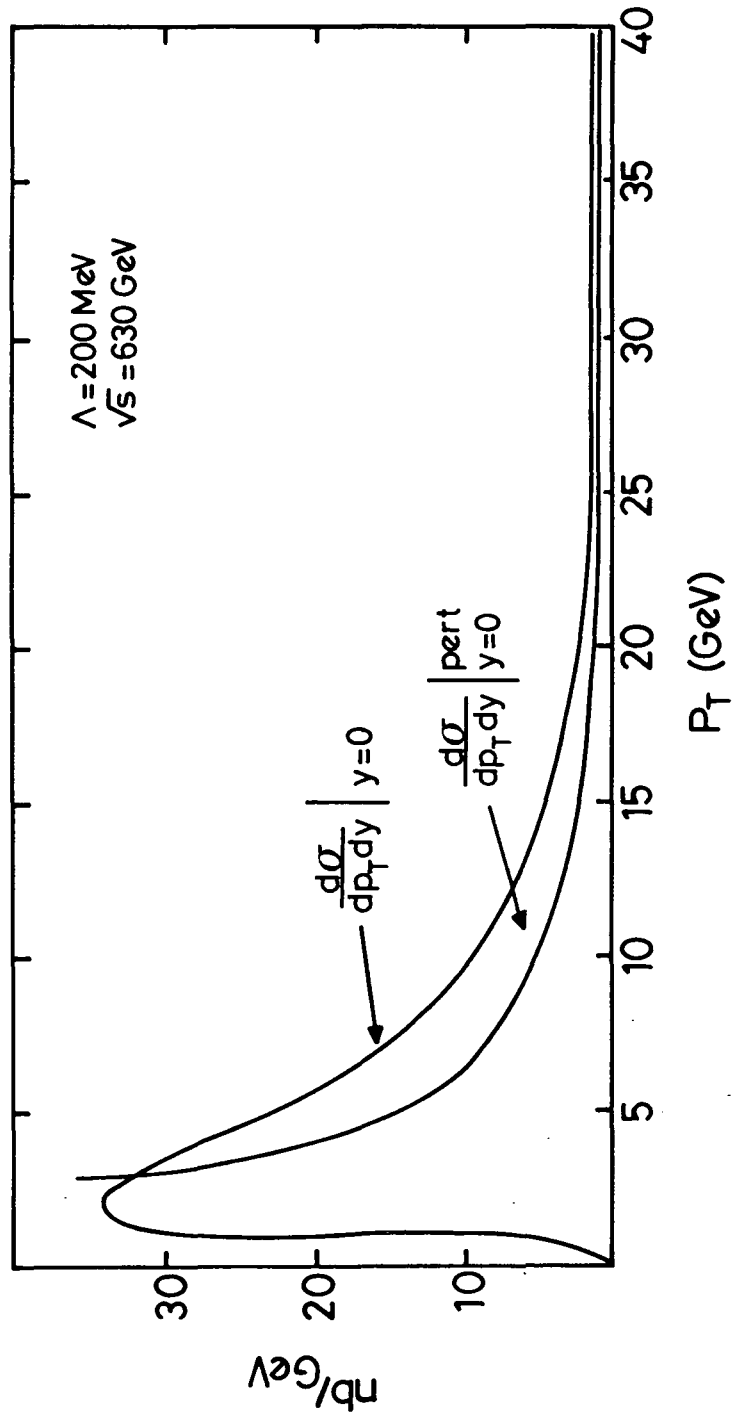

Figure II.1.5 Altarelli *et. al.*

Q_T-distributions to first and second order in α_s. Q_T is the lepton pair transverse momentum in hadron-hadron collisions. The $O(\alpha_s^2)$ Q_T-distribution reproduces the perturbative $O(\alpha_s)$ result at large Q_T and sums the multigluon emissions to DLLA at small Q_T.

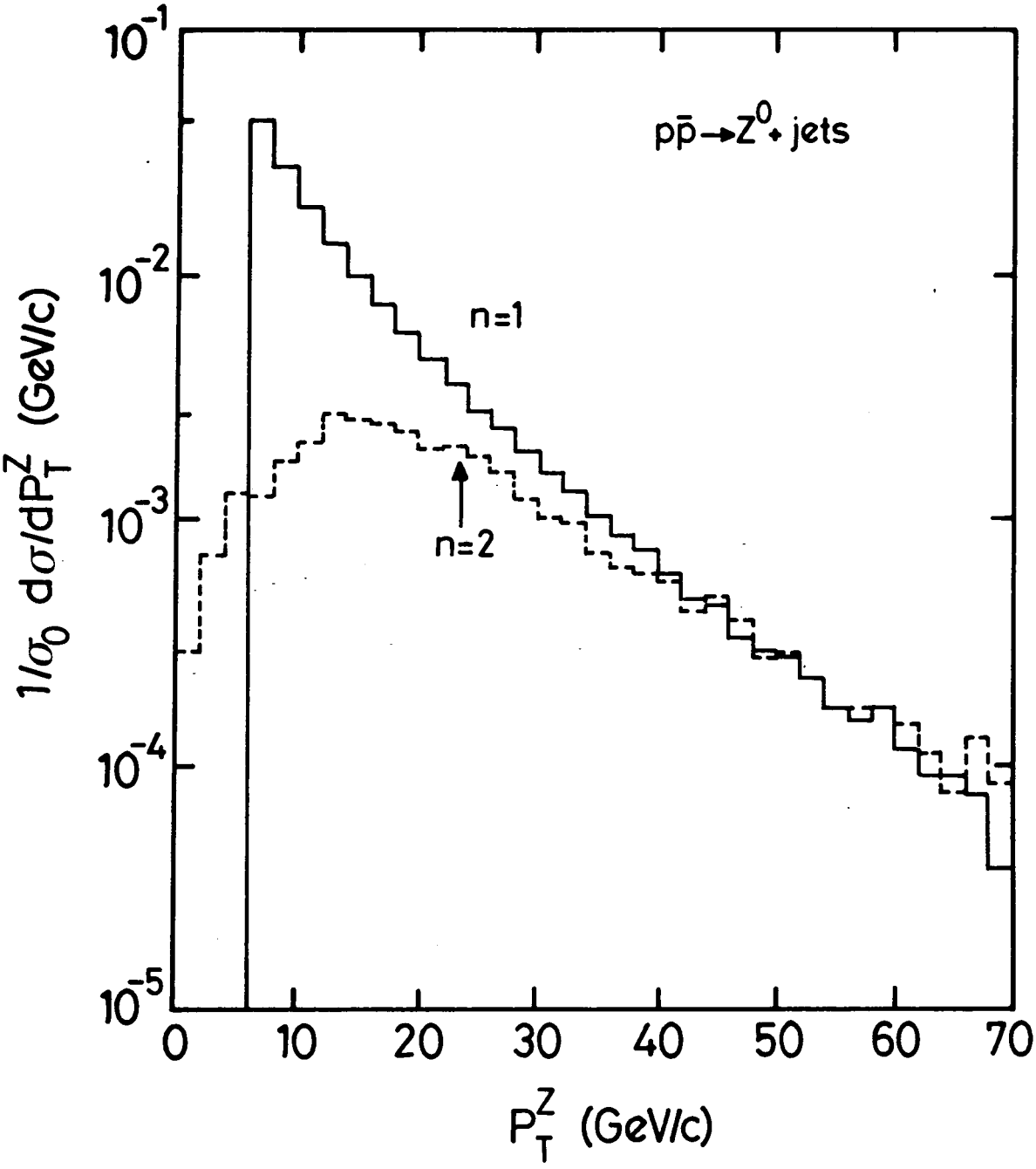

Figure II.1.6 Stirling *et.al.*

Distibution for the quantity $\frac{dR_n^Z}{dp_T^Z}$

$$R_n^Z = \frac{\sigma(Z + n\,jets)}{\sigma_0(Z)} \qquad n = 1, 2$$

II.2 $e^+e^- \to q\bar{q}g$.

II.2.1 Kinematics.

We work in the rest frame of the photon of mass Q and we introduce the dimensionless energy fraction variables:

$$x_i = \frac{2E_i}{Q} \qquad (i = 1,2,3 \qquad 0 \leq x_i \leq 1)$$

for the quark, antiquark and gluon (fig.II.2.1).

The four momenta of q, $\bar{q}$, and g are

$$\begin{aligned} p_1 &= \frac{Q}{2}(x_1; 0, 0, x_1) \\ p_2 &= \frac{Q}{2}(x_2; x_T, 0, -x_L) \\ p_3 &= \frac{Q}{2}(x_3; -x_T, 0, x_L - x_1) \end{aligned} \qquad \text{II.2.1}$$

respectively, where

$$x_T = \frac{2Q_T}{Q} \qquad \text{and} \qquad x_L = \frac{2Q_L}{Q}$$

Longitudinal and transverse momentum conservation are already embodied in eq.II.2.1 but energy conservation demands:

$$x_1 + x_2 + x_3 = 2 \qquad \text{II.2.2}$$

For massless $\bar{q}$ and g we also have the relations:

$$x_2^2 - x_T^2 - x_L^2 = 0$$

$$x_3^2 - x_T^2 - (x_L - x_1)^2 = 0 \qquad \text{II.2.3}$$

From eqs.II.2.2 and II.2.3 it then follows that:

$$x_T^2 = \frac{4}{x_1^2}(1 - x_1)(1 - x_2)(1 - x_3) \qquad \text{II.2.4}$$

The physical region for the above process is defined by:

$$0 \leq x_i \leq 1 \qquad \text{and} \qquad x_1 + x_2 + x_3 = 2$$

and is drawn as the Dalitz plot of fig.II.2.2.

II.2.2 Cross-Sections.

In terms of these variables, the differential cross-sections for $e^+e^- \rightarrow q\bar{q}g$, given by the graphs of fig.II.2.3b for single gluon emission and normalised by σ_0, the point-like cross-section of fig.II.2.3a is given by: [ref.II.11]

$$\frac{1}{\sigma_0}\frac{d^2\sigma}{dx_1 dx_2} = \frac{\alpha_s}{2\pi}C_F \quad \frac{x_1^2 + x_2^2}{(1-x_1)(1-x_2)} \qquad \text{II.2.5}$$

where $C_F = \frac{4}{3}$ the colour Casimir for $SU(3)_c$.

To get the x_T-distribution, we first go from (x_1, x_2) to (x_1, x_T). Specifying the values of the variables x_1, x_T fixes two kinematic points in the Dalitz plot of fig.II.2.2, related by $x_2 \leftrightarrow x_3$. So, adding the contributions of the graphs of fig.II.2.3b with x_2, x_3 interchanged, we have from eq.II.2.5:

$$\frac{1}{\sigma_0}\frac{d^2\sigma}{dx_1 dx_T^2} = \frac{\alpha_s}{2\pi}\frac{C_F}{x_T^2} \left[\frac{x_1^2+1}{1-x_1} - \frac{x_T^2(1-\frac{1}{4}x_1)}{(1-x_1)^2}\right]\left[1 - \frac{x_T^2}{1-x_1}\right]^{-\frac{1}{2}}$$

We can now integrate over x_1 (for $x_T \neq 0$) to obtain:

$$\frac{1}{\sigma_0}\frac{d\sigma^{(1)}}{dx_T^2} = \int_0^{1-x_T^2} dx_1 \quad \frac{d^2\sigma}{dx_1 dx_T^2} \quad ,$$

$$\frac{1}{\sigma_0}\frac{d\sigma^{(1)}}{dx_T^2} = \frac{2\alpha_s}{\pi}\frac{C_F}{x_T^2}\left[\left(1 - \frac{1}{4}x_T^2 + \frac{1}{4}x_T^4\right)\ln\left(\frac{1+\sqrt{1-x_T^2}}{x_T}\right) - \frac{1}{4}\sqrt{1-x_T^2}\,(3-x_T^2)\right] \qquad \text{II.2.6}$$

In the limit $x_T << 1$ we get from eq.II.2.6 the leading log formula (LLA):

$$\frac{1}{\sigma_0}\frac{d\sigma^{(1)}}{dx_T^2} = \frac{\alpha_s C_F}{\pi} \quad \frac{1}{x_T^2}\ln\left(\frac{1}{x_T^2}\right) \qquad \text{II.2.7}$$

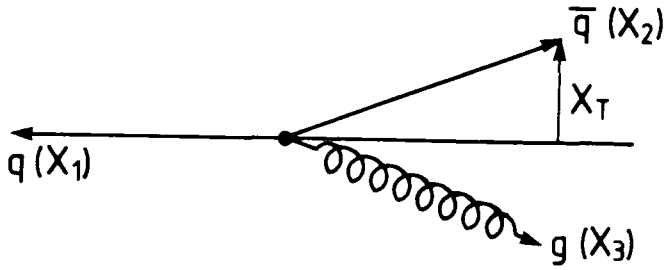

Figure II.2.1 The process $e^+e^- \to q\bar{q}g$ in the centre-of-mass frame.

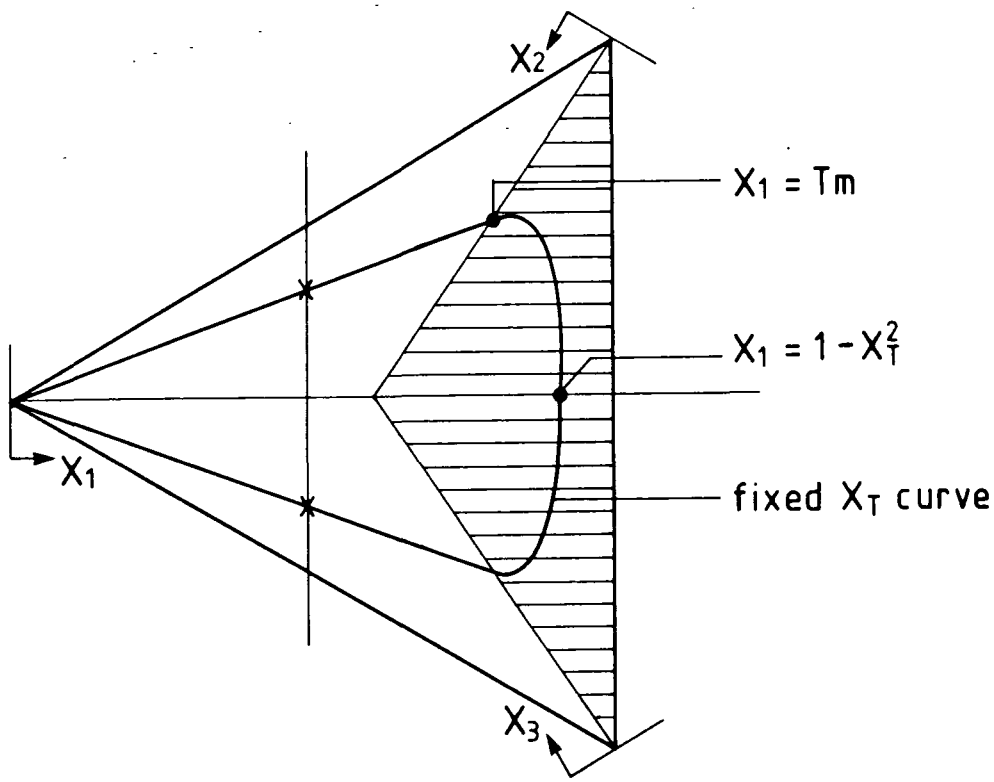

Figure II.2.2 Fixed x_T-line in the Dalitz plot

(x_T measured with respect to x_1)

In the shaded region x_1 is the largest energy fraction (thrust) $x_1 \geq x_2, x_3$

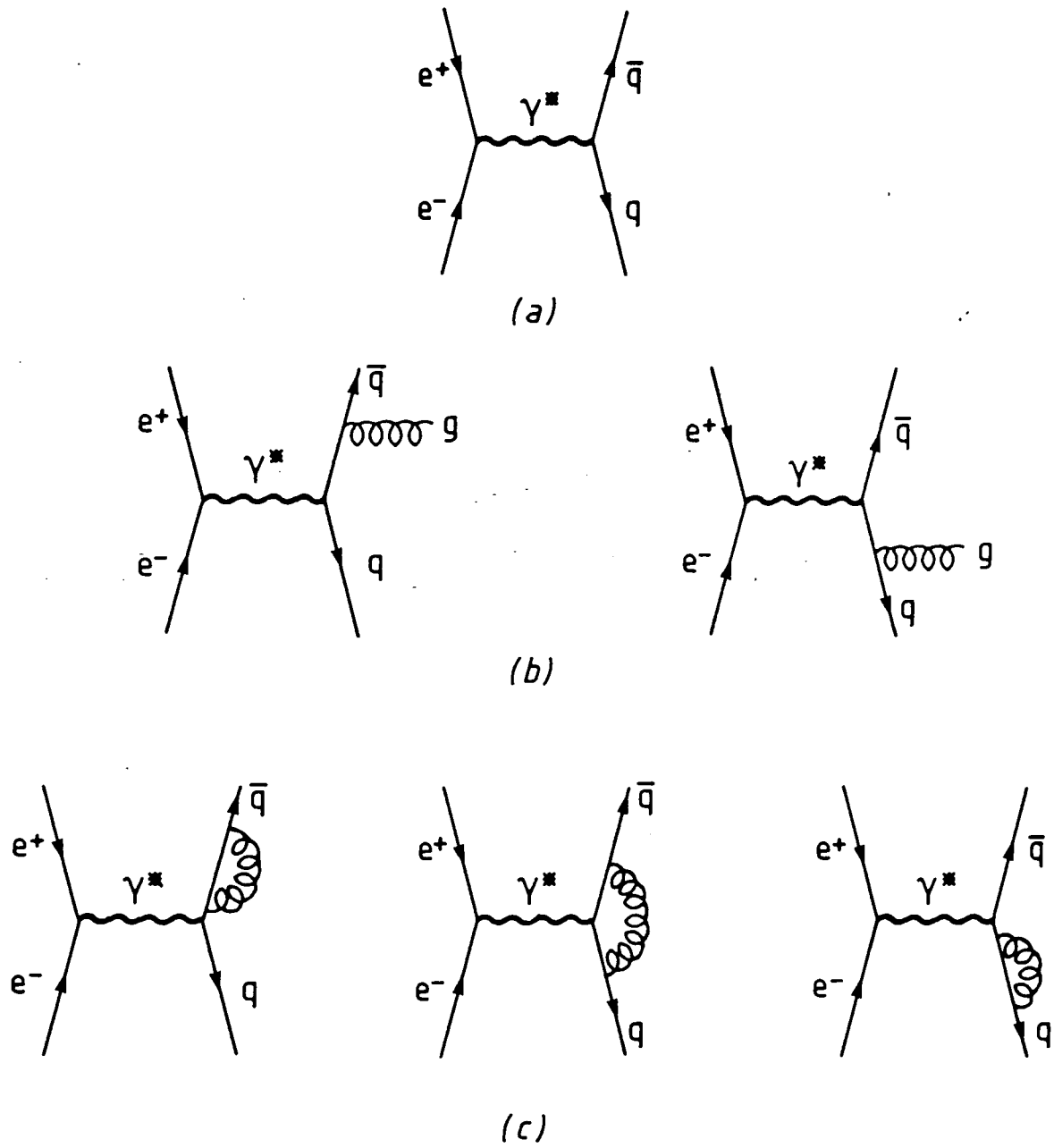

Figure II.2.3 Feynman diagrams for $e^+e^- \rightarrow$ jets

3a] Zeroth order contribution

3b] Graphs of $O(\alpha_s)$ for real gluon emission

3c] Graphs giving virtual contributions to $O(\alpha_s)$

Note that in eq.II.2.7 the argument of the logarithm was chosen to be $1/x_T^2$ and not $4/x_T^2$, that we really get in the limit $x_T \ll 1$. Of course, both choices are equivalent in the LLA, but the chosen one has bigger range of validity in phenomenological applications [ref. II.12].

In all the above formulae, x_T has been defined to be transverse to either the quark or the antiquark carrying momentum fraction x_1. However, in jet production in e^+e^- annihilation it is experimentally more feasible to define the transverse momentum relative to the parton with the maximum energy i.e. with largest x_i (called *thrust*). The kinematically allowed range of x_T is then $0 \leq x_T^2 \leq \frac{1}{3}$ (fig. II.2.2) and the differential cross-section for one gluon emission is given by: [ref.II.13]

$$\frac{1}{\sigma_0}\frac{d\sigma^{(1)}}{dx_T^2} = \frac{4\alpha_s C_F}{\pi x_T^2}\left[(1-\frac{1}{4}x_T^2+\frac{1}{4}x_T^4)\ln\left(\frac{\sqrt{1-T_m}+\sqrt{1-T_m-x_T^2}}{x_T}\right)\right.$$
$$\left.-\sqrt{1-\frac{x_T^2}{1-T_m}}\cdot\left(3-T_m-\frac{T_m^2}{2}-x_T^2(1-T_m)\right)\right] \qquad \text{II.2.8}$$

where T_m is the minimum value of the thrust variable at a given x_T, i.e. the root of the cubic:

$$x_T^2 T_m^2 = 4(1-T_m^2)(2T_m-1)$$

with (see fig.II.2.2):

$$\frac{2}{3} \leq T_m \leq 1$$

T_m can be usefully approximated by:

$$T_m \simeq 1-\frac{x_T^2}{2}-\frac{x_T^3}{16}-\frac{x_T^4}{16}-\frac{19x_T^5}{256}-\frac{3x_T^6}{32}-\frac{253x_T^7}{2048}$$

which is accurate to a fraction of one percent for most of the x_T-range, i.e. for $x_T^2 < 0.3$.

Note, parenthetically that eq.II.2.8, of course, reduces to eq.II.2.6 if $T_m \to 0$, as appropriate for x_T defined relative to the 1 axis.

II.1.3 The role of the virtual graphs.

As displayed in eq.II.2.5 the cross-section for real gluon emission diverges in the limit $x_1 \to 1$ and/or $x_2 \to 1$. Because of the relation:

$$2p_ip_j \quad = \quad Q^2(1-x_k) \quad = \quad 2E_iE_j(1-\cos\theta_{ij}) \qquad \text{II.2.9}$$

which, with θ_{ij} the angle between the partons i and j, is valid for massless quarks and gluons, it is easy to identify the configurations which give rise to these singularities, namely those where: (fig.II.2.4)

a] The gluon is soft $\to$ infrared divergence

b] The gluon is collinear with one of the fermions $\to$ collinear divergence

To keep away from these singularities and define a finite cross-section, we require a non-zero minimum value of x_T : $x_T \geq x_T^0$ (fig.II.2.4)

It is important to emphasize here, that the above singular configurations are exactly those in which we cannot distinguish experimentally between three jets ($e^+e^- \to q\bar{q}g$) and two back-to-back jets ($e^+e^- \to q\bar{q}$). Therefore, the requirement of a minimum transverse momentum plays an important experimental role, as well as a theoretical one. Theoretically, it keeps us away from both the soft and collinear singularities and experimentally, it defines three distinct jets from the final state paricles (see also §III.3).

In the two-jet region now, our analysis to first order in α_s can only be complete, if we consider the $O(\alpha_s)$ virtual corrections to the process $e^+e^- \to q\bar{q}g$. The corresponding cross-section is given by the graphs of fig.II.2.3c and involves the same infrared and collinear singularities appearing in the real $O(\alpha_s)$ contribution, in such a way, that the total $O(\alpha_s)$ answer (sum of real and virtual graphs) is finite. Kinoshita, Lee and Nauenberg [ref.II.14] have proved that such cancellations *do* occur to all orders in perturbation theory, provided all indistinguishable configurations are included.

The regularised $O(\alpha_s)$ cross-section is then given by:

$$\frac{d\Sigma^{(1)}}{dx_T^2} \quad = \quad \frac{d\sigma^{(1)}}{dx_T^2} \quad - \quad \delta(x_T^2)\int dx_T^2 \frac{d\sigma^{(1)}}{dx_T^2}$$

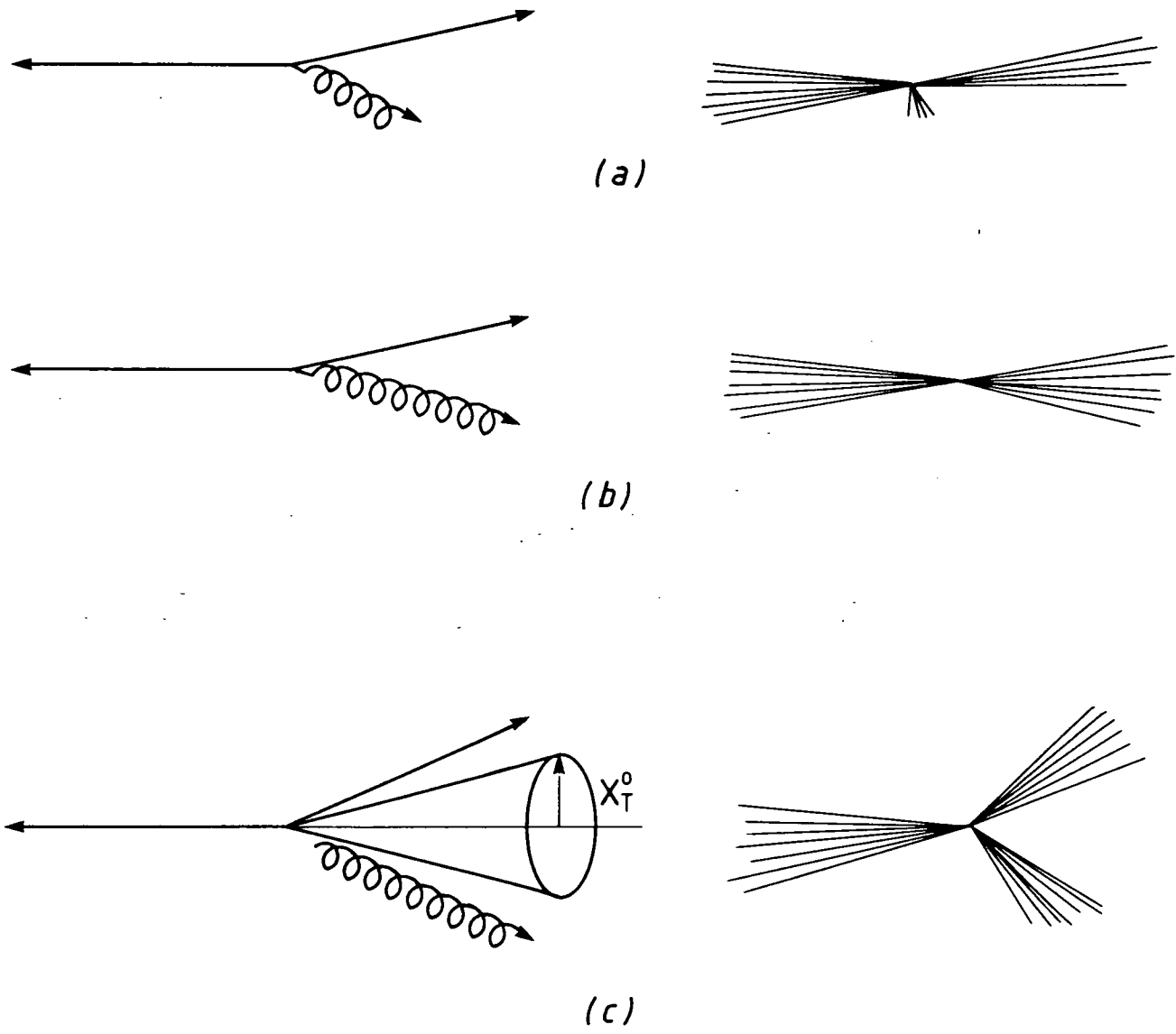

Figure II.2.4 When is a $q\bar{q}g$ final state distinguishable (on hadronisation) from a $q\bar{q}$ one ?

4a] Soft gluon (two jets)

4b] Collinear gluon (two jets)

4c] $\bar{q}, g$ have to be outside the cone defined by x_T^0 in order to give a clear three-jet event

II.3 ALL ORDERS CONSIDERATION.

Eq.II.2.8 gives the cross-section to $O(\alpha_s)$ for the emission of a single gluon with transverse momentum Q_T. Because of the property of Asymptotic Freedom at large x_T, i.e. $Q_T \sim Q$, we expect it to dominate over two, three, ..., gluon emissions. On the other hand, as x_T decreases, i.e. $\Lambda << Q_T << Q$, the simple perturbative expansion breaks down (see §II.1). Multigluon emissions become increasingly important and cannot be neglected any more. However, because of the limited value of Q_T, the compensation between real and virtual graphs is no longer complete and large logarithms appear as a result of collinear and soft gluon emissions. In order to give a practically useful answer the perturbative series must be resummed. Before going into the details of the resummation techniques for multigluon emissions, we can make the following approximation:

II.3.1 The Independent Emission Approximation (I E A).

Recall that the probability of a gluon emission is inversely proportional to the square of the transverse momentum of the emitted gluon. So, the emission of 'soft' gluons is most likely. However, if the gluons are 'soft' compared to the fast moving quark or antiquark that emits them, ($x_{T_i} << 1$), we can regard their emissions as approximately independent.

To appreciate this approximation, we look at the emission of two gluons from a quark leg (fig.II.3.1). If the gluon is soft ($k_1 << p$) then the quark momentum after the emission is (approximately) the same as it was before the emission ($p' \simeq p$). Then the emission of a second soft gluon ($k_2 << p'$) can be seen as an (approximately) independent event, in the sense that the second gluon knows nothing about the emission of the first one !

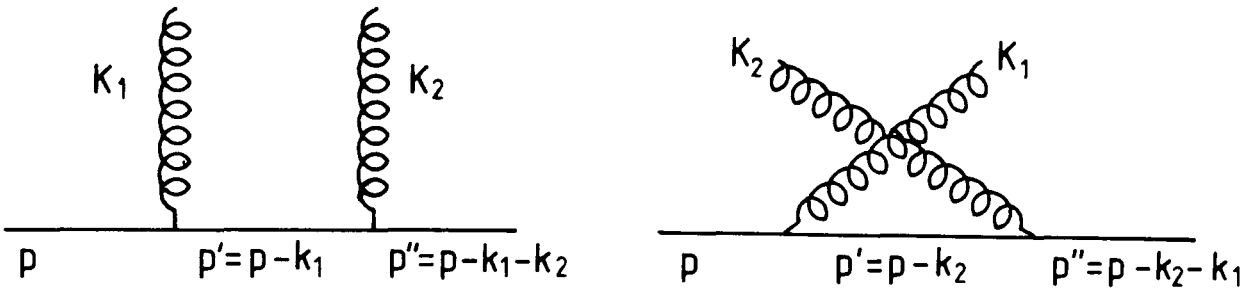

Figure II.3.1 Two contributions to the amplitude for two gluon emission, defining the relevant momenta.

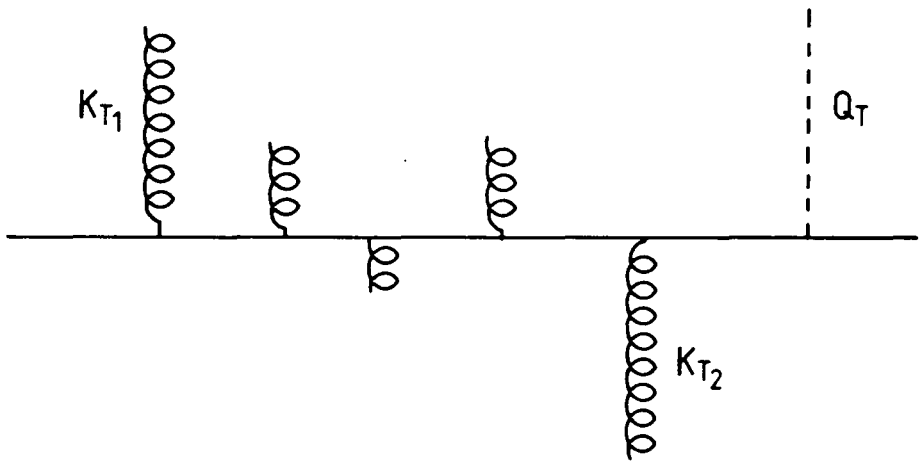

Figure II.3.2 Next-to-leading contribution

Two gluons with large but almost equal and opposite k_T (which balance the total Q_T) plus any number of soft gluons.

If we now look at just the propagators of the graphs of fig.II.3.1, we can see that for massless quarks and gluons, with $k_1, k_2 << p$: [ref.II.15]

$$\frac{\not p - \not k_1}{(p-k_1)^2}\frac{\not p - \not k_1 - \not k_2}{(p-k_1-k_2)^2} + \frac{\not p - \not k_1}{(p-k_2)^2}\frac{\not p - \not k_1 - \not k_2}{(p-k_1-k_2)^2}$$

$$\simeq \quad \frac{\not p}{2pk_1}\frac{\not p}{2p(k_1+k_2)} + \frac{\not p}{2pk_2}\frac{\not p}{2p(k_1+k_2)}$$

$$= \quad \frac{\not p}{2pk_1}\frac{\not p}{2pk_2} \qquad \text{II.3.1}$$

And this factorisation generalizes to any number of soft gluon emissions [ref.II.16]. The only constraint these soft and 'independent'gluons have to obey is the overall transverse momentum conservation:

$$Q_T = \sum_i k_{T_i}$$

II.3.2 Resummation of multigluon emissions in DLLA.

We recall the LLA result for the emission of one gluon (eq.II.2.7) and calculate the cross-section for two gluon emission from that for one:

$$\frac{1}{\sigma_0}\frac{d\sigma^{(2)}}{dQ_T^2} = \left[\frac{C_F\alpha_s}{\pi}\right]^2 \frac{1}{2\pi}\int \frac{d^2\mathbf{k}_{T_1}}{k_{T_1}^2}\frac{d^2\mathbf{k}_{T_2}}{k_{T_2}^2} \times$$

$$\times \ln\left(\frac{k_{T_1}^2}{Q^2}\right) \ln\left(\frac{k_{T_2}^2}{Q^2}\right) \delta^{(2)}(\mathbf{k}_{T_1} + \mathbf{k}_{T_2} + \mathbf{Q}_T) \qquad \text{II.3.2}$$

It has been shown [ref.II.17] that in the DLLA approximation, the dominant regions of integration correspond to the case where the emitted gluons are strongly ordered : $k_{T_1}^2 << k_{T_2}^2 \sim Q_T^2$ and $k_{T_2}^2 << k_{T_1}^2 \sim Q_T^2$ when monentum conservation is trivially fulfilled. Then:

$$\frac{1}{\sigma_0}\frac{d\sigma^{(2)}}{dQ_T^2} = \left[\frac{C_F\alpha_s}{\pi}\right]^2 \frac{1}{Q_T^2}\ln\frac{Q_T^2}{Q^2}\int_0^{Q_T^2}\frac{dk_T^2}{k_T^2}\ln\frac{k_T^2}{Q^2} \qquad II.3.3$$

The apparent divergence at the lower limit of the k_T^2 intergration is cancelled by the the contributions from the $O(\alpha_s^2)$ virtual graphs. (This can be done by introducing a λ^2 infrared cut-off, which will be removed eventually by the virtual graphs).

The regularized $O(\alpha_s^2)$ cross-section is then finite:

$$\frac{1}{\sigma_0}\frac{d\Sigma^{(2)}}{dQ_T^2} = -\left[\frac{C_F\alpha_s}{\pi}\right]^2 \frac{1}{2Q_T^2}\ln^3\frac{Q^2}{Q_T^2}$$

$$\frac{1}{\sigma_0}\frac{d\Sigma^{(2)}}{dQ_T^2} = -\left[\frac{1}{\sigma_0}\frac{d\sigma^{(1)}}{dQ_T^2}\right]_{LLA} \frac{C_F\alpha_s}{2\pi}\ln^2\frac{Q^2}{Q_T^2} \qquad \text{II.3.4}$$

Note that this $O(\alpha_s^2)$ contribution, being negative, tends to cancel the $O(\alpha_s)$ cross-section (in other words, leading logs tend to cancel in the region $Q_T^2 << Q^2$). We can now write:

$$\frac{1}{\sigma_0}\frac{d\sigma}{dQ_T^2} = \frac{1}{\sigma_0}\left[\frac{d\sigma^{(1)}}{dQ_T^2} + \frac{d\sigma^{(2)}}{dQ_T^2}\right] \quad ,$$

$$\frac{1}{\sigma_0}\frac{d\sigma}{dQ_T^2} = \frac{1}{\sigma_0}\frac{d\sigma^{(1)}}{dQ_T^2}\left[1 - \frac{\alpha_s C_F}{2\pi}\ln^2\frac{Q^2}{Q_T^2}\right] \qquad \text{II.3.5}$$

and we can understand the two terms in eq.II.3.5 as the beginning of a series which sums all such multigluon emissions.

In fact, multigluon emissions can be calculated in the same way as for the two gluon case. These have been summed to give the well known Sudakov form factor: [ref.II.18]

$$\frac{1}{\sigma_0}\frac{d\sigma}{dQ_T^2}|_{LLA} = \frac{1}{\sigma_0}\frac{d\sigma^{(1)}}{dQ_T^2}|_{LLA} \exp\left[-\frac{C_F\alpha_s}{2\pi}\ln^2\frac{Q^2}{Q_T^2}\right] \qquad \text{II.3.6}$$

The appearance of the Sudakov form factor has been seen as an incomplete cancellation between virtual and real gluon emision in the region $Q_T^2 << Q^2$. This form factor, if exact, would imply a total suppression of the cross-section at small Q_T, while giving the $O(\alpha_s)$ LLA result at large $Q_T \sim Q$.

II.3.3 Beyond DLLA.

We have just seen that in DLLA multigluon emissions can be factorised and allow summation. However, Collins, Soper and Sterman [ref.II.8,17] were among the first to question the validity of the leading double logarithmic approximation. They noticed that it is possible to find kinematic regions where both $\alpha_s << 1$ and $\alpha_s \ln \frac{Q^2}{Q_T^2} < 1$ (so that DLLA is appropriate) and yet $\alpha_s \ln^2 \frac{Q^2}{Q_T^2} > 1$, so that terms beyond the leading logs have to be included in a complete analysis to all orders.

We can appreciate the importance of non-leading terms, ignored in the derivation of eq.II.3.6, if we recall the approximation of ordered gluons (valid in DLLA). The above cross-section vanishes as $Q_T \to 0$, but in this limit the approximation of ordered gluons breaks down (as there is no phase space left!)

A typical example of important next-to-DLLA terms which have been left over so far, is shown in fig.II.3.2 . It involves two gluons with large but almost equal and opposite transverse momenta k_{T_i} which balance the overall transverse momentum Q_T, together with any number of soft gluons. These contributions are suppressed by at least three large logarithms, but they might give a non-zero cross-section in the limit $Q_T \to 0$.

Then, in order to deal with these contributions, a more careful treatment of the transverse momentum conservation is needed.

II.3.4 Impact Parameter Summation.

Parisi and Petronzio [ref.II.6] noted that by going to 'impact parameter space', both the factorization of the k_{T_i} integrals and *exact* transverse momentum conservation can be achieved. The idea is to write the transverse momentum δ-function in the form:

$$\delta^{(2)}(\mathbf{k}_{T_1} + \mathbf{k}_{T_2} + \ldots + \mathbf{k}_{T_n} + \mathbf{Q}_T) = \frac{1}{(2\pi)^2} \int d^2b \; e^{i(\mathbf{k}_{T_1} + \ldots + \mathbf{Q}_T).\mathbf{b}} \quad \text{II.3.7}$$

Each multigluon contribution (for example eq.II.3.2) is then a completely factorized product of k_{T_i} integrals, every one of which is given by:

$$\Delta(b) \quad = \quad \frac{1}{\pi} \int d^2k_T \quad \left[\frac{1}{\sigma_0}\frac{d\sigma}{dk_T^2}\right] \quad \left[e^{i\,\mathbf{k_T}\cdot\mathbf{b}} - 1\right]$$

and performing the angular integration:

$$\Delta(b) \quad = \quad \int dk_T^2 \quad \left[\frac{1}{\sigma_0}\frac{d\sigma}{dk_T^2}\right] \quad \left[J_0(k_T b) - 1\right] \qquad \text{II.3.8}$$

where the -1 arises from the virtual gluon diagrams which regulate the infrared ($k_T \to 0$) divergences. The Q_T distribution arising from these multigluon emissions is then a power series in Δ , which is found to sum to an exponential:

$$\frac{1}{\sigma_0}\frac{d\sigma}{dQ_T^2} \quad = \quad \frac{1}{2}\int db\, b \quad \exp\left[\Delta(b)\right] \quad J_0(Q_T b) \qquad \text{II.3.9}$$

It should be noted that eq.II.3.9 has the following properties: [ref.II.7]

a) $d\sigma/\sigma_0 dQ_T^2$ is now non-zero as $Q_T \to 0$

b) It reproduces the $O(\alpha_s)$ perturbative result as $Q_T \to Q$

$$\frac{1}{\sigma_0}\frac{d\sigma}{dQ_T^2} \longrightarrow \left[\frac{1}{\sigma_0}\frac{d\sigma^{(1)}}{dQ_T^2}\right]_{O(\alpha_s)}$$

c) The resummation does not change the total integrated cross- section σ_0

$$\int dQ_T^2 \quad \frac{1}{\sigma_0}\frac{d\sigma}{dQ_T^2} \quad = \quad \frac{1}{\sigma_0}\sigma_0 e^{\Delta(0)} \quad = \quad 1$$

d) Although multigluon emission ($n \geq 2$) regularizes and alters the shape of the $O(\alpha_s)$ distribution, it does not change the average value of Q_T^2

$$\langle Q_T^2\rangle \quad = \quad \int dQ_T^2 \quad Q_T^2 \quad \left[\frac{1}{\sigma_0}\frac{d\sigma}{dQ_T^2}\right] \quad = \quad \langle Q_T^2\rangle^{(1)}_{O(\alpha_s)}$$

II.4 SUMMARY OF CHAPTER II.

Studies of transverse momentum distributions are of great theoretical importance, particularly as they enable us to investigate the structure of perturbtive QCD in some detail, and can be divided in two distinct kinematical regimes: At large transverse momenta ($Q_T \sim Q$) the perturbative expansion is rapidly convergent and the property of Asymptotic Freedom ensures the dominance of the emission of a single, hard gluon to balance the relative Q_T of the process. On the other hand, as Q_T becomes smaller, the coupling constant $\alpha_s(Q_T)$ increases and the emission of many, relatively 'soft' gluons gives rise to large logarithms so that the applicability of perturbative QCD in this regime is under question.

In this chapter we have seen how multigluon emissions can be resummed to all orders in α_s in a model where the gluons are emitted independently and transverse momentum conservation is treated in a exact way. The nice properties of the final expression, eq.II.3.9, indicate that this simple model has some useful features which may help to shed light on how the Q_T distribution is generated by multigluon emissions, as well as allow the individual multijet cross-sections to be studied.

The use of this model to attack the theoretical problems formulated in the introduction to this chapter is described in the following chapters.

CHAPTER III e^+e^- → 4 JETS

III.1 INTRODUCTION.

As outlined in the last chapter, in the Independent Emission Approximation (I E A), n-gluon cross-sections are constructed in terms of that for a single gluon emission in a simple way (eq.II.3.2). In this chapter, we use the formalism of I E A to study two gluon emission in some detail. As it will be explained in §III.3, the four final-state particles can define four-jets, provided they are well defined and well separated in phase space. Details of the numerical integration for calculating the four-jet cross-section are in §III.4 and the comparison with an 'exact' calculation is described and discussed in §III.5.

Our calculations will be performed at Q = 100 GeV, the energy of phenomenological relevance at LEP.

III.2 TWO GLUON EMISSION IN I E A.

In I E A, the two gluon contribution can be easily constructed in terms of that for a single gluon emission:

$$\frac{1}{\sigma_0}\frac{d\sigma^{(n)}}{d^2\mathbf{Q}_T\, d^2\mathbf{k}_{T_1}\ldots d^2\mathbf{k}_{T_n}} = \frac{1}{n!}\;\frac{1}{\sigma_0}\frac{d\sigma^{(1)}}{d^2\mathbf{k}_{T_1}}\;\frac{1}{\sigma_0}\frac{d\sigma^{(1)}}{d^2\mathbf{k}_{T_2}}\ldots\times$$

$$\times\frac{1}{\sigma_0}\frac{d\sigma^{(1)}}{d^2\mathbf{k}_{T_n}}\;\delta^{(2)}(\,\mathbf{k}_{T_1}+\mathbf{k}_{T_2}\ldots+\mathbf{Q}_T\,) \qquad \text{III.2.1}$$

Expressing the two-dimensional momentum conserving δ-function in terms of its b-space integral representation (eq.II.3.7) makes it easy to integrate out the angular dependences, since the cross-sections depend only on the moduli of the transverse momenta and not on their direction. This gives a regularized factor $\Delta(b)$ (eq. II.3.8) for each gluon.

We can then re-write the regularized two-gluon cross-section as:

$$\frac{1}{\sigma_0}\frac{d\Sigma^{(2)}}{dQ_T^2} = \frac{1}{2}\int dk_{T_1}^2\,\frac{1}{\sigma_0}\frac{d\sigma^{(1)}}{dk_{T_1}^2}\;\int dk_{T_2}^2\,\frac{1}{\sigma_0}\frac{d\sigma^{(1)}}{dk_{T_2}^2}\times$$

$$\frac{1}{2}\int_0^\infty db\,b\;\;\Big[J_0(k_{T_1}b)-1\Big]\;\;\Big[J_0(k_{T_2}b)-1\Big]\;\;J_0(Q_Tb) \qquad \text{III.2.2}$$

The integration of the product of Bessel functions [ref.III.1] gives:

$$\frac{1}{\sigma_0}\frac{d\Sigma^{(2)}}{dQ_T^2} = \frac{1}{4}\int dk_{T_1}^2\,\frac{1}{\sigma_0}\frac{d\sigma^{(1)}}{dk_{T_1}^2}\;\int dk_{T_2}^2\,\frac{1}{\sigma_0}\frac{d\sigma^{(1)}}{dk_{T_2}^2}\;\;W_3(k_{T_1},k_{T_2},Q_T)$$

$$-\frac{1}{\sigma_0}\frac{d\sigma^{(1)}}{dQ_T^2}\;\int dk_T^2\,\frac{1}{\sigma_0}\frac{d\sigma^{(1)}}{dk_T^2}\;+\frac{1}{2}\,\delta(Q_T^2)\;\;\Big[\int dk_T^2\,\frac{1}{\sigma_0}\frac{d\sigma^{(1)}}{dk_T^2}\Big] \qquad \text{III.2.3}$$

where

$$W_3(k_{T_1},k_{T_2},Q_T) = \frac{2}{\pi}\,\frac{1}{\Big[(k_{T_1}+k_{T_2})^2-Q_T^2\Big]^{\frac{1}{2}}\;\;\Big[Q_T^2-(k_{T_1}-k_{T_2})^2\Big]^{\frac{1}{2}}} \qquad \text{III.2.4}$$

Since W_3 just results from performing the angular intergrations of the two dimensional δ-function, $\delta^{(2)}(\mathbf{k}_{T_1} + \mathbf{k}_{T_2} + \mathbf{Q}_T)$, we can easily understand why W_3 is only defined if these vectors of length k_{T_1} , k_{T_2} , Q_T can form a closed triangle:

$$(k_{T_1} + k_{T_2})^2 \quad \geq \quad Q_T^2 \quad \geq \quad (k_{T_1} - k_{T_2})^2$$

It should be also noted that the singularity in the first term of eq.III.1.4 arising from the $1/k_{T_i}^2$ in $d\sigma^{(1)}/dk_{T_i}^2$ (eq. II.2.8) when either $k_{T_i} = 0$, is cancelled by the second term, giving a finite answer.

III.3 JET IDENTIFICATION CRITERIA.

The four final state partons ($q\bar{q}gg$) will only define four distinct jets, provided they are well defined (i.e. every one is energetic enough to be identified as a different jet) and they are well separated from each other (by a minimum relative angle) [ref.III.2].

The situation here is very similar to the one described in §II.2.3. There we saw how the introduction of a certain cut (the requirement for a non-zero minimum transverse momentum x_T^0) not only ensured distinct jets in the final state, but also guaranteed a finite tree level result in the allowed region of the phase space.

In general, such cuts are needed both theoretically, to define infrared- and collinear-safe cross-sections for partons, and experimentally, to group the final state hadrons into jets. Theoretically, these cuts can have any non-zero value, while experimentally, they must be specified with regard to the experimental acceptances. [ref.III.3]

It has also been emphasised, that the soft and collinear divergences of the tree graphs, which occur in those regions of phase space where the final state partons are not well defined (which, from an experimental point of view, means not distinct jets) are compensated by similar divergences in the virtual graphs (which have to be taken into account to the same order in α_s). Then, the K L N theorem ensures that a finite answer is obtained everywhere in phase space.

We can therefore write our $O(\alpha_s^2)$ cross-section schematically as:

$$d\sigma \quad = \quad \left[d\sigma^{(4)} - d\sigma^{(s)} \right] \quad + \quad \left[d\sigma^{(s)} + d\sigma^{(3)} \right] \qquad \text{III.3.1}$$

where $d\sigma^{(s)}$ contains the singularities in the region where four jets are indistinguishable from three jets:

$$d\sigma^{(4)} \underset{region}{\overset{singular}{-}} \rightarrow d\sigma^{(s)} \qquad \text{III.3.2}$$

Each term in eq.III.3.2 is then finite. The first is finite by construction and contributes to the four-jet result and the second is finite by virtue of the K L N theorem and contributes to the three-jet answer.

III.3.1 Sterman-Weinberg Cuts.

The most commonly used set of cuts defines three- and four-jets as those three- and four-parton configurations which satisfy the following criteria proposed by Sterman and Weinberg: [ref.III.4]

(i) Every parton energy is greater than some minimum, so that $x_i > \epsilon$

(ii) The angle between every possible parton pair is larger than 2δ

These criteria lead us to the following formal definition:

'By n-jet cross-section we shall understand the cross-section for events which have all but a fraction $\epsilon/2$ of the total- energy distributed within n separated cones of (full) opening angle δ'. As an illustration a three-jet event is shown in fig.III.3.1. At the parton level, an event is called a three-jet event (with the jet axis and ϵ , δ specified before hand) if all the parton momenta fall inside the phase volume shown in fig.III.3.1. By construction, this includes the singular region associated with one of the partons of the four-parton state, being soft and/or collinear with another. The three-jet cross-section is known to be finite by virtue of the K L N theorem.

III.3.2 Invariant Mass Cut.

Another procedure for defining irresolvable jets is based on an invariant mass cut-off on the parent partons [ref.III.5]. In this case, we say that two partons are irresolvable if:

$$s_{ij} \quad = \quad (p_i + p_j)^2 \quad \leq \quad yQ^2$$

where Q^2 is the total energy. By three-jet cross-section then, we understand the cross-section for events which consist of three clusters, each having an invariant mass squared smaller than yQ^2.

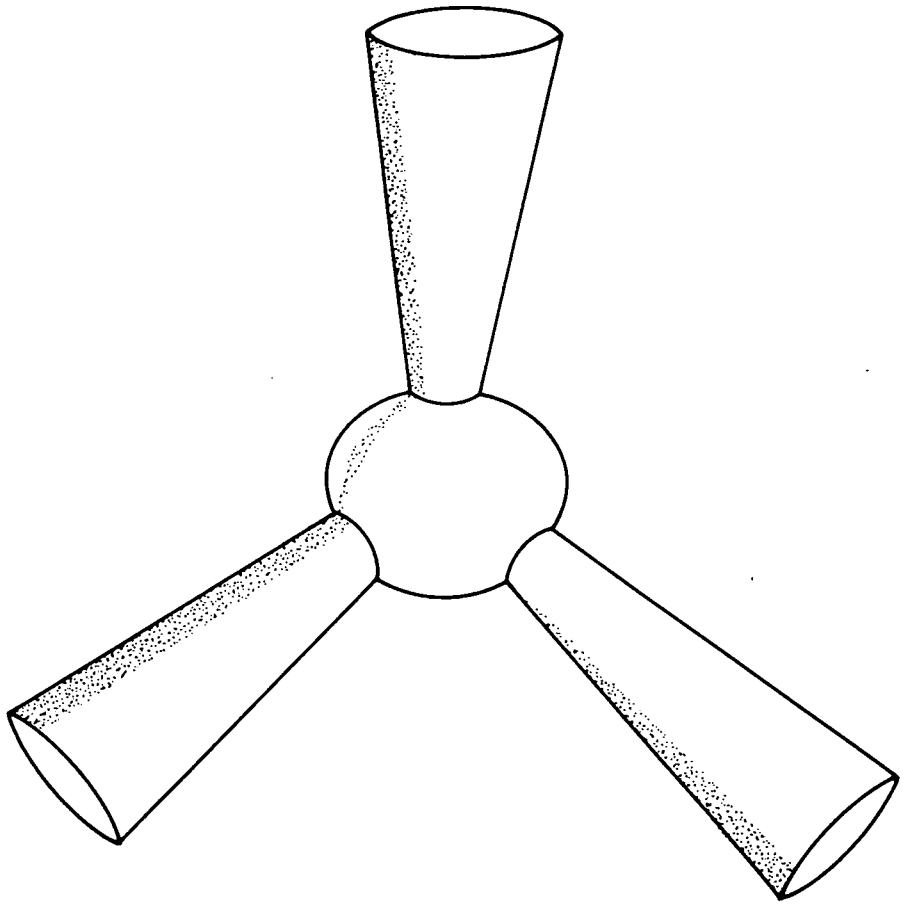

Figure III.3.1 Three-jets phase space

Defined using Sterman-Weinberg cuts (ϵ, δ).

ϵ : minimum energy fraction

δ : minimum angular separation

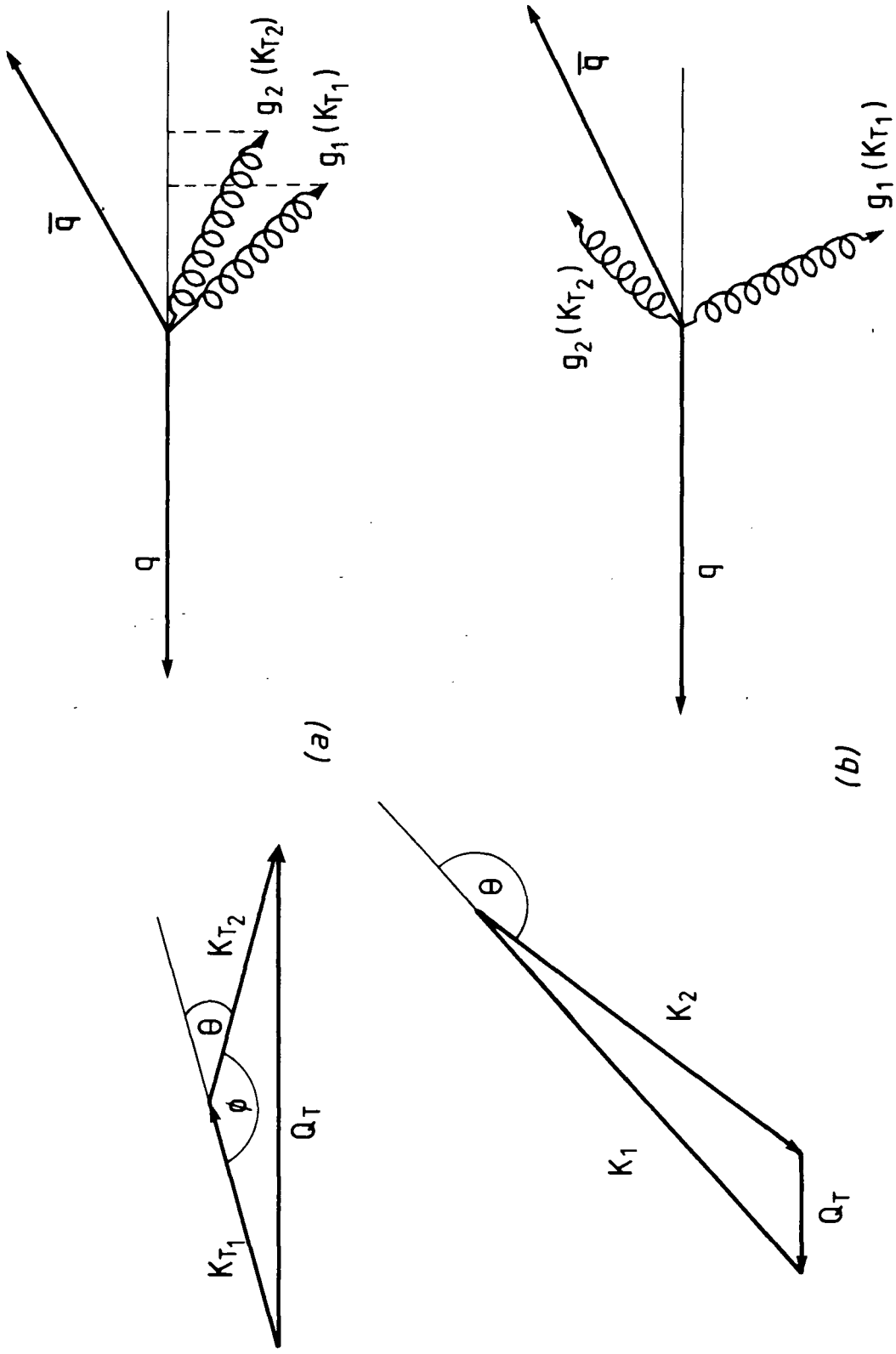

Figure III.3.2 Collinear configurations

a] Collinear gluons

b] Gluon collinear with fermion

III.3.3 Cuts in I E A.

Because the independent emission model is only transverse momentum dependent, the cuts needed to ensure four distinct jets can only be defined in terms of transverse momentum variables. As we shall see later in some detail, transverse momentum cuts are rather severe, as they remove more configurations than necessary.

a] Soft Partons

Recall that Q_T has been defined with respect to the fermion with largest thrust (§II.2.2). That fermion then is guaranteed to be energetic enough to produce a well defined jet. To prevent the other fermion and the two gluons from being soft, we impose the constraints:

$$Q_T\,,\, k_{T_i} \quad \geq \quad k_0 \qquad , \qquad i = 1,2 \qquad \text{III.3.3}$$

where k_0 some minimum transverse momentum cut

b] Collinear Partons

As Q_T has been restricted to be greater than a minimum k_0, the two fermions can never be collinear with each other. Moreover, the requirement of non-zero transverse momenta k_{T_i} for the gluons prevent each one of them from becoming collinear with the most energetic fermion (from which transverse momenta are measured). To deal with the remaining gluon-gluon and gluon-second fermion collinear configurations, we recall that the vectors of length k_{T_1} , k_{T_2} and Q_T have to form a triangle. We now require this triangle to be non-degenerate. This constraint removes away the remaining collinear configurations (fig. III.2.3) and can be expressed by the following closed formula:

$$\theta_0 \quad < \quad \theta(k_{T_1}\,,\, k_{T_2}) \quad < \quad \pi - \theta_0 \qquad \text{III.2.4}$$

It is interesting to note that in I E A, collinear gluon configurations (excluded by the requirement of distinct jets in the final state) do *not* give rise to any singularities, as there are no triple gluon interactions included in IEA. These do, of course, occur in the full answer for QCD.

We can now understand why these cuts have removed more phase space configurations than was actually needed. Consider, for instance, the configuration shown in fig.III.3.3. All four partons are apparently energetic enough to define (upon hadronisation) four distinct jets. Hence, this event should be classified as a four-jet event. However, gluon g_1 has so small transverse momentum, that the event fails one of our cuts, namely the requirement for a minimum transverse momentum, and therefore will be excluded in a four-jet analysis!

Eq.III.3.4 can be expressed in terms of transverse momentum variables, using the following relations (fig. III.3.2a).

$$\cos\theta_0 \quad \geq \quad \cos\theta \quad \geq \quad \cos(\pi - \theta_0)$$

$$\cos\theta \quad = \quad -\cos\phi$$

$$\cos\phi \quad = \quad \frac{Q_T^2 - k_{T_1}^2 - k_{T_2}^2}{2\,k_{T_1}\,k_{T_2}}$$

to obtain the constraint:

$$-z_0 \quad \leq \quad \frac{Q_T^2 - k_{T_1}^2 - k_{T_2}^2}{2\,k_{T_1}\,k_{T_2}} \quad \leq \quad z_0$$

where

$$z_0 \quad = \quad \cos\theta_0$$

The four-jet phase space, defined by the kinematical relations of §III.1 and restricted by the above cuts, is then shown in fig.III.3.4.

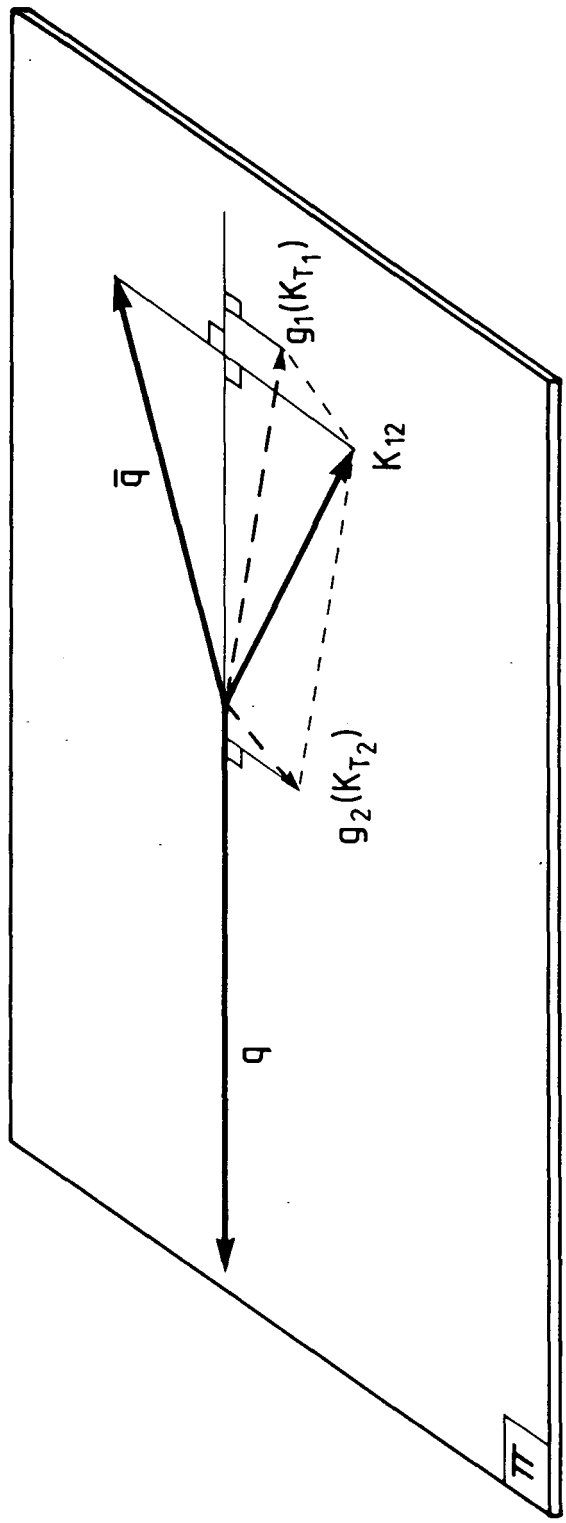

Figure. III.3.3 An 'almost' four-jet event.

Due to large longitudinal momenta, each parton is hard enough to be identified as a distinct jet. However, gluon g_1 fails the requirement of a minimum transverse momentum! (Solid lines on the plane II, dashed lines outside it)

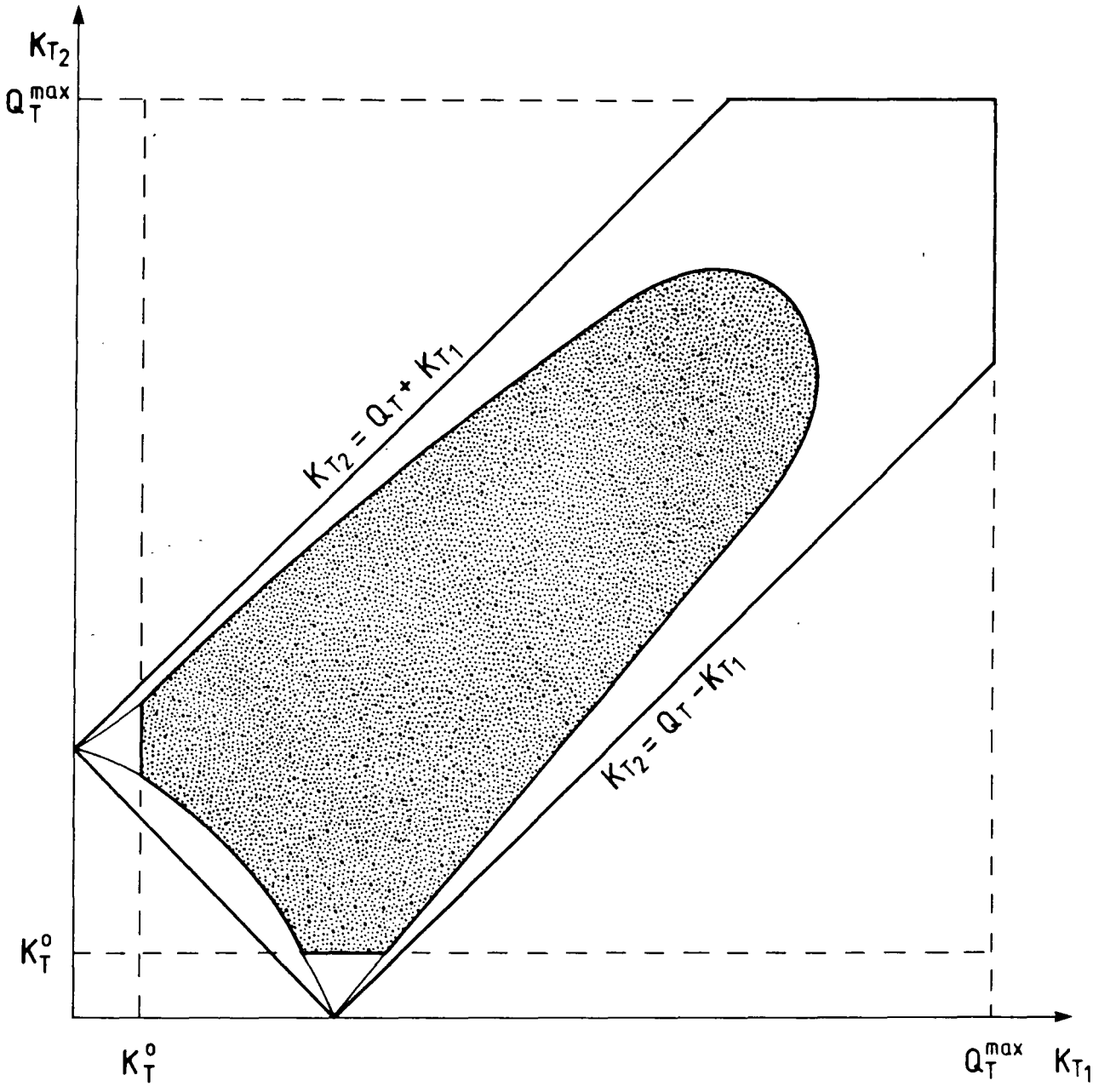

Figure III.3.4 Four-jet phase space.

It is defined by the kinematical constraint (the vectors of length k_{T_1}, k_{T_2}, Q_T must form a triangle) and the soft and collinear cuts (the above triangle is not degenerate)

III.3.4 Relations between the Cuts.

Second order corrections to three-jet cross-sections have been calculated using either of the above set of cuts ($\epsilon\,\delta$ cuts, invariant mass, minimum transverse momentum) [ref.III.6] and it has been noted [ref.III.7] that the results show great similarities in form. In fact, with a little algebraic manipulation, the leading logarithmic terms

$$\ln\epsilon\,\ln\Big(\frac{1-\cos\delta}{2}\Big) \quad , \quad \ln^2 y \quad \text{and} \quad \ln^2 x_T^0$$

can become identical, with particular choices of the values of the cuts:

$$\epsilon = x_T^0 \quad , \quad \delta = 4x_T^0 \quad \text{and} \quad y = \epsilon^2$$

The above relations can also be justified on the ground that, all these different cuts , if chosen carefully, remove (more or less) the same regions of phase space, namely those where the final-state particles become soft and/or collinear. An illustration of such a situation is shown in figure III.3.5, for a three-jet event.

These relations then enable us to compare calculations and translate results obtained using different sets of cuts (see also §III.5). In particular,it is worth noting the following choice:

$$\epsilon = 0.1 \quad , \quad \delta = 4\epsilon = 25^o\,(\cos\delta = 0.92)$$

$$y = \epsilon^2 = 0.01$$

$$x_T^0 = \epsilon = 0.1 \qquad (k_0 = 5GeV \text{ at } Q = 100GeV)$$

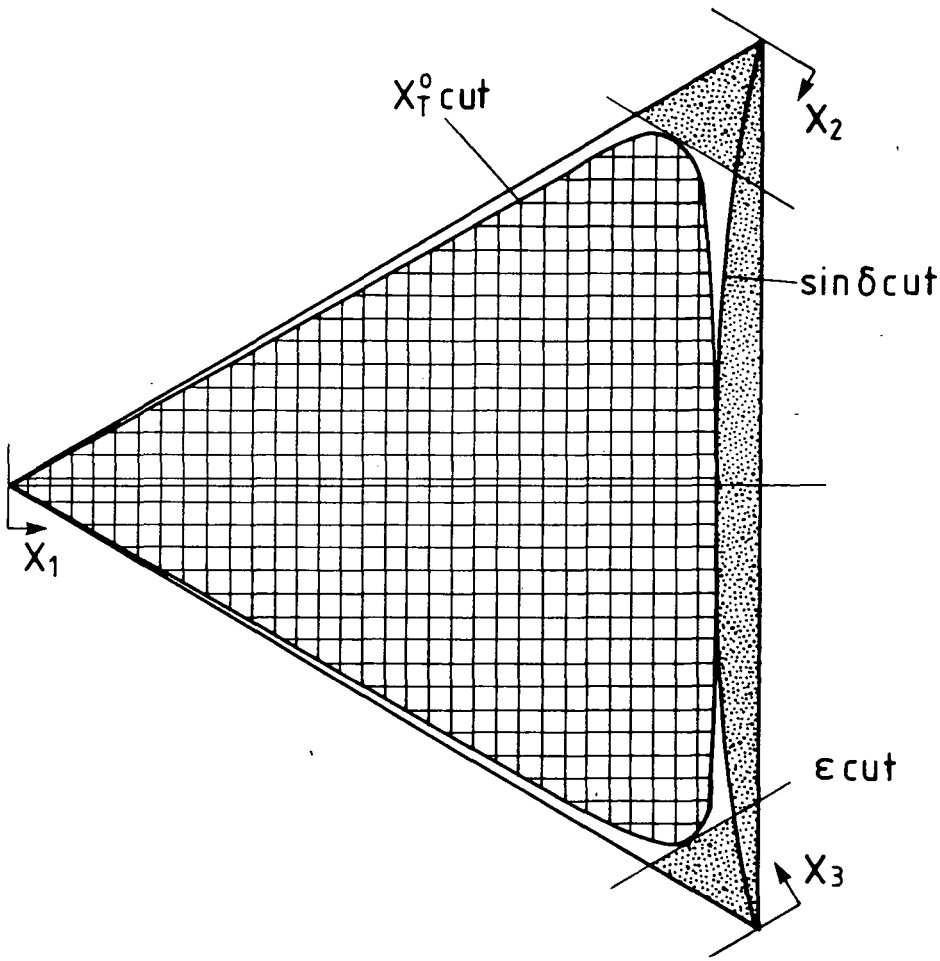

Figure III.3.5 The Dalitz plot for $e^+e^- \rightarrow q\bar{q}g$

When the shaded region with soft and collinear singularities is excluded by Sterman-Weinberg cuts, the remaining phase space is not very different from that allowed by a minimum transverse momentum cut (hatched area)

III.4 NUMERICAL INTEGRATION.

We can now calculate the contribution of the two gluon emission to the four-jet cross-section in the I E A by integrating the first part of eq.III.2.3 over the phase space determined by the kinematics and the cuts introduced in the last section.

Note that our integral is perfectly finite, even though W_3 is singular, because these infinities occur at the edges of phase space where they are integrable. However, to ensure maximum numerical stability, we prefer to work in terms of more appropriate variables. The study of these changes of variables is the subject of this section.

(i) $(\mathbf{k_{T_1}}, \mathbf{k_{T_2}}) \longrightarrow (\mathbf{x}, \mathbf{y})$

We first go from the dimensionful variables (k_{T_1}, k_{T_2}) to the dimensionless ones (x, y) defined as follows:

$$k_{T_1} = \frac{Q_T}{2}(x+y) \quad , \quad x = \frac{k_{T_1} + k_{T_2}}{Q_T}$$

$$k_{T_2} = \frac{Q_T}{2}(x-y) \quad , \quad y = \frac{k_{T_1} - k_{T_2}}{Q_T} \qquad \text{III.4.1}$$

with the corresponding change in the measure given by:

$$dk_{T_1}\, dk_{T_2} \quad = \quad 2\,\frac{Q_T}{2}\,\frac{Q_T}{2}\,dx\,dy$$

The transformed phase space and the new limits are shown in fig.III.4.1

Before expressing our integral (eq.III.2.3 and 4) in terms of these new variables, we introduce the notation:

$$\frac{1}{\sigma_0}\frac{d\sigma^{(1)}}{dk_{T_i}^2} \quad = \quad \frac{1}{k_{T_i}^2}\, f(k_{T_i}) \qquad \text{III.4.2}$$

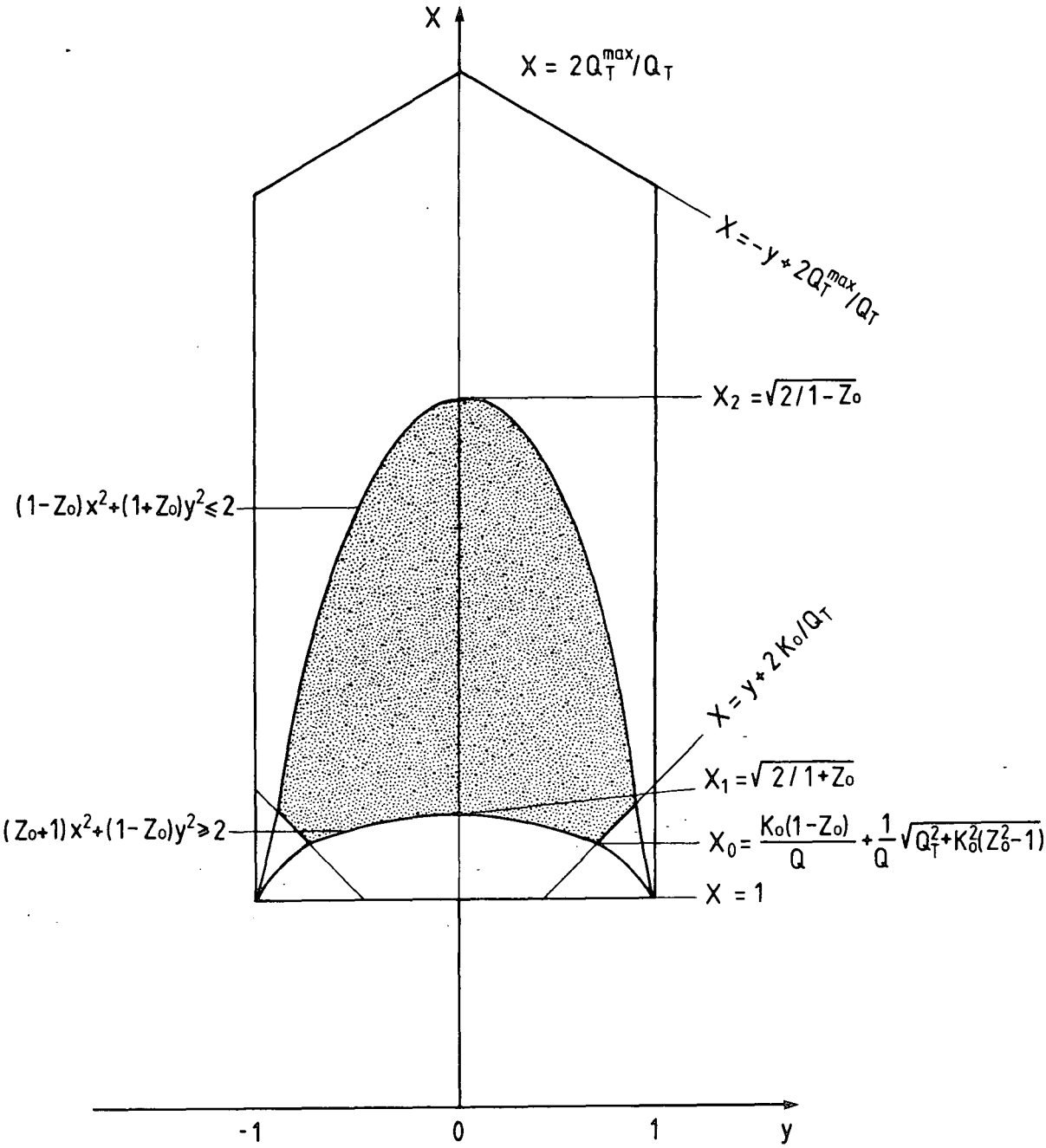

Figure III.4.1 Four-jet phase space

With its boundaries defined for numerical integration

so that we can write:

$$\frac{1}{\sigma_0}\frac{d\sigma^{(2)}}{dQ_T^2} = \frac{1}{2\pi}\int dk_{T_1}^2 \frac{1}{k_{T_1}^2} f(k_{T_1}) \; dk_{T_2}^2 \frac{1}{k_{T_2}^2} f(k_{T_2}) \times$$

$$\times \frac{1}{\left[(k_{T_1}+k_{T_2})^2 - Q_T^2\right]^{\frac{1}{2}} \left[Q_T^2 - (k_{T_1}-k_{T_2})^2\right]^{\frac{1}{2}}}$$

and with a little algebra:

$$\frac{1}{\sigma_0}\frac{d\sigma^{(2)}}{dQ_T^2} = \frac{4}{\pi Q_T^2}\int \frac{dx\,dy}{x^2-y^2} f\left[\frac{Q_T}{2}(x+y)\right] \times$$

$$\times f\left[\frac{Q_T}{2}(x-y)\right] \frac{1}{(x^2-1)^{\frac{1}{2}}(1-y^2)^{\frac{1}{2}}} \qquad \text{III.4.3}$$

The limits of the y-integral (shown in fig.III.4.1) are such that we can make use of the following identities:

$$\frac{1}{x^2-y^2} = \frac{1}{2x}\left[\frac{1}{x+y} - \frac{1}{y-x}\right]$$

and

$$\int_{-\alpha}^{\alpha} \frac{dy}{y+x} = \int_{-\alpha}^{\alpha} \frac{dy}{x-y} \quad , \quad \int_{-\alpha}^{-\beta} \frac{dy}{y+x} = \int_{\alpha}^{\beta} \frac{dy}{x-y}$$

and re-write eq.III.3.3 as:

$$\frac{1}{\sigma_0}\frac{d\sigma^{(2)}}{dQ_T^2} = \frac{4}{\pi Q_T^2}\int \frac{dx\,dy}{x(x+y)} \frac{f\left[\frac{Q_T}{2}(x+y)\right] f\left[\frac{Q_T}{2}(x-y)\right]}{(x^2-1)^{\frac{1}{2}}(1-y^2)^{\frac{1}{2}}}$$

(ii) $(\mathbf{x}, \mathbf{y}) \longrightarrow (\mathbf{x}, \theta)$

Though we know our cross-section is finite, it is not yet ready for numerical integration, as we see from the last expression, because of the singularities as $x \rightarrow 1$ and $y \rightarrow 1$. To show these are artifacts of the integration, we introduce the following change of variables, for x , y close to 1:

$$x = x \quad , \quad x = x$$

$$y = \frac{-1 + x\sin\theta}{x - \sin\theta} \quad , \quad \sin\theta = \frac{xy+1}{x+y} \qquad \text{III.4.4}$$

so that

$$\frac{dy}{(x+y)(y^2-1)^{\frac{1}{2}}} \longrightarrow \frac{d\theta}{(x^2-1)^{\frac{1}{2}}}$$

and the $y \to 1$ pole has been absorbed in the change of measure.

Note that:

$$x + y = \frac{x^2-1}{x-\sin\theta} \qquad x - y = \frac{x^2 - 2x\sin\theta + 1}{x - \sin\theta}$$

so we can write

$$\frac{1}{\sigma_0}\frac{d\sigma^{(2)}}{dQ_T^2} = \frac{4}{\pi Q_T^2}\int_{x_{min}}^{x_{max}} \frac{dx}{x(x^2-1)^{\frac{1}{2}}} \int_{\theta_{min}}^{\theta_{max}} \frac{d\theta}{(x^2-1)^{\frac{1}{2}}} \times$$

$$\times f\left[\frac{Q_T}{2}\left(\frac{x^2-1}{x-\sin\theta}\right)\right] \; f\left[Q_T\left(\frac{x^2-2x\sin\theta+1}{x-\sin\theta}\right)\right] \qquad \text{III.4.5}$$

where

$$\theta_{min(max)} = \arcsin\left(\frac{xy_{min(max)}+1}{x+y_{min(max)}}\right)$$

(iii) $(\mathbf{x}, \theta) \to (\xi, \psi)$

We finally deal with the pole at $x = 1$, which we have arranged to appear twice, in both the x- and θ-integrals, so that each appearance can be treated independently. In fact, we can re-write our integral schematically as:

$$I = \int_{x=1}^{x_{max}} \frac{dx}{x(x^2-1)^{\frac{1}{2}}} \; \phi(x) \qquad (I_1)$$

where

$$\phi(x) = \frac{1}{(x^2-1)^{\frac{1}{2}}} \int_{\theta_{min}}^{\theta_{max}} d\theta \, f_1 f_2 \qquad (I_2)$$

The I_1 integral is well behaved. All we need to see that explicitly, is a suitable change of variables to cancel the $x = 1$ pole. In fact, if we choose:

$$x = \cosh\xi$$

with

$$\xi_{min(max)} = ln\left[x_{min(max)} + \sqrt{x^2_{min(max)} - 1}\right]$$

then

$$dx = \sinh\xi\, d\xi = (x^2-1)^{\frac{1}{2}}\, d\xi$$

and

$$\frac{dx}{x(x^2-1)^{\frac{1}{2}}} = \frac{d\xi}{\cosh\xi}$$

so that the pole at $x = 1$ is indeed absorbed.

On the other hand, I_2 needs more careful treatment. In this case the cancellation of the pole at $x = 1$ is more subtle, as it is due to an extra $(x^2-1)^{\frac{1}{2}}$ factor in the numerator coming from the behaviour of the limits of the θ-integration as $x \rightarrow 1$. To see how this happens, let us consider (without loss of generality) the case when $f = 1$.

If we change variables according to:

$$\theta \longrightarrow \psi = \frac{\pi}{2} - \theta$$

then (using eq.III.4.4)

$$\cos\psi = \sin\theta = 1 - \frac{(x-1)(1-y)}{x+y} \qquad \text{III.4.6}$$

We then expand in a power series:

$$\cos\psi = 1 - \frac{1}{2}\psi^2 + \ldots \qquad \text{III.4.7}$$

and note that ψ and $y(\theta)$ have opposite limits.

From eqs.III.4.5 and 6 we can write:

$$1 - \frac{1}{2}\psi_{max}^2 = 1 - \frac{(x-1)(1-y_{min})}{x+y_{min}}$$

$$1 - \frac{1}{2}\psi_{min}^2 = 1 - \frac{(x-1)(1-y_{max})}{x+y_{max}}$$

We recall that if $y_{max} = Y$ then $y_{min} = -Y$ thus:

$$\psi_{max} = \left[\frac{2(x-1)(1+Y)}{x-Y}\right]^{\frac{1}{2}} \quad , \quad \psi_{min} = \left[\frac{2(x-1)(1-Y)}{x+Y}\right]^{\frac{1}{2}}$$

Therefore:

$$\psi_{max} - \psi_{min} = (x-1)^{\frac{1}{2}} \left[\left(\frac{2(1+Y)}{x-Y}\right)^{\frac{1}{2}} - \left(\frac{2(1-Y)}{x+Y}\right)^{\frac{1}{2}}\right]$$

and the pole at $x = 1$ is cancelled:

$$\phi(x) = \frac{\psi_{max} - \psi_{min}}{(x^2-1)^{\frac{1}{2}}} = \left[\frac{2}{x+1}\right]^{\frac{1}{2}} \left[\left(\frac{1+Y}{x-Y}\right)^{\frac{1}{2}} - \left(\frac{1-Y}{x+Y}\right)^{\frac{1}{2}}\right]$$

The above analysis leads us to introduce our last change of variables:

$$\omega = \frac{\frac{\pi}{2} - \theta}{(x^2-1)^{\frac{1}{2}}} \quad , \quad \sin\theta = \cos\left[\omega(x^2-1)^{\frac{1}{2}}\right] \qquad \text{III.4.8}$$

with the ω-limits determined from the θ-limits, for all values of x, unless $x = 1$, in which case:

$$\omega_{min} = \left[\frac{1-Y}{1+Y}\right]^{\frac{1}{2}} \quad , \quad \omega_{max} = \left[\frac{1+Y}{1-Y}\right]^{\frac{1}{2}} \qquad \text{III.4.9}$$

and the cross-section finally reads:

$$\frac{1}{\sigma_0}\frac{d\sigma^{(2)}}{dQ_T^2} = \frac{4}{\pi Q_T^2} \int_{\xi_{min}}^{\xi_{max}} \frac{d\xi}{\cosh\xi} \int_{\omega_{min}}^{\omega_{max}} d\omega\, f(k_{T_1})\, f(k_{T_2})$$

which is explicitly finite.

The limits of the integration are given by eqs.III.4.5 and III.4.9, while k_{T_1}, k_{T_2} are expressed in terms of the variables ξ, ω via eqs. III.4.1, 4, 5 and 8.

III.5 RESULTS AND DISCUSSION.

Now that our integrals are perfectly finite, with all singularities under control, we can numerically calculate the two gluon contribution to the four-jet cross-section. We present here our results for $d\sigma^{(2)}/\sigma_0 dQ_T^2$, where Q_T is defined with respect to the quark or antiqurk with the largest thrust, so that we use eq.II.2.8 as our input for $d\sigma^{(1)}/\sigma_0 dQ_T^2$.

Our results will depend on the following parameters:

a] The centre-of-mass energy (mass of the virtual photon)
We choose to work at $Q = 100\text{GeV}$

b] The choice of the cuts which define a hadron jet from a mass of hadrons. Theoretically, these cuts can have any non-zero value, while experimentally, they must be specified with regard to the experimental acceptances.Typically, UA1 for instance, impose: (see also §III.3.4) [ref.III.8]

$$p_T^{min} = 20\,\text{GeV} \qquad \text{at} \qquad \sqrt{s} = 640\,\text{Gev}$$

and

$$\cos\theta_0 = 0.9$$

We repeat our calculation for the following values of the cut-parameters:

$k_0 = 1,\ 4,\ 6,\ 10\,\text{GeV}$ Fig.III.5.1,2,3,4

$\cos\theta_0 = 0.75,\ 0.90,\ 0.99$ Fig.III.5.2,5,6

c] The way the coupling constant runs

The choice of the scale in the running formula for the coupling constant has been the subject of great theoretical dispute in the past, and the following choices have been proposed:

(i) The scale is set by the total energy of the process, i.e. $\alpha_s^2 = \alpha_s^2(Q^2)$ which effectively fixes α_s (Fig. III.5.2).

(ii) In calculations of transverse momentum distibutions, the scale is set by the overall Q_T : $\alpha_s^2 = \alpha_s^2(Q_T^2)$ (Fig. III.5.7).

(iii) The fact that we allow two gluons to balance the total transverse momentum, suggests that the scale is set by each individual gluon, that is : $\alpha_s^2 = \alpha_s(k_{T_1})\,\alpha_s(k_{T_2})$ (Fig. III.5.8).

The suggestion for using gluon transverse momenta k_T^2 in the argument of α_s has its origin in the resummation of large logarithmic corrections which modify the Altarelli-Parisi evolution equation of naive perturbative QCD [ref.III.9].

However, it has been emphasized by Pennington, Roberts and Ross [ref. III.10], that in time-like processes like e^+e^- annihilation, when next-to-leading corrections are included, large π^2-terms do occur at $O(\alpha_s^2)$ and above which can be resummed, if the $\ln k_T^2/Q^2$ term in the formula for the running coupling is replaced by $[\ln^2 k_T^2/Q^2 + \pi^2]^{1/2}$. These resummed π^2-terms represent corrections of order $O(\alpha_s^3(Q^2))$ and give eq.III.5.a the following properties: [ref.III.11]

α] It 'freezes' the running coupling at a constant value as $k_T^2 \rightarrow 0$,

β] it allows perturbative QCD to be used without requiring:

$$\alpha_s(Q^2) \ll 1 \quad \text{and} \quad \alpha_s(Q^2) \ln k_T^2/Q^2 \ll 1$$

γ] it has been used successfully to extract the value of Λ_{QCD} from various sets of data (a procedure which is very sensitive to second and higher order terms) [ref. III.12] (see also chapter IV).

In the light of the above remarks, we let the following formula to govern the running of α_s

$$\alpha_s(\chi^2) = \frac{4\pi}{\beta_0\sqrt{ln^2\left(\frac{\chi^2}{\Lambda^2_{QCD}}+1\right)+\pi^2}}$$

where

$$\beta_0 = 11 - \frac{2N_F}{3}$$

N_f being the number of flavours

and

$$\Lambda_{QCD} = 0.2 \quad \text{and} \quad 0.5\,\text{GeV} \qquad \text{Fig.III.5.8,9}$$

III.5.1 Comparison with the full answer.

The two gluon emission contribution we consider here is a key pointer to the accuracy of the summation of many gluons that we have seen is needed to describe experiment in the small Q_T region. Since it is only the one and two gluon emissions that have been calculated exactly, these low order calculations must serve as a guide to the multigluon contributions. In order to check the accuracy of our approximate model, we now compare our results with the full two gluon emission cross-section. By doing so, we determine the kinematic region and the range of values of the parameters introduced in the last section for which our model is most likely to be a good approximation to the fixed order result.

The full two gluon cross-section has been evaluated [ref.III.13] using a Monte-Carlo generation of events using the matrix elements of ref.[III.14] and imposing identical cuts with the ones we considered in the I E A model. In this case, these cuts play a more important role. They not only guarantee four distinct jets in the final state, but also serve to regularize the infrared and collinear singularities of the full perturbative calculation.

To write down the expressions for the matrix elements, we first introduce the following notation for the four-momenta and helicities of the particles in the process:

$$e^+(p_+) + e^-(p_-) \rightarrow \bar{q}(k_3) + q(k_4) + g(k_1) + g(k_2)$$

Let $M(\lambda_1, \lambda_2, \lambda_3, \lambda_4, \lambda_5, \lambda_6)$ denote the helicity amplitude with λ_1 the helicity for the e^+ , λ_2 the one for e^- , λ_3 for $\bar{q}$, λ_4 for q , λ_5 the one for $g(k_1)$ and λ_6 for $g(k_2)$.

The helicities of the leptons must necessarily be opposite, because of the $\frac{(1\pm\gamma_5)}{2}$ projection operators, and the same holds for the quarks. A non-zero helicity amplitude is then $M(-,+,-,+,-,-)$ for which we have:

$$|M(-,+,-,+,-,-)|^2 = \left[\frac{(N^2-1)}{2N}\right] \frac{Q_f^2 e^4 g^4}{A} k_{4-}^2 (k_3 k_4) \times$$

$$\times \left[N^2\Big((k_1k_3)(k_2k_4) + (k_1k_4)(k_2k_3)\Big) - (k_1k_2)(k_3k_4)\right] \qquad \text{III.5.1}$$

where Q_f is the fractional quark charge and g is the SU(N) gauge coupling constant. (k_ik_j) is the dot product of four-vectros k_i and k_j, while A is given by:

$$A = (k_1k_2)(k_1k_3)(k_1k_4)(k_2k_3)(k_2k_4)(k_3k_4)$$

Working in the e^+e^- centre-of-mass frame, with the z-direction along p_+, the following notation has been introduced:

$$k_\pm = k_0 \pm k_z \qquad \text{and} \qquad k_\perp = k_x + \mathrm{i}k_y$$

for any vector k.

All other non-zero helicity amplitudes, for which the gluon helicities are equal, have the same structure as in eq.III.5.1. They only differ in the appearance of k_{3+}, k_{3-} or k_{4+} instead of k_{4-}.

On the other hand, the helicity amplitudes with opposite helicities for the gluons are generated by the expression:

$$|M(-,+,-,+,-,+)|^2 = \left[\frac{(N^2-1)}{128N}\right] \left[\frac{Q_f^2 e^4 g^4}{A}\right] \times$$

$$\times \left[\frac{k_3 k_4}{E^2(k_1 k_2) k_{1+}^2 k_{2-}^2 k_{3+} k_{4-}}\right] \left[(N^2-2)|c_1+c_2|^2 + N^2|c_1-c_2|^2\right] \qquad \text{III.5.2}$$

where:

E : the beam energy

$$c_1 = |\alpha|^2 + \left[\frac{k_2 k_4}{2E(E-k1_{30})}\right]\alpha\beta + \left[\frac{k_1 k_3}{2E(E-k_{40})}\right]\alpha^*\gamma$$

$$c_2 = \beta\gamma + \left[\frac{k_1 k_4}{2E(E-k_{30})}\right]\alpha\beta + \left[\frac{k_2 k_3}{2E(E-k_{40})}\right]\alpha^*\gamma$$

$$\alpha = Z_{12}Z_{34} - Z_{14}Z_{32}$$

$$\beta = Z_{32}^*[Z_{12}^* + Z_{14}^*]$$

$$\gamma = Z_{14}[Z_{12} + Z_{32}]$$

$$Z_{ij} = k_{i+}k_{j-} - k_{i\perp}^* k_{j\perp} \quad , \quad i,j = 1,2,3,4$$

Of course, the remaining non-zero helicity amplitudes, with opposite gluon helicities, can all be obtained from eq.III.5.2, by interchanging k_1 and k_2, and/or k_3 and k_4.

To obtain the four-jet cross-section, one must sum all the absolute squared values of the helicity amplitudes, perform the colour sum, average over the initial lepton helicities, symmetrize appropriately for identical gluons and sum over quark flavours.

So that:

$$d\sigma(four.jet) = \frac{\delta^4(p_+ + p_- - k_1 - k_2 - k_3 - k_4)}{128E^2(2\pi)^8} |\bar{M}_g|^2 \frac{d^3\mathbf{k}_1 d^3\mathbf{k}_2 d^3\mathbf{k}_3 d^3\mathbf{k}_4}{k_{10}k_{20}k_{30}k_{40}}$$

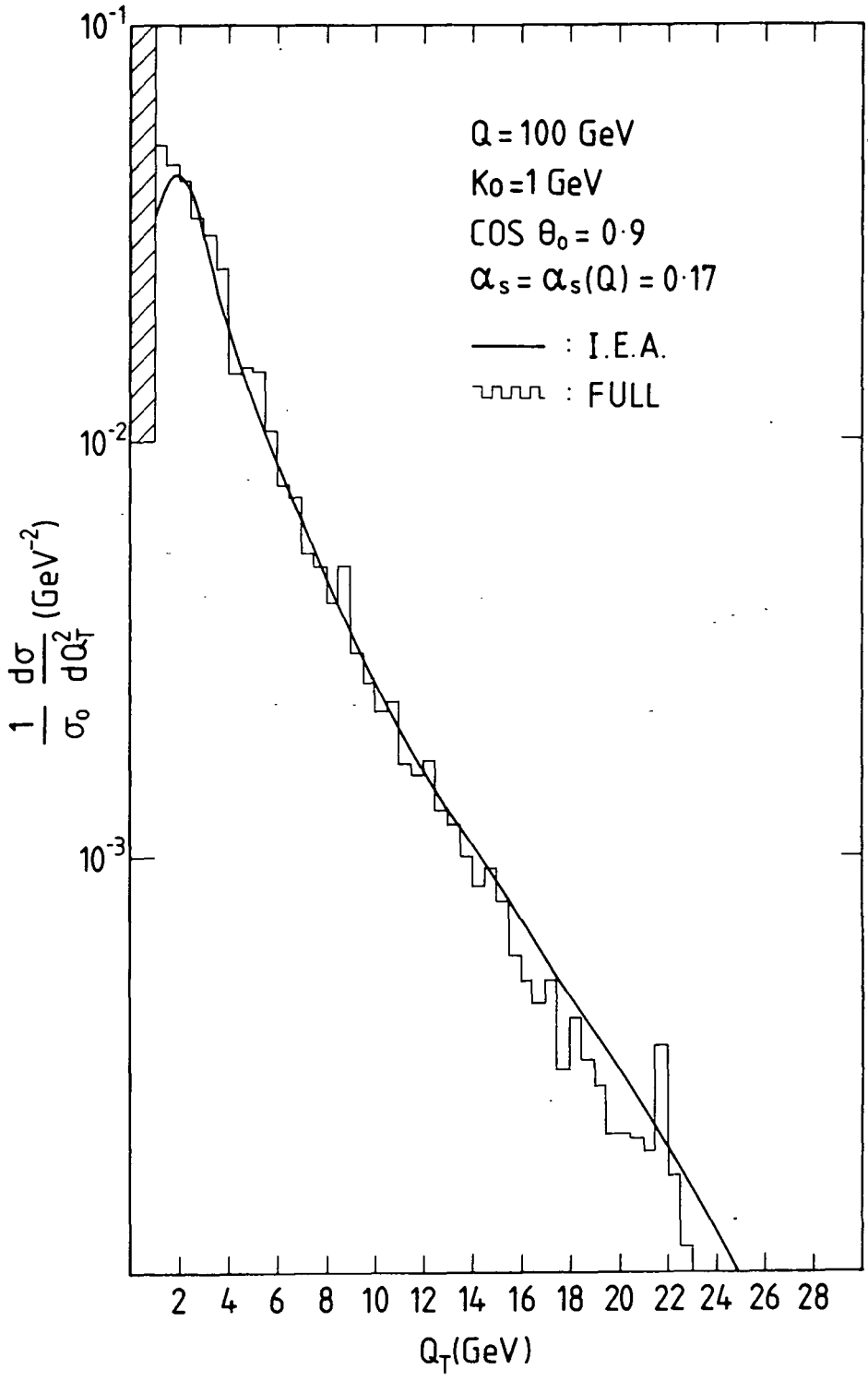

Figure III.5.1

Q_T-distribution of a four-jet enent in electron-positron annihilation. Comparison of IEA with the full QCD result.

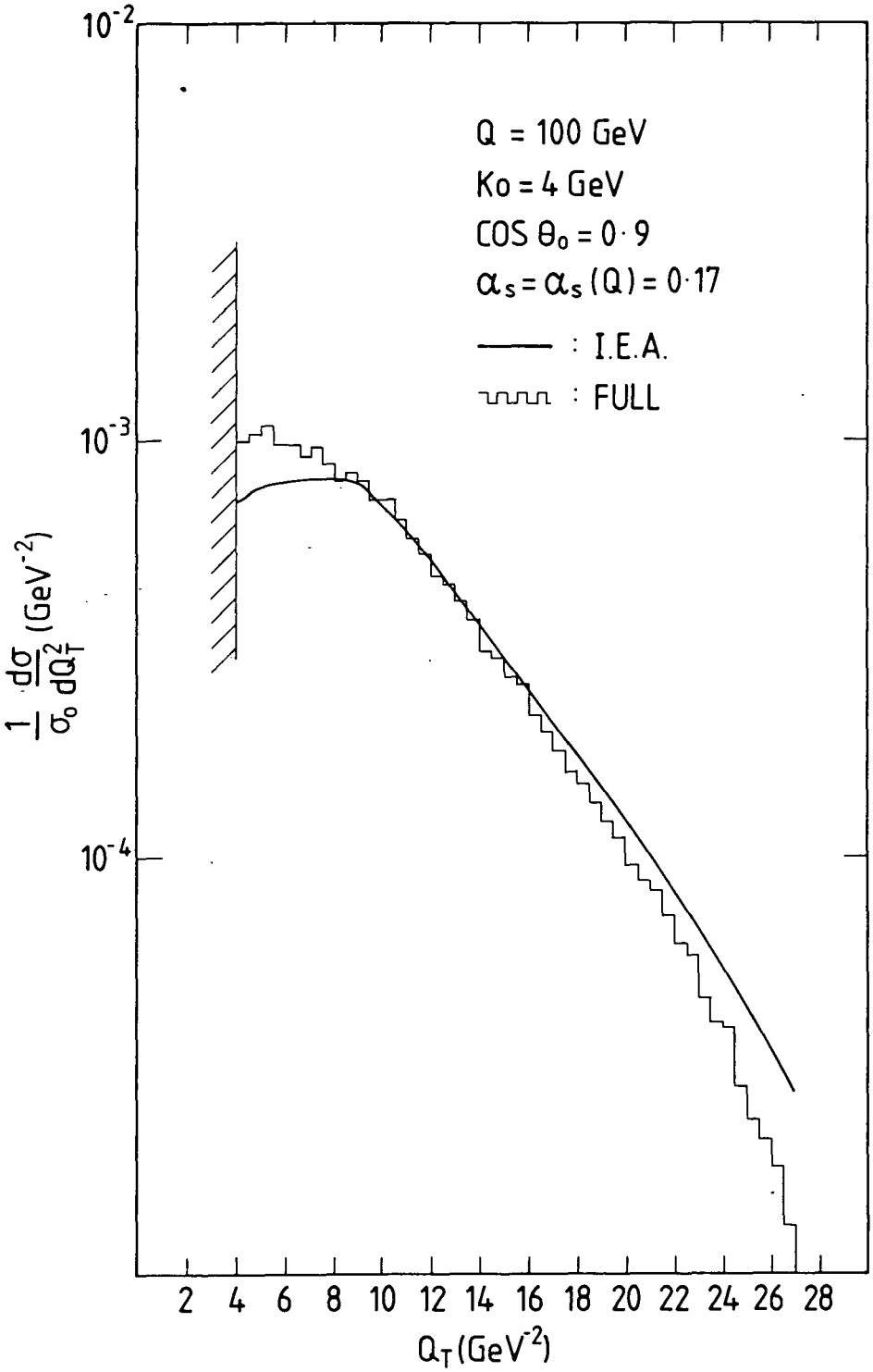

Figure III.5.2

Q_T-distribution of a four-jet enent in electron-positron annihilation. Comparison of IEA with the full QCD result.

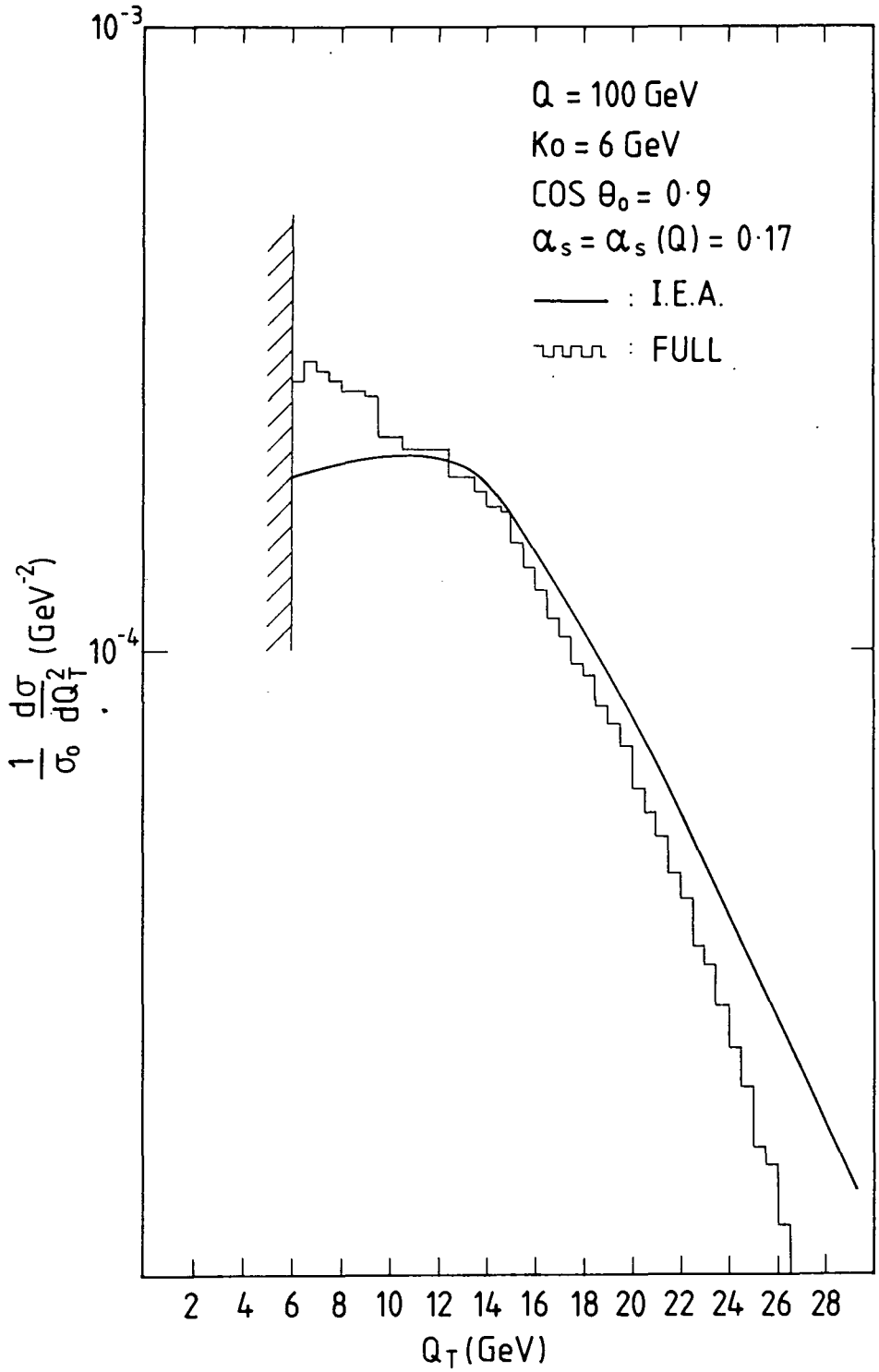

Figure III.5.3

Q_T-distribution of a four-jet enent in electron-positron annihilation. Comparison of IEA with the full QCD result.

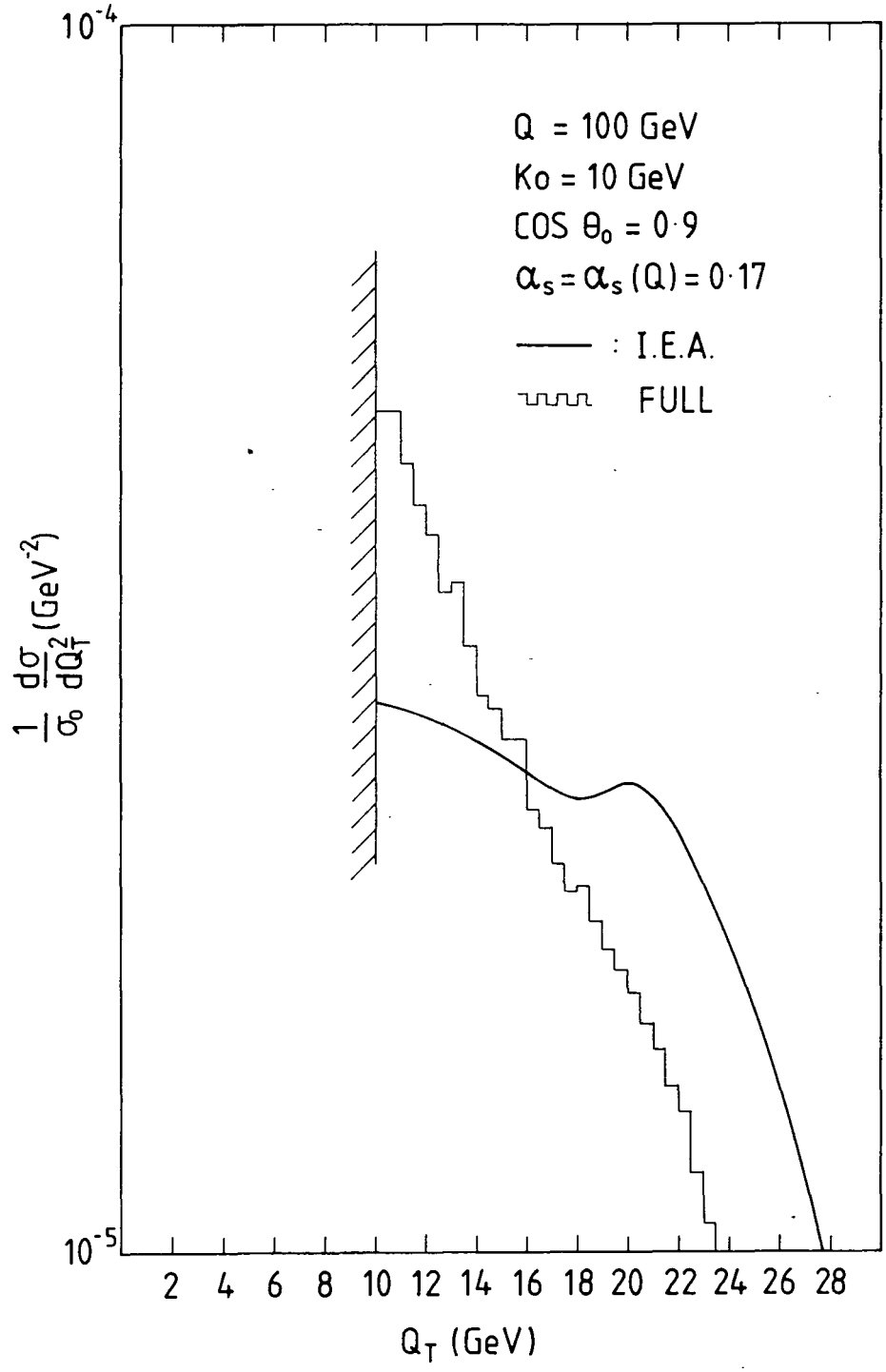

Figure III.5.4

Q_T-distribution of a four-jet enent in electron-positron annihilation. Comparison of IEA with the full QCD result.

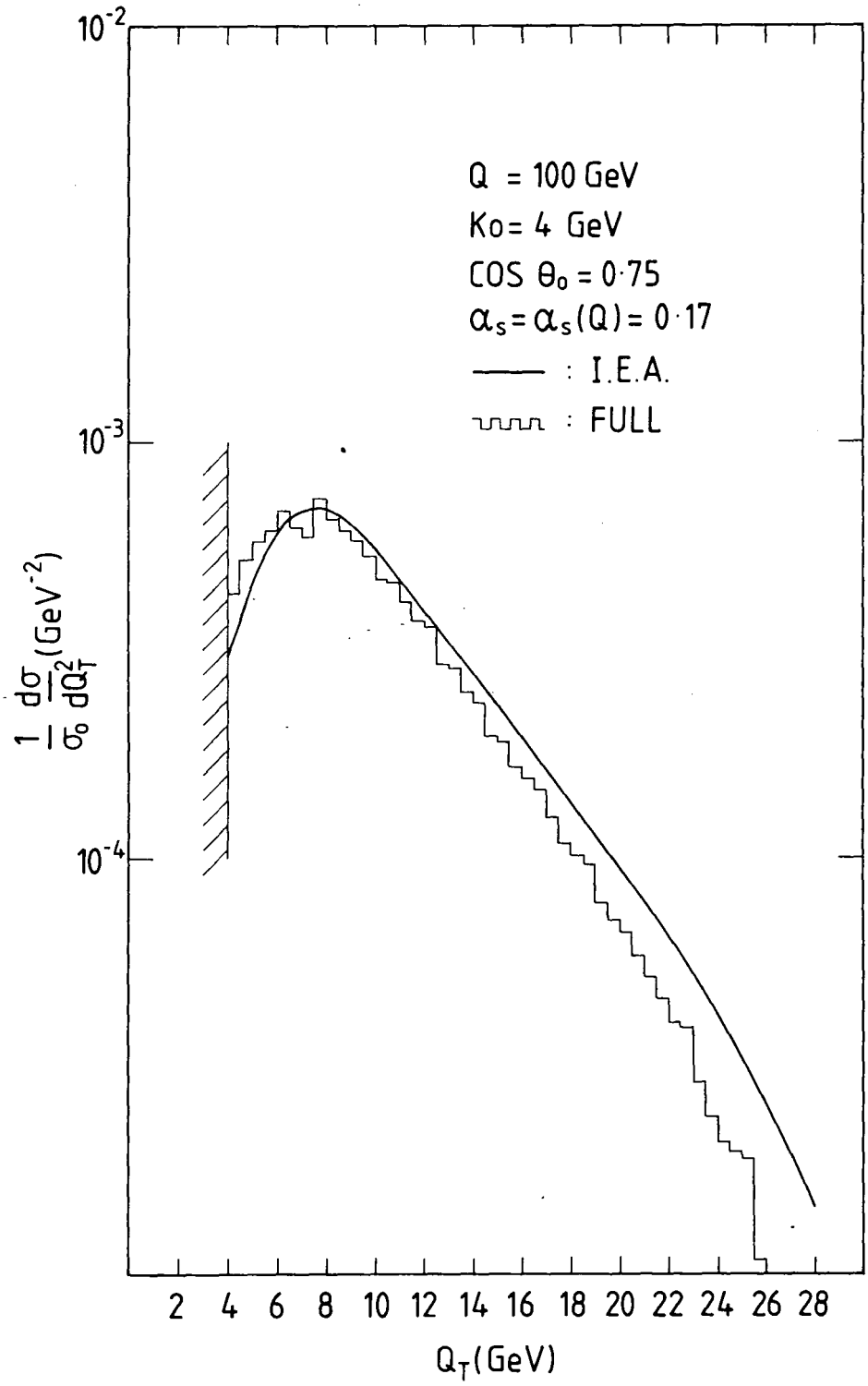

Figure III.5.5

Q_T-distribution of a four-jet enent in electron-positron annihilation. Comparison of IEA with the full QCD result.

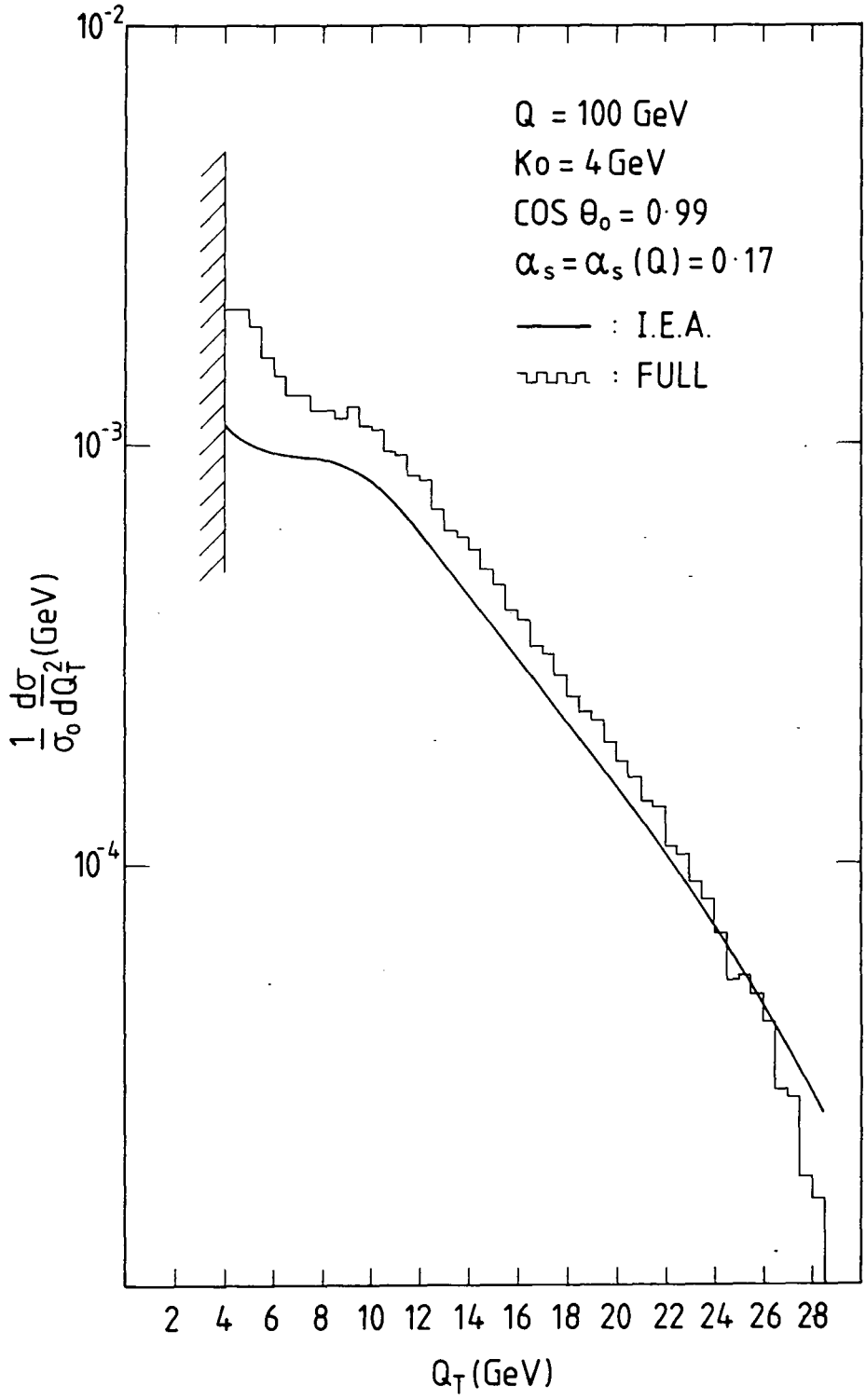

Figure III.5.6

Q_T-distribution of a four-jet enent in electron-positron annihilation. Comparison of IEA with the full QCD result.

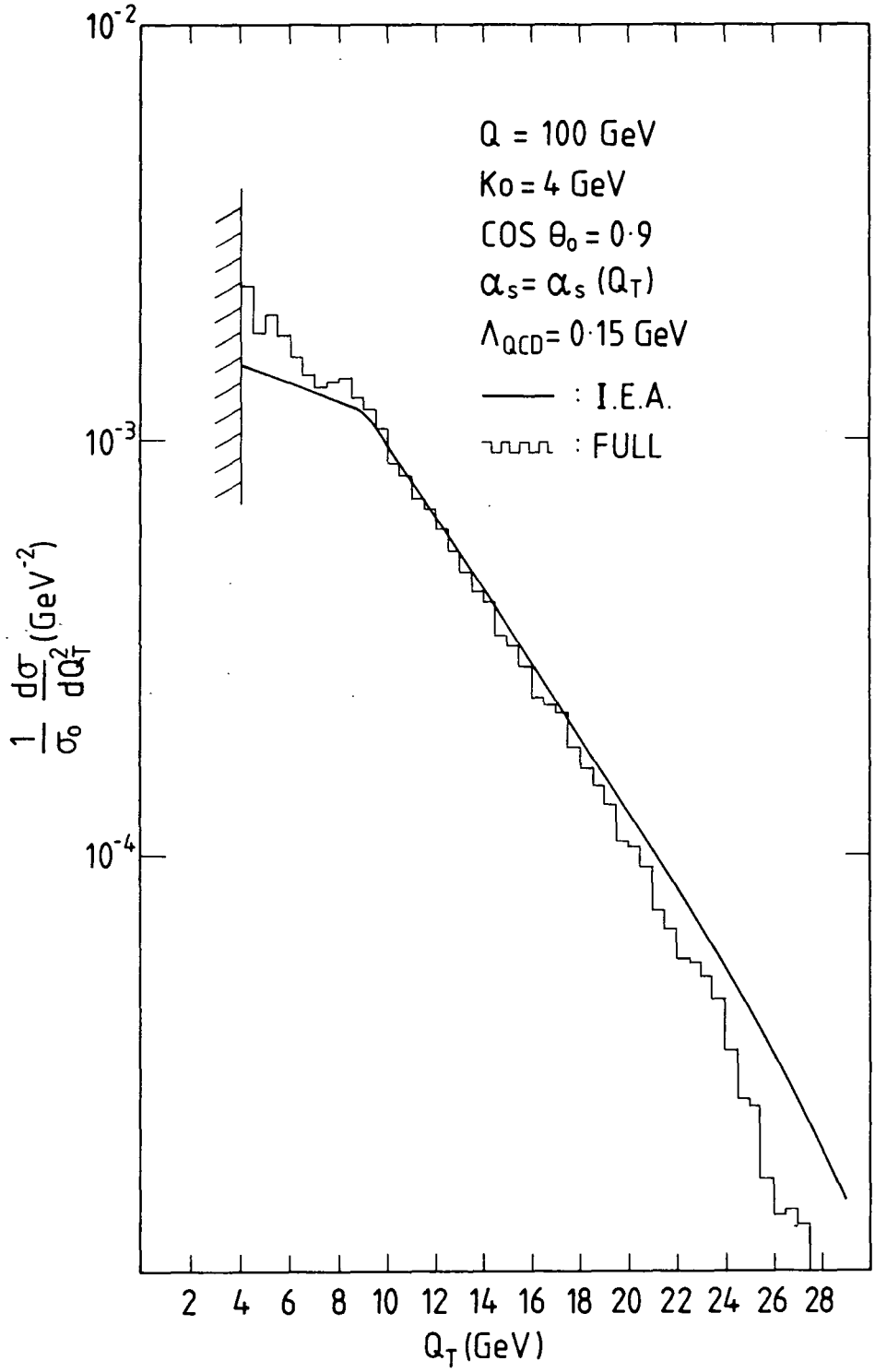

Figure III.5.7

Q_T-distribution of a four-jet enent in electron-positron annihilation. Comparison of IEA with the full QCD result.

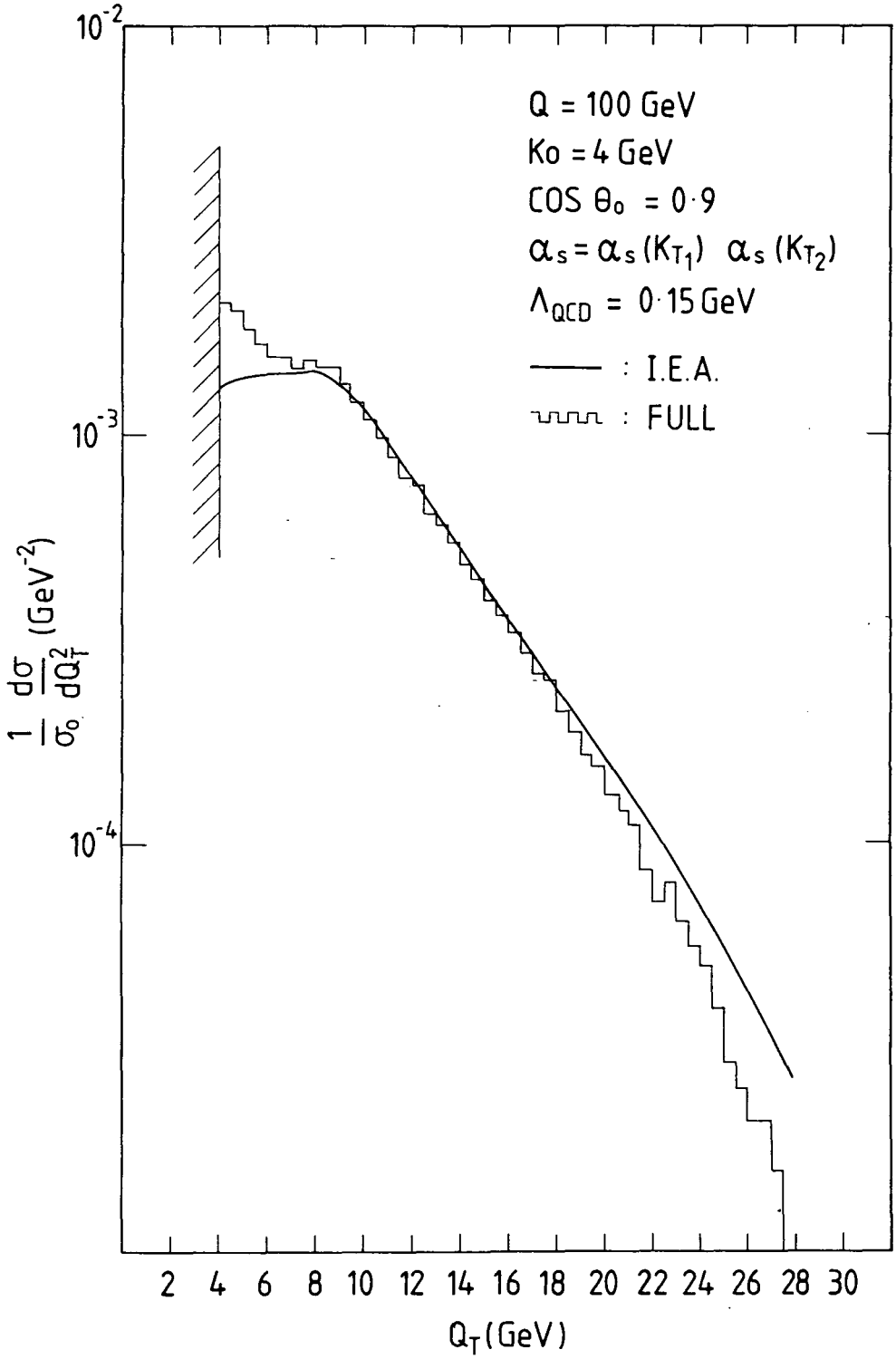

Figure III.5.8

Q_T-distribution of a four-jet enent in electron-positron annihilation. Comparison of IEA with the full QCD result.

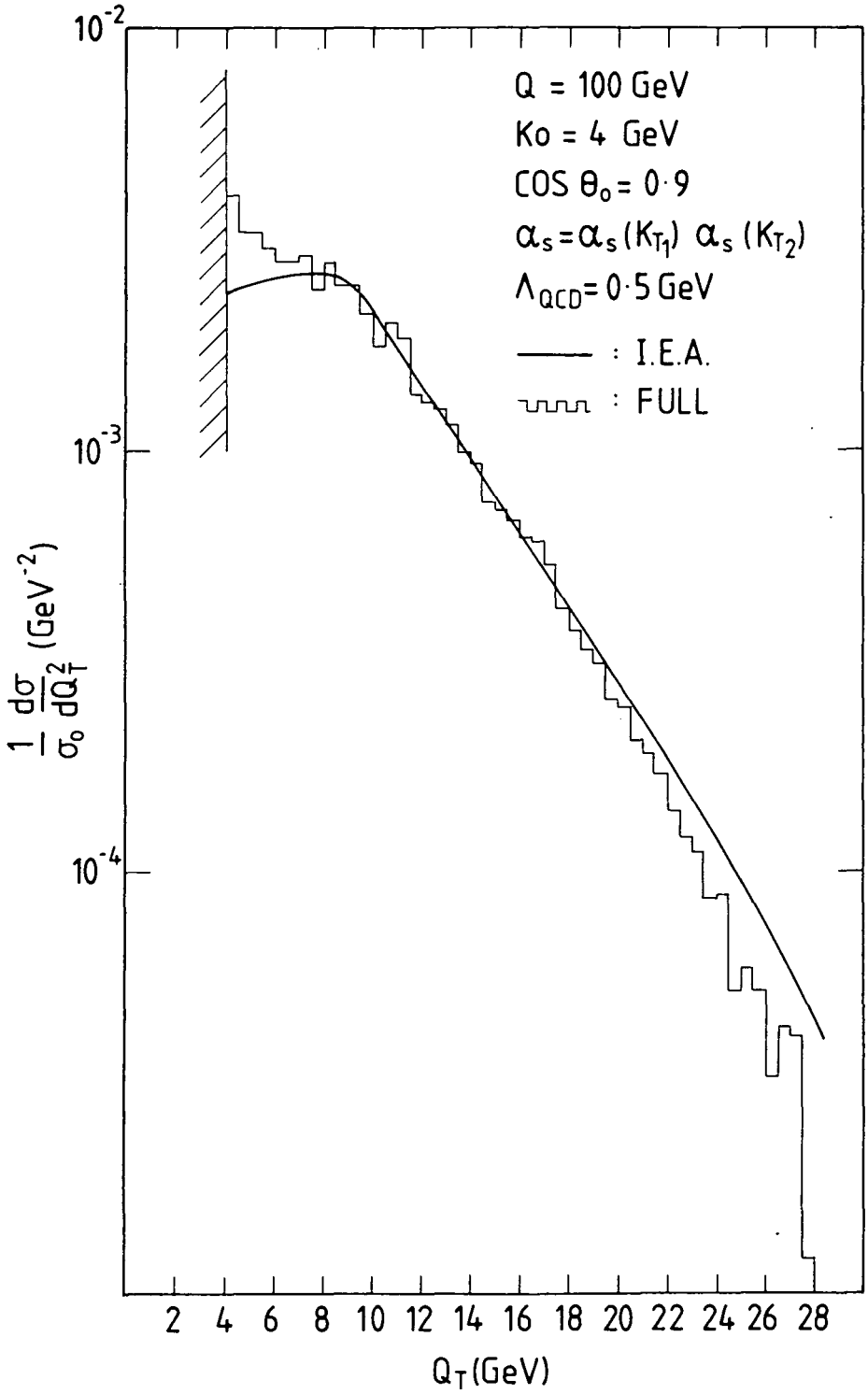

Figure III.5.9

Q_T-distribution of a four-jet enent in electron-positron annihilation. Comparison of IEA with the full QCD result.

III.5.2 Dependence on the choice of parameters.

a] Dependence on Q_T

We found that for fixed k_0 , θ_0 , the I E A model agrees remarkably well with the full answer in the region (for Q=100 GeV) :

$$2k_0 \quad \leq \quad Q_T \quad \leq \quad 20\,\mathrm{GeV} \qquad \text{III.5.3}$$

remembering $Q_T^{max} = Q/2\sqrt{3} \sim 28.9$ GeV in this case. This agreement is almost independent of the way the coupling constant runs! The above statement can be understood in the light of the following observations:

(i) I E A breaks down at large values of transverse momenta (because the gluons cannot be seen as independently emitted anymore) so that no agreement is expected as we approach large values of Q_T towards the edge of the phase space. Also note that at large Q_T, the Monte Carlo generation has the correct kinematic limit, whereas the the IEA ansatz allows the transverse momentum of *each* gluon to reach this limit separately and so their vector sum can exceed the kinematic bound on Q_T.

(ii) As we move towards the other end of the phase space (small transverse momenta) the full result is approaching its collinear gluon singularities, as the triple gluon interactions included in it become increasingly important. On the other hand, I E A is rather suppressed by non-leading contributions, as large transverse momenta for the individual gluons are needed to balance the small total Q_T.

(iii) Finally, we note that as we move from the $Q_T \leq 2k_0$ region to the $Q_T \geq 2k_0$ region, new configurations with leading contributions take over, to give rise to the peak at $Q_T = 2k_0$.

b] Dependence on k_0

As mentioned above, the region of best agreement between the I E A model and the full answer is given by eq.III.5.3. That is the smaller the value of k_0, the bigger the region of agreement.

Recall that k_0, being a transverse momentum cut, removes more phase space than necessary, so that we need to go to rather small values of k_0 in order to make the removed area of phase space comparable with the one removed by the $\epsilon Q/2$ cut. However, we do not want to go to *very* small values of k_0, if we want to avoid soft singularities and stay close to the experimental values of cuts.

c] Dependence on θ_0

The agreement seems to be best for a moderate value of θ_0 (namely $\cos\theta_0 \sim 0.9$), which is not very different from the experimentally favoured values for the δ-angle, introduced by Sterman and Weinberg.

It should be pointed out here, that the I E A cross-section remains finite in the limit $\cos\theta_0 \to 1$ (as it is free of collinear gluon singularities) whereas the full result diverges in the same limit, as a result of these singularities from graphs containing triple gluon interactions. Though these singularities are removed by the cut in $\cos\theta$, eq.II.3.4, the smaller θ_0 is, the more closely these are felt, as apparent from the curves in fig.III.5.1,5 and 6.

d] Dependence on α_s

Recall that we considered the following possibilities for the momentum dependence of the running coupling constant α_s (§III.5):

(i) $\alpha_s^2 = \alpha_s^2(Q^2)$ (essentially a fixed α_s)

(ii) $\alpha_s^2 = \alpha_s^2(Q_T^2)$ (scale set by the total Q_T)

(iii) $\alpha_s^2 = \alpha_s(k_{T_1}^2)\,\alpha_s(k_{T_2}^2)$ (each gluon emitted sets its own scale)

It is perhaps surprising, but we found the agreement of the I E A model with the full result to be rather insensitive to this freedom in the choice of the scale, and this statement seems independent of the values of the parameters Λ_{QCD} , β_0, etc. However, it should be noted that for the purpose of comparing the two results, choices (i) and (ii) are effectively the same, as (ii) only multiplies (i) by the same factor in both cases.

III.6 SUMMARY OF CHAPTER III.

In this chapter, we have set up a model for quick and reliable calculations of multigluon cross-sections in $e^+e^- \rightarrow q\bar{q} + (ng)$. The model is based on the approximation that the gluons are emitted independently (apart from momentum conservation) and it is particularly useful for calculating momentum distributions in the multijet case.

To ascertain when and where such a model is a good approximation to the fixed order result, we looked at two-gluon emission in some detail. To ensure that our final state particles are well defined and well separated in phase space, we imposed suitable cuts, namely that each parton has a minimum transverse momentum and that there is a minimum angular separation between each pair. Identical cuts were implemented for the full two-gluon distribution, obtained by a Monte-Carlo generation of events using the exact matrix elements.

The comparison of the two results helped to identify the kinematic region in which our model is most likely to be reliable and to determine the choice of the various parameters (k_0 , $\theta_0 \ldots$) for maximal agreement.

CHAPTER IV I E A IN PRACTICE

IV.1 INTRODUCTION

In the last chapter, we justified the use of a simple model (based on the approximation of independently emitted gluons) for quick and reliable calculations of multijet cross-sections. The calculation of the four-jet cross-section in electron-positron annihilation was the first application of this model. Its predictions were successfully compared with the exact results obtained using a Monte Carlo generation of events, according to the full matrix elements.

In this chapter, we explore the possibility of using our model in other processes which are not very different from the one described in the last chapter. The comparison of our results with the full ones will serve as further tests of its potential to be used as a tool to study the structure of multijet final states, thus providing us with some answers to the main theoretical questions formulated in §II.1.2.

First of all, we recall that independent emission means that the gluons necessarily do not interact with each other so that the approximation is of an essentially Abelian theory. This suggests we to compare the IEA results with the exact ones obtained in an 'Abelian QCD' theory. Then we use the IEA formalism to calculate distributions in other variables that have been proposed to describe the multijet structure of the final hadronic state in e^+e^- annihilation. Finally, we compare IEA predictions for multijet cross-sections with the more exact ones obtained using an algorithm that has been recently proposed by Altarelli *et. al.* for calculating transverse momentum distributions.

IV.2 ABELIAN Q C D TESTS

As has already been emphasized (§II.3.1), our assumption of independent multigluon emissions requires that gluons do *not* interact with each other, so that no triple gluon graphs are included in our analysis of multijet cross-sections. Remembering that the gluon self-interaction is one of the most characteristic manifestations of the non-Abelian nature of QCD, this means that our approximation is that of an essentially Abelian theory! Therefore, we would expect our model to agree better with the exact results obtained in an Abelian QCD (QCD with massless and colourless quarks, which is gauge invariant in itself).

In this section, we compare the four-jet cross-section we obtained in our model (which is already Abelian!) with the full one, derived using the Abelian limit of the matrix element. This limit is realized by the following substitutions in the expression for the non-Abelian matrix element (eq.III.4.1,2) [ref.III.15]

$$C_F \to 1 \quad , \quad C_A \to 0 \quad \text{and} \quad N_c \to 1$$

To make the comparison of the results straightforward, we redefine the coupling constant:

$$\alpha_s(\text{Abelian}) \quad = \quad \frac{4}{3} \quad \alpha_s(\text{non} - \text{Abelian})$$

and also take into account the fact that for colourless quarks the pointlike cross-section σ_0 is normalized according to:

$$\sigma_0(\text{Abelian}) \quad = \quad \frac{1}{3} \quad \sigma_0(\text{non} - \text{Abelian})$$

We then repeat the calculations of the last chapter for the following values of the jet-defining parameters:

$$k_0 \quad = \quad 4\,,\,10\,GeV \qquad \text{Fig. IV.2.1, 2, 4}$$

$$\cos\theta_0 \quad = \quad 0.9 \quad , \quad 0.99 \qquad \text{Fig. IV.2.2, 3}$$

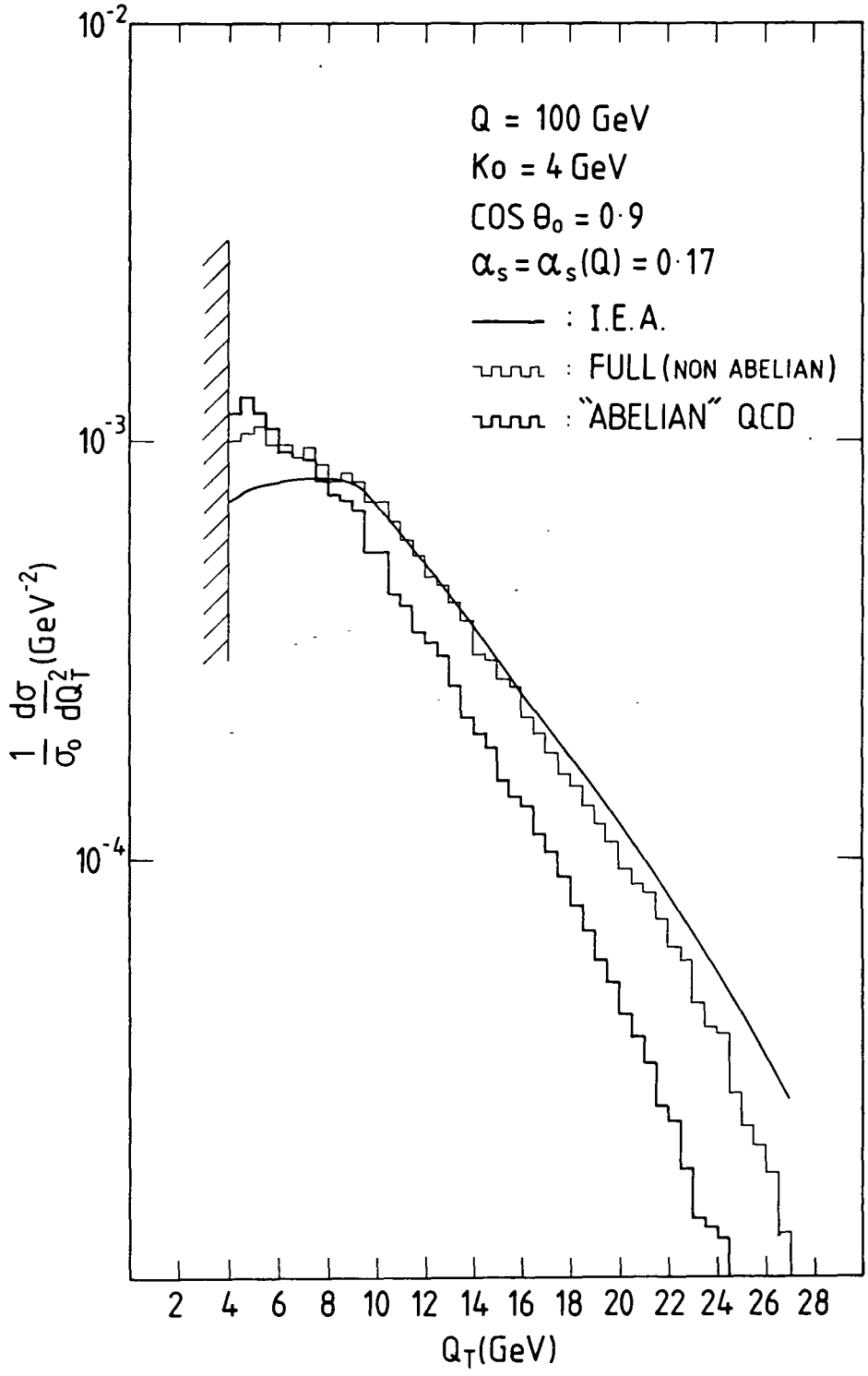

Figure IV.2.1

Q_T-distribution of a four-jet event in electron-positron annihilation. IEA compared with an Abelian QCD theory.

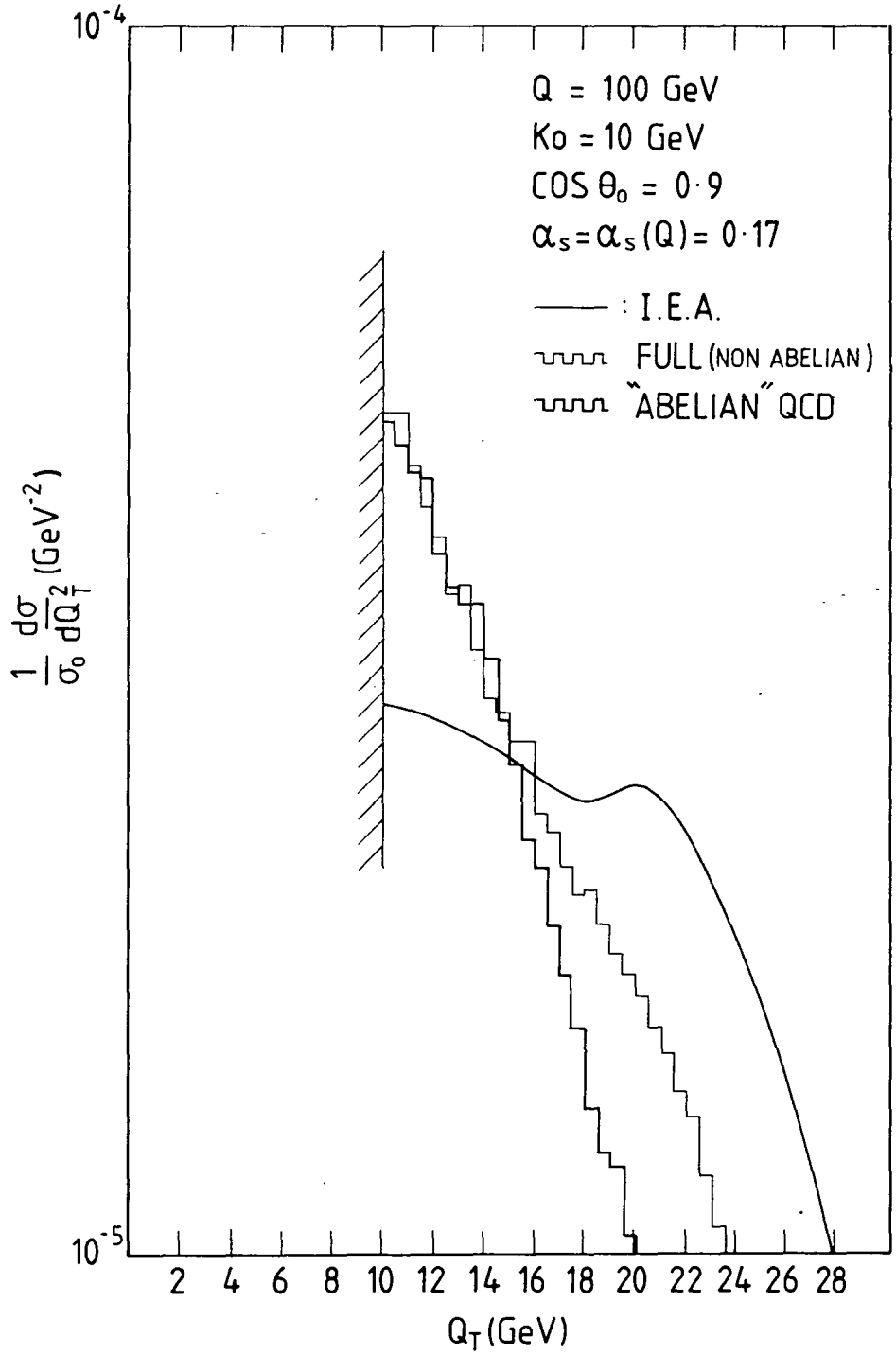

Figure IV.2.2

Q_T-distribution of a four-jet event in electron-positron annihilation. IEA compared with an Abelian QCD theory.

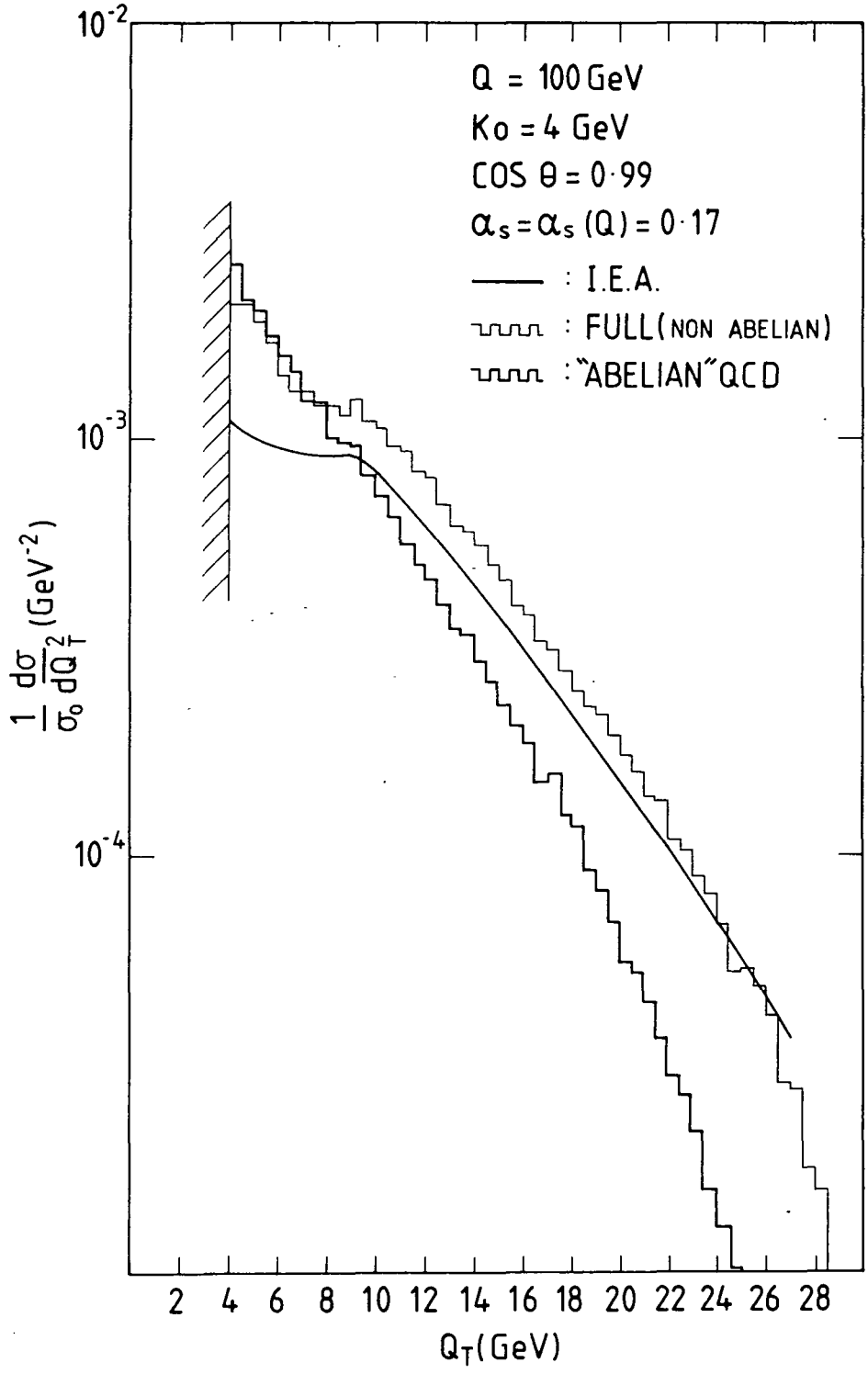

Figure IV.2.3

Q_T-distribution of a four-jet event in electron-positron annihilation. IEA compared with an Abelian QCD theory.

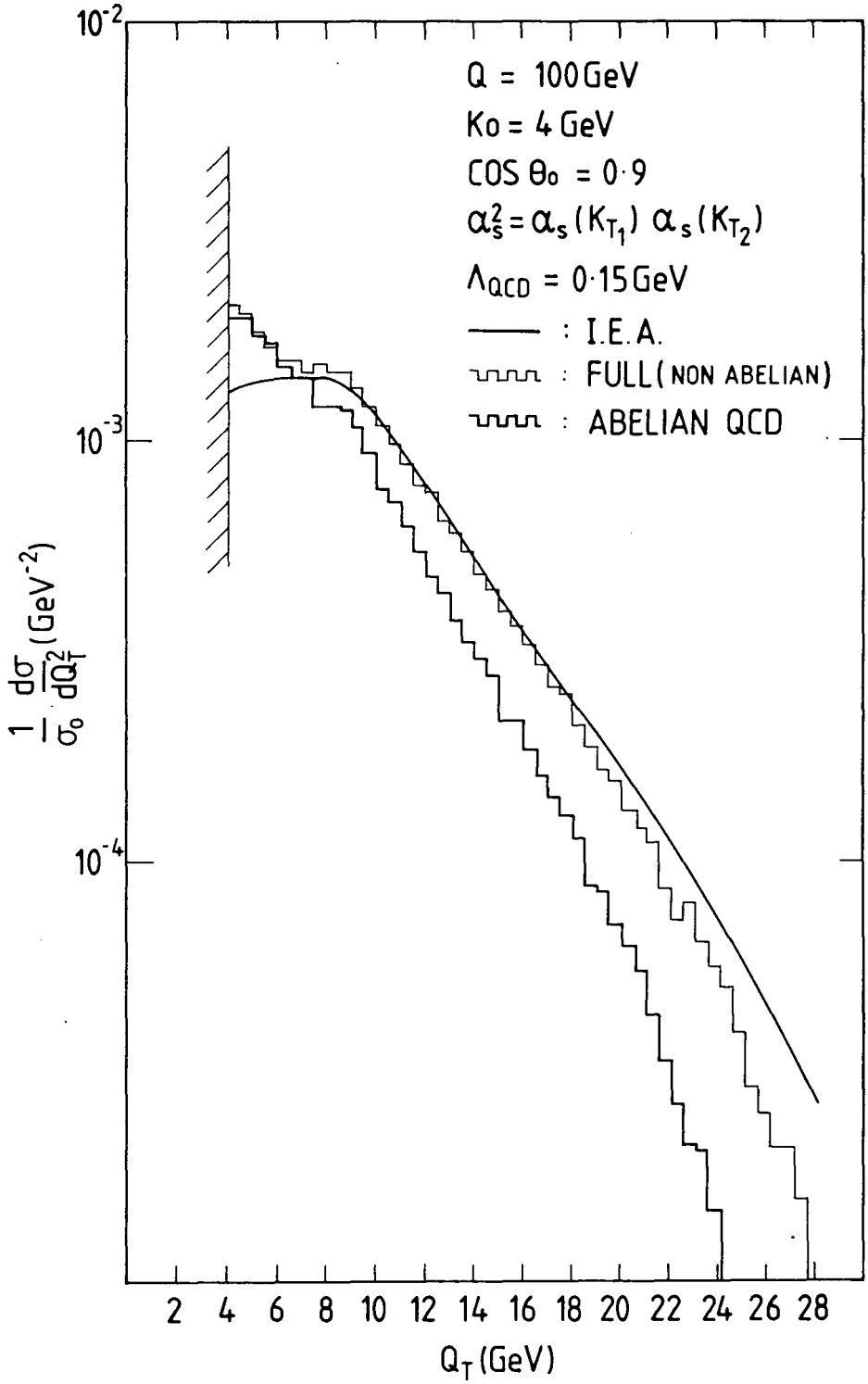

Figure IV.2.4

Q_T-distribution of a four-jet event in electron-positron annihilation. IEA compared with an Abelian QCD theory.

It is then quite surprising to note that there does not seem to be any agreement between IEA and Abelian QCD. Recall that, for the same values of the jet-defining cuts, there was a kinematic region (eq.III.5.3) in which IEA results agreed remarkably well with the exact, non-Abelian answer and that this agreement was expected to improve in the Abelian limit. Instead, it has become worse. So we have to address the question: Why does IEA tend to agree with non-Abelian results rather than Abelian ones? Looking for an explanation, we examine the following possibilities:

a] The agreement between IEA and non-Abelian QCD is just a coincidence and our 'soft' approximation to the full gluon emission matrix element is not valid. A more careful analysis of the effect of non-leading terms which are not already included in IEA is needed before the validity of the approximation is justified.

b] Q_T is *not* the appropriate variable to study the jet structure of the final-state hadrons! It has been pointed out [ref. II.17] that, while non-leading contributions associated with an exact treatment of transverse momentum conservation are included in IEA (see §II.3.3), there are further non-leading contributions associated with energy conservation, which may have significant influence but are more difficult yet to treat precisely! (The use of other variables to describe multijet final states in IEA is studied in some detail later on in this chapter).

c] A more careful investigation of the diagram structure of our model is needed. Recall that when we add and square the Feynman diagrams for the process $e^+e^- \rightarrow q\bar{q}gg$, we get contributions of the following types (see fig.IV.2.5)

1. 'Planar' graphs, which come with colour factor $C_F^2 N$
2. 'Non-Planar' graphs, with colour factor $C_F N(C_F - C_A/2)$
3. Triple-gluon graphs, with colour factor $-C_A C_F N$

(see Appendix A for calculation of the colour factors)

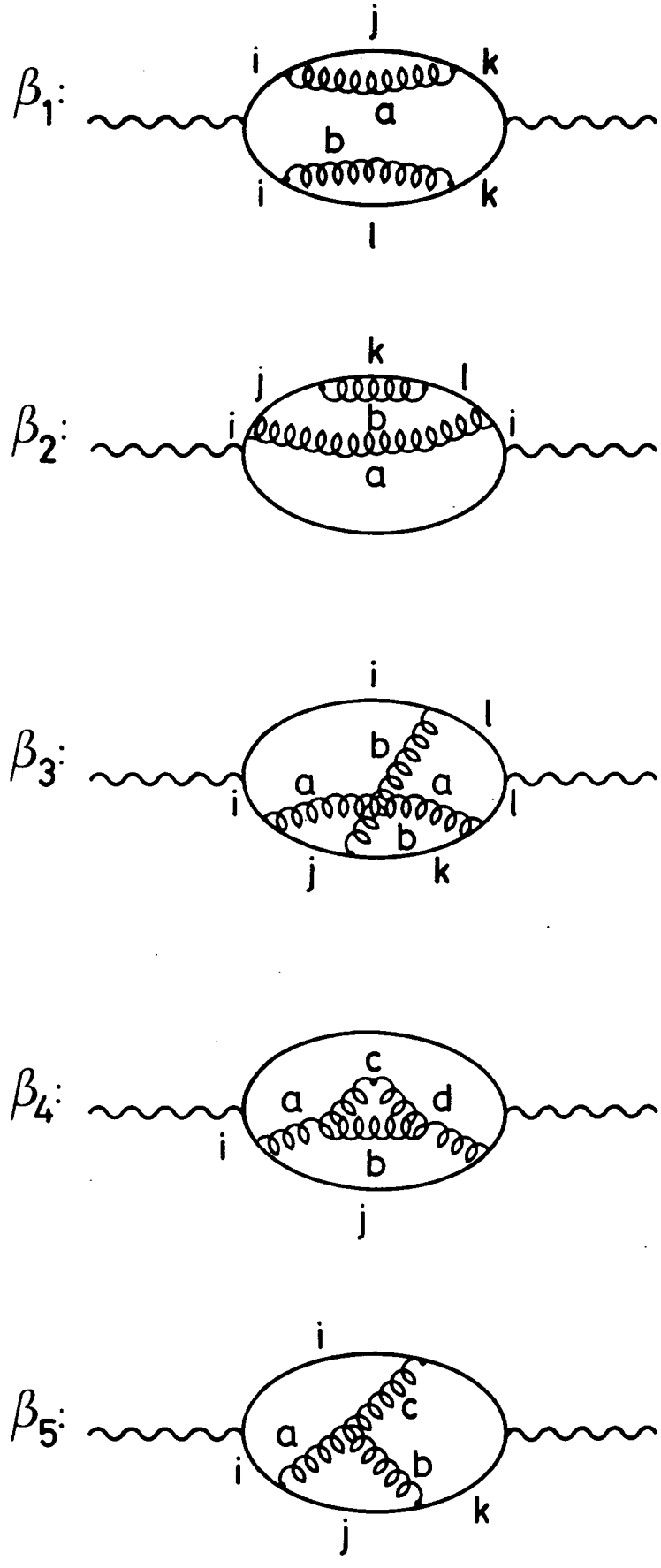

Figure IV.2.5 Feynman diagrams for $e^+e^- \to q\bar{q}gg$

Triple-gluon graphs are obviously excluded in IEA but non-planar graphs are not included either! This is because the model is constructed in terms of products of cross-sections (rather than Feynman diagrams) so that no interference terms are included.

If we now note that non-planar diagrams are somewhat suppressed in non-Abelian QCD ($C_F - C_A/2 = -1/6$ as opposed to $C_F^2 = 16/9$ and $C_A C_F = 4$) but *not* in Abelian QCD ($C_F - C_A/2 = 1, C_F^2 = 1$), it is quite easy to understand why IEA does not agree with Abelian QCD: Simply because they do not contain the same subset of diagrams!

IV.2.1 Planar Abelian Q C D

The above analysis suggests a better test for our model, that is to compare our results with those obtained using the 'planar Abelian' limit of the exact matrix element, which is realized by the following substitutions:

$$C_F \to 1 \quad , \quad C_A \to 2C_F \quad \text{and} \quad N_c \to 1$$

Results for the 'standard' choice of the jet-defining cuts ($k_0 = 4 \text{ and } 6\, Gev, \cos\theta_0 = 0.9$) are presented in figure IV.2.6,7,8.

Clearly, the agreement between IEA and the full answer has been restored, but it is not any better than the original agreement between IEA and non-Abelian QCD. This is because the full answer is not as Abelian as it might thought to be. In fact, triple gluon graphs *do* survive in the limit $C_A \to 2C_F$ which are needed to eliminate the non-planar contributions. To see how this happens, let us parametrize the contributions from each subset of diagrams in the following way:

$$2XC_F^2N \quad + \quad 2YC_F(C_F - C_A/2)N \quad + \quad ZC_AC_FN$$

for the planar, non-planar and triple-gluon graphs respectively. Now, as $C_A \to 2C_F$ the colour weight of the last term becomes C_F^2 just as for the first one; thus the two terms are not colour-distinguished any more!

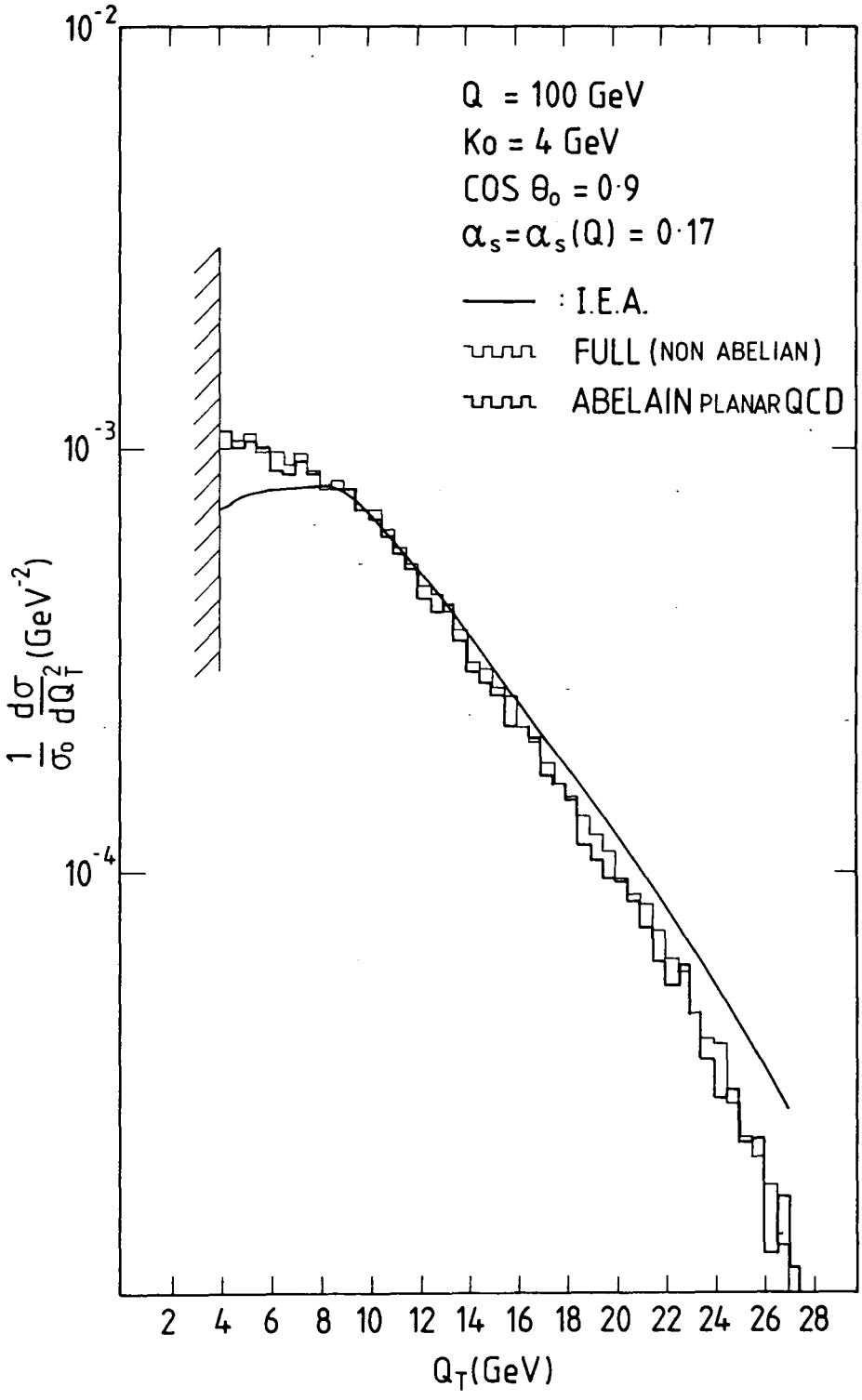

Figure IV.2.6

Q_T-distribution of a four-jet event in electron-positron annihilation. IEA compared with a Planar-Abelian QCD theory.

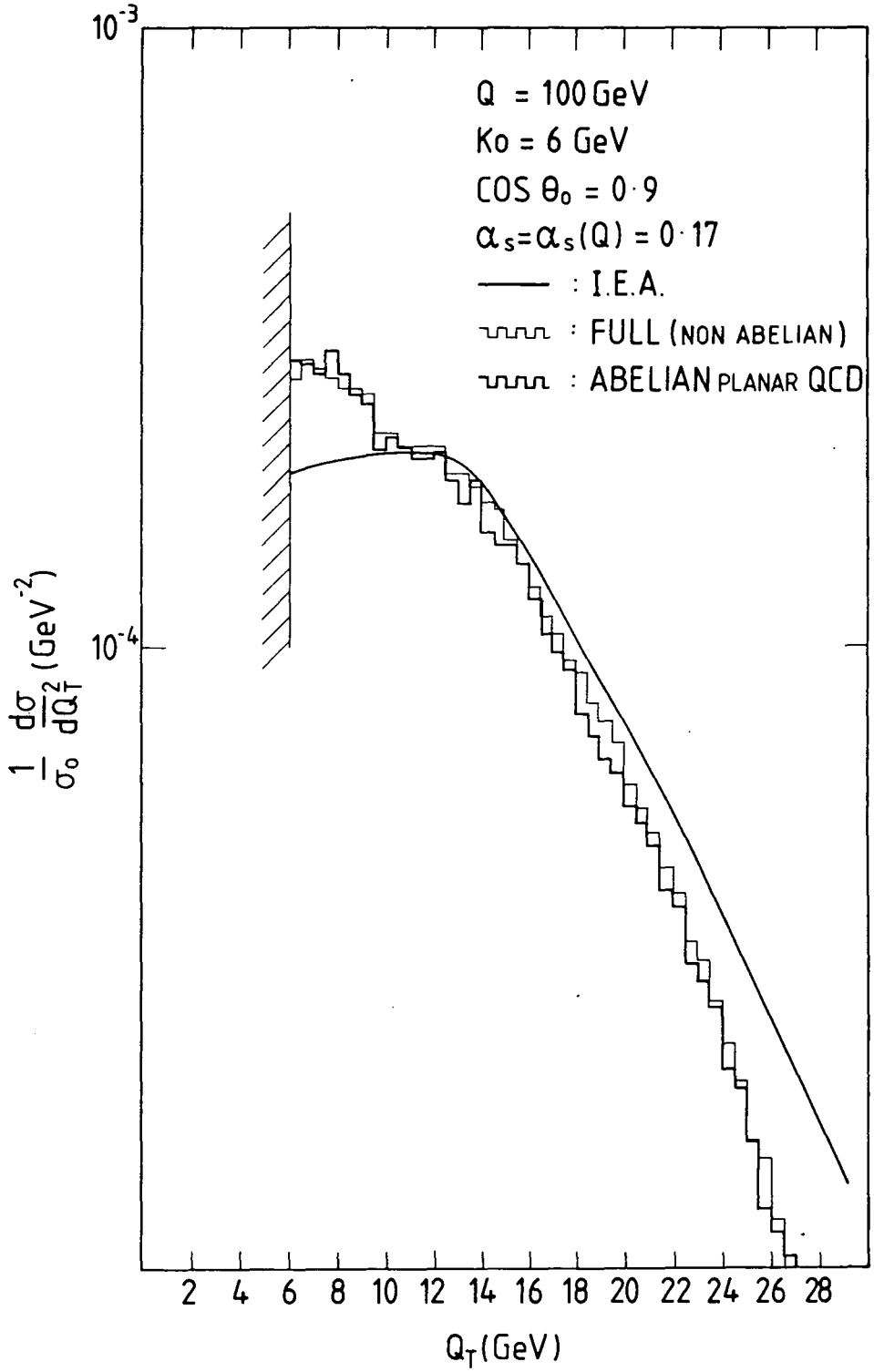

Figure IV.2.7

Q_T-distribution of a four-jet event in electron-positron annihilation. IEA compared with a Planar-Abelian QCD theory.

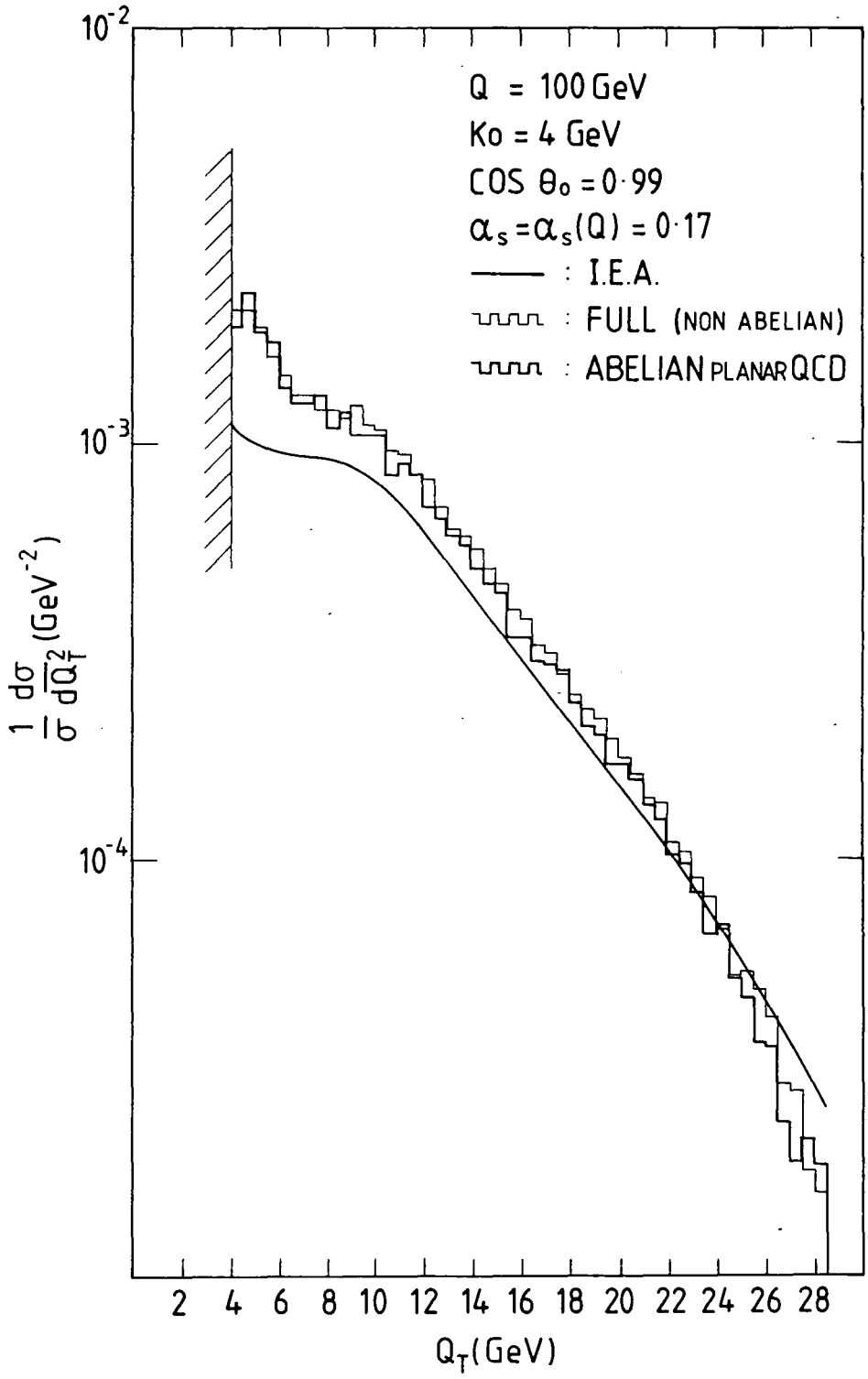

Figure IV.2.8

Q_T-distribution of a four-jet event in electron-positron annihilation. IEA compared with a Planar-Abelian QCD theory.

Unfortunately, we only have the full matrix elements (after the substitutions $C_F = (N^2-1)/2N$ and $C_A = N$).in the form: $C_F(\alpha N^2 - \beta)$ α, β given in eqs.III.4.1 and 2.

Clearly, with only two known variables (α, β) we cannot determine all three unknown (X , Y and Z) without recalculating the individual Feynman amplitudes. However, the fact that the full planar non-Abelian result compares very well with the planar Abelian IEA results suggests that the kinematical coefficient of the remaining triple gluon term is rather small.

To summarize, we conclude that the agreement of our IEA model (which is effectively planar and Abelian) with the full, non-Abelian answer is due to the following facts:

(i) Non-planar graphs are colour-suppressed, as ($C_F - C_A/2$) is small

(ii) Triple-gluon graphs are suggested to be kinematically small (Z small).

IV.3 MULTIJET SHAPE VARIABLES

IV.3.1 The D-distribution

The D-variable is one of the many variables that have been introduced to describe the jet structure of the final state hadrons in electron-positron annihilation, along with Thrust (T), Sphericity (S), Accoplanarity (A), Tripodity (D_3) to name but a few [ref. IV.2]. All these variables satisfy the following properties:

a] They are insensitive to the emission of soft and/or collinear gluons (and this makes them theoretically acceptable).

b] They are also quite insensitive to the process of hadronization (so that an interpretation of experimental data in terms of perturbative QCD is possible).

To see how the D-variable comes about, we have to start from the 3x3 tensor [ref. IV.3].

$$\theta^{ij} \quad = \quad \frac{\sum_\alpha \frac{p_\alpha^i p_\alpha^j}{|p_\alpha|}}{\sum_\alpha |p_\alpha|}$$

where the α-sum runs over all final state particles and p_α^i is the centre-of-mass three-momentum of the α^{th} particle.

By a principal axes transformation, we can reduce θ to a diagonal tensor, the eigenvalues of which are given by the roots of the characteristic equation:

$$\lambda^3 - \lambda^2 + \frac{1}{3}C\lambda - \frac{1}{27}D \quad = \quad 0$$

where the factors of 1/3 and 1/27 are included so that the variables span the range from 0 to 1.

In terms of the eigenvalues of θ, C and D are given by:

$$D = 27\lambda_1\lambda_2\lambda_3 \qquad , \qquad C = 3(\lambda_1\lambda_2 + \lambda_2\lambda_3 + \lambda_3\lambda_1)$$

For a two-jet event, both C and D vanish, while for a planar event $C = 3\lambda_1(1-\lambda_1)$ and D vanishes. D is only non-zero for non-planar events. It is then clear that distributions in C and D can provide measures of the multijet structure of an event. The D-distribution in particular, seems very appropriate for a discussion of four-jet events, as D is a clear measure of the accoplanarity of an event. (Recall that three-jet events are bound to be planar events).

To make things more transparent, we can explicitly relate the D-variable defined above, to our familiar Dalitz plot variables x_i, (i=1,2,3,4) defined to be the fractions of the maximum available energy carried by the quark, the antiquark and the two gluons respectively.

If we also define:

x_T: to be the corresponding fraction of the maximum transverse momentum relative to the most energetic fermion (labelled as parton 1) so that $x_T = 2Q_T/Q$ and

x_k: to be the fraction of the maximum momentum out of the plane defined by the two fermions ,

we can then show (Appendix B)

$$D = \frac{27}{4}\frac{x_1^2 x_T^2 x_k^2}{x_1 x_2 x_3 x_4}$$

an expression with some interesting properties:

First of all, it shows explicitly that D vanishes for a planar event ($x_k = 0$). It also exhibits some symmetry in the definition of the thrust axis to the extent that, if we choose to define x_T from the second fermion, then we just replace x_1 by x_2 in the above expression for D.

Although there is no problem in reproducing the calculation for the D-distribution in both Abelian and non-Abelian QCD for the full case [ref.IV.4], its calculation in the IEA is not possible, as the latter is (by construction) only tranverse momentum dependent.

However, we can still get an idea of what is happening out of the plane by considering the distribution of a new variable $x_\Delta^2 = x_T^2 x_k^2$, which shares some features of the proper D-variable. The calculation of the distribution in this D-like variable (which still vanishes for planar events) in the IEA model is the subject of the next section.

IV.3.2. The Calculation.

In IEA, two-gluon cross-sections are easily constructed in terms of that for one-gluon:

$$\frac{1}{\sigma_0}\frac{d\sigma}{dQ_T^2} = \frac{1}{2\pi}\int d^2\mathbf{k}_1 d^2\mathbf{k}_2 \left[\frac{1}{\sigma_0}\frac{d\sigma^{(1)}}{dk_1^2}\right]\left[\frac{1}{\sigma_0}\frac{d\sigma^{(1)}}{dk_2^2}\right]\delta^{(2)}(\mathbf{k}_1+\mathbf{k}_2-\mathbf{Q}_T)$$

$$= \frac{1}{2\pi}\int dk_{1x}dk_{1y}dk_{2x}dk_{2y}\, h(k_1^2)\, h(k_2^2)\, \delta(k_{1x}+k_{2x}-Q_T)\, \delta(k_{1y}-k_{2y})$$

where we have introduced the notation:

$$\frac{1}{\sigma_0}\frac{d\sigma}{dk_i^2} \quad = \quad h(k_i^2) \quad \equiv \quad h_i$$

Performing the k_{2x} , k_{2y} integrals using the δ-functions we set :

$$k_{2y} \quad = \quad k_{1y} \qquad , \qquad k_{2x} \quad = \quad Q_T - k_{1x}$$

so that:

$$\frac{1}{\sigma_0}\frac{d\sigma}{dQ_T^2 dk} \quad = \quad \frac{1}{2\pi}\int dk_{1x} h(k_{1x}^2+k^2) h[(Q_T-k_{1x})^2+k^2]$$

where $k \equiv k_{1y}$

We now introduce the variable : $\Delta = Q_T \cdot k$ and change variables according to :

$$(Q_T^2 \quad , \quad k) \qquad \rightarrow \qquad (Q_T \quad , \quad \Delta)$$

with

$$\frac{d\sigma}{dQ_T^2 dk} \quad = \quad \frac{d\sigma}{dQ_T d\Delta}\begin{vmatrix} \frac{\partial Q_T}{\partial Q_T^2} & \frac{\partial \Delta}{\partial Q_T^2} \\ \frac{\partial Q_T}{\partial k} & \frac{\partial \Delta}{\partial k} \end{vmatrix} \quad = \quad \frac{1}{2}\frac{d\sigma}{dQ_T d\Delta}$$

so that

$$\frac{1}{2\sigma_0}\frac{d\sigma}{dQ_T d\Delta} = \frac{1}{2\pi}\int dk_{1x} h_1 h_2$$

Integrating over Q_T:

$$\frac{1}{\sigma_0}\frac{d\sigma}{d\Delta} = \frac{2}{2\pi}\int dQ_T \int dk_{1x}\, h_1 h_2$$

which can be expressed in terms of Δ^2:

$$\frac{1}{\sigma_0}\frac{d\sigma}{d\Delta^2} = \frac{1}{2\pi}\frac{1}{\Delta}\int dQ_T \int dk_{1x}\, h_1 h_2$$

Integration Limits

a.] For fixed Δ , Q_T k is given by $k = \Delta/Q_T$

b.] Now, recall the kinematical limit:

$$-Q_T^{max} \leq k_1 \leq Q_T^{max}$$

$$-Q_T^{max} \leq \sqrt{k_{1x}^2 + k_{1y}^2} \leq Q_T^{max}$$

$$-\sqrt{(Q_T^{max})^2 - k^2} \leq k_{1x} \leq \sqrt{(Q_T^{max})^2 - k^2}$$

that is:

$$-\omega \leq k_{1x} \leq \omega$$

where

$$\omega = \sqrt{(Q_T^{max})^2 - k^2}$$

Similarly, we require :

$$-\omega \leq k_{2x} \leq \omega$$

Finally, noting that k_{1x} , k_{2x} must satisfy the constraint:

$$k_{1x} + k_{2x} = Q_T$$

we conclude:

$$\text{when} \quad Q_T > 0 \qquad -\omega + Q_T \;\leq\; k_{1x} \;\leq\; \omega$$

$$\text{when} \quad Q_T < 0 \qquad -\omega \;\leq\; k_{1x} \;\leq\; \omega + Q_T$$

c. On the other hand, the Q_T-limits are given by:

$$\lambda \;=\; max[k_0\,,\,\Delta] \;\leq\; Q_T \;\leq\; Q_T^{max}$$

Therefore we have :

$$\frac{1}{\sigma_0}\frac{d\sigma}{d\Delta^2} = \frac{1}{2\pi}\frac{1}{\Delta}\left[\int_\lambda^{Q_T^{max}} dQ_T \int_{Q_T-\omega}^{\omega} dk_{1x} h_1 h_2 + \int_{-Q_T^{max}}^{\lambda} dQ_T \int_{-\omega}^{\omega+Q_T} dk_{1x} h_1 h_2\right]$$

and combining the two integrals together:

$$\int_\lambda^{Q_T^{max}} dQ_T \quad \int_{Q_T-\omega}^{\omega} dk_{1x}\, h_1 h_2 \quad + \quad \int_\lambda^{Q_T^{max}} dQ_T \quad \int_{-\omega}^{\omega-Q_T} dk_{1x}\, h_1 h_2$$

$$= \int_\lambda^{Q_T^{max}} dQ_T \quad \int_{Q_T-\omega}^{\omega} dk_{1x} h_1 h_2 \quad + \quad \int_\lambda^{Q_T^{max}} dQ_T \quad \int_{-\omega+Q_T}^{\omega} dk_{1x} h_1 h_2$$

$$= \quad 2\int_\lambda^{Q_T^{max}} dQ_T \quad \int_{-\omega+Q_T}^{\omega} dk_{1x}\, h_1 h_2$$

we obtain:

$$\frac{1}{\sigma_0}\frac{d\sigma}{d\Delta^2} \quad = \quad 2\frac{1}{2\pi}\frac{1}{\Delta}\int_\lambda^{Q_T^{max}} dQ_T \quad \int_{Q_T-\omega}^{\omega} dk_{1x} h_1 h_2$$

Finally, we introduce momentum-fractions:

$$x_k = \frac{2k_{1x}}{Q} \quad , \quad x_T = \frac{2Q_T}{Q} \quad , \quad x_\Delta = x_k \cdot x_T$$

in terms of which we express our final result:

$$\frac{1}{\sigma_0}\frac{d\sigma}{dx_\Delta^2} \quad = \quad 2\frac{1}{2\pi}\frac{1}{x_\Delta}\int_{x_T^{min}}^{x_T^{max}} dx_T \quad \int_{x_k^{min}}^{x_k^{max}} dx_k \quad \times$$

$$\times h\left[x_k^2 + \frac{x_\Delta^2}{x_T^2}\right] \quad h\left[\left(x_T - \frac{x_\Delta}{x_T}\right)^2 + \frac{x_\Delta^2}{x_T^2}\right]$$

with

$$x_T^{min} = \frac{2\lambda}{Q} \quad , \quad \lambda = max(\Delta, k_0)$$

$$x_T^{max} = \frac{2Q_T^{max}}{Q}$$

$$x_k^{max} = \frac{2\omega}{Q} \quad , \quad \omega = \left[(Q_T^{max})^2 - \frac{\Delta^2}{Q_T^2}\right]^{1/2}$$

$$x_k^{min} = \frac{2[Q_T - \omega]}{\omega}$$

IV.3.3 Results and Discussion.

IEA results for the $1/\sigma_0 d\sigma/dx_\Delta^2$ distribution are presented in figures IV.3.1 and 2. If we compare them with the full answers obtained using the exact matrix elements in both Abelian and non-Abelian QCD, we can easily see that there is a kinematic region in which IEA agrees rather well with non-Abelian results, and this agreement gets worse in the Abelian limit.

However, because of the way x_Δ^2 is defined (it is only non-vanishing for non-planar events but not *all* four-jet events are non-planar) we need to go to rather small values of x_Δ^2 to see our approximation working. Typically, we expect a good agreement in the region around the critical value:

$$x_\Delta^2 \sim (x_{k_0})^4 = \left(\frac{2k_0}{Q}\right)^4 = (0.04)^4$$

and this is confirmed when comparing figures IV.3.1 and 2. Finally, we note that there is no agreement between IEA and full results for large values of x_Δ^2, as IEA breaks down for large values of momenta (see also §III.5.2).

Noting that these results are in agreement with those of the last chapter, we conclude that the study of distributions in this D-like variable confirms the conclusions obtained from studing transverse momentum distributions and so provides another successful test of the applicability of our model to the investigation of the multijet structure of hadronic final states.

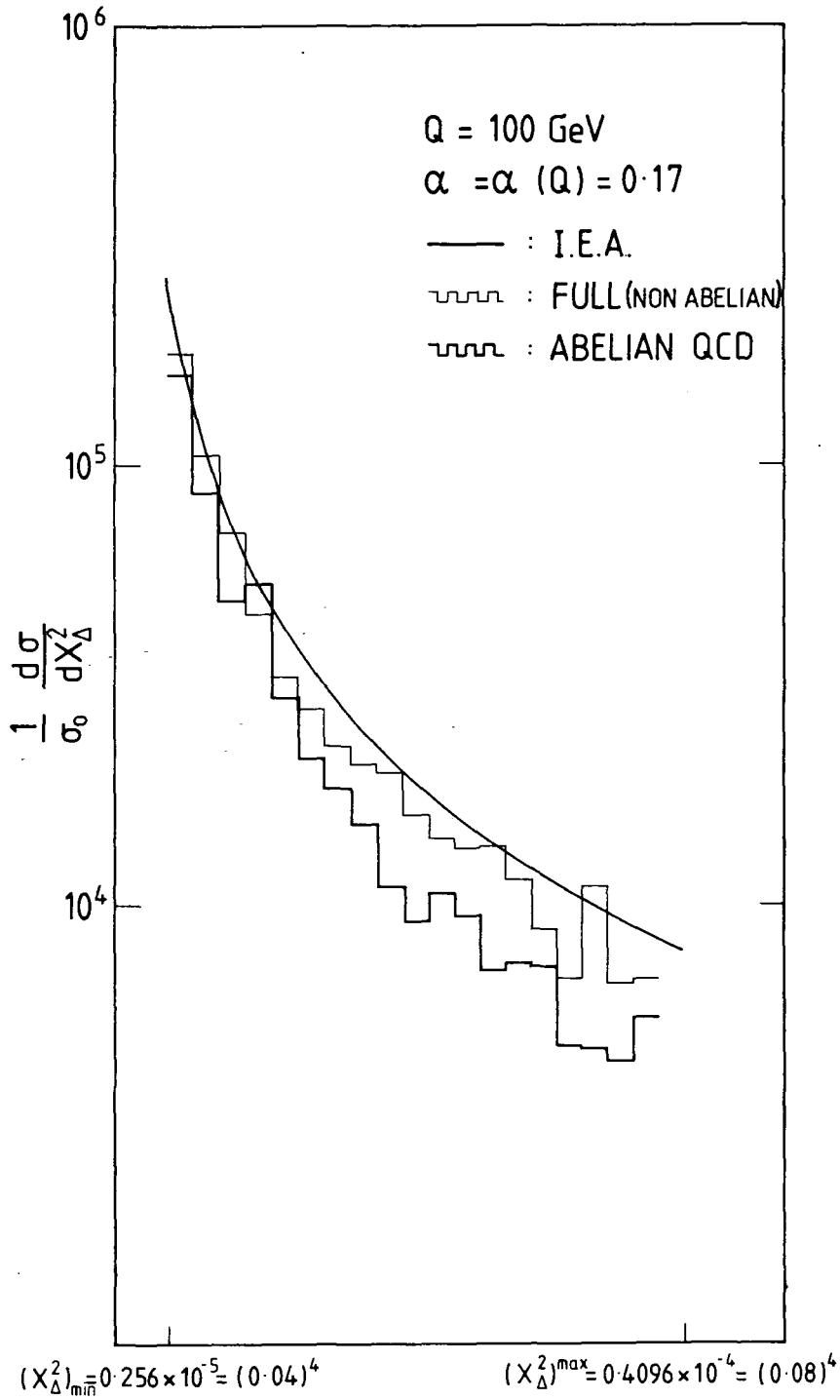

Figure IV.3.1

Distributions in x_Δ^2. IEA compared with the full QCD results.

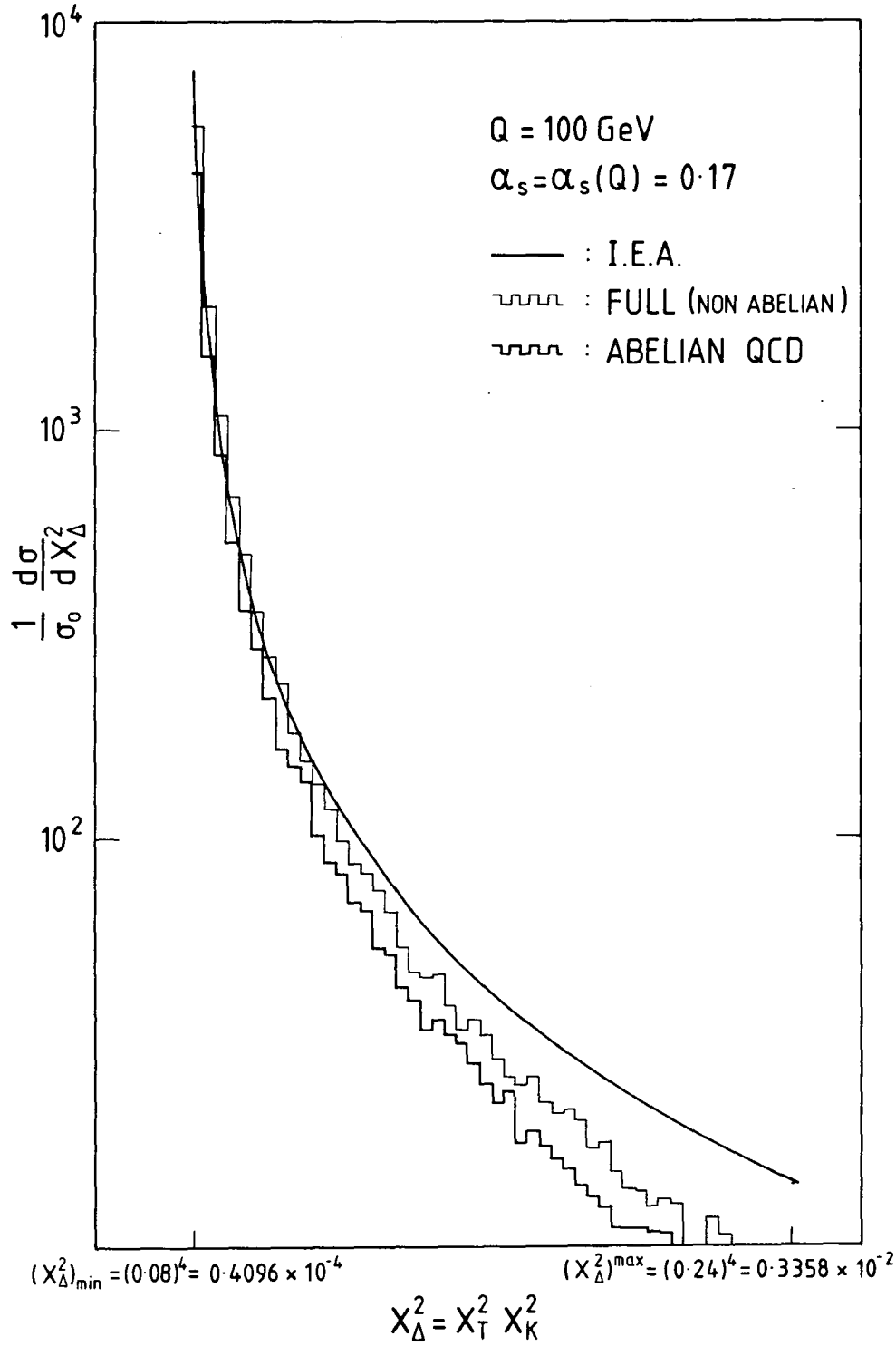

Figure IV.3.2

Distributions in x_Δ^2. IEA compared with the full QCD results.

IV.3.4 The Total Tranverse Momentum W_T.

The total transverse momentum W_T of the final state particles is yet another observable that has been used in QCD studies of hadron production in e^+e^- annihilation, and has recently attracted theoretical as well as experimental interest [ref IV.5]. As it probes the transverse spread of the final state particles, it is particularly useful to test QCD predictions when studying the multijet structure of the final hadronic state.

One of the most characteristic QCD predictions is the expectation of growing transverse momentta at higher and higher energies, a phenomenon known as 'jet broadening' that has been observed in both e^+e^- annihilation and hadron-hadron scattering [ref.IV.6]. Jet broadening is best parametrized in terms of mean values of transverse momenta and $\langle W_T \rangle$ is easily calculated to lowest order in α_s (see also §V.4).

However, it has been recently anticipated [ref. ellis] that there must be large higher order corrections to the lowest order result if unitarity is to be respected. To compute the $O(\alpha_s^2)$ corrections for instance, we would have to consider not only four parton final states, but also loop-corrections to the three parton process ; a non-trivial calculation.

On the other hand, we might expect that these higher order corrections can be easily calculated in our I E A model (which is naturally tranverse momentum defined) in a way which is very similar to the calculations described so far. To justify our claim, let us recall the definition of W_T

First of all, we define the transverse thrust axis with respect to which all transverse momenta are measured. This is determined by the unit vector $\vec{n}$ which maximizes the quantity :

$$T \quad = \quad \max \sum_k \frac{|\vec{p} \cdot \vec{n}|}{2Q}$$

where the k sum runs over all final state particles. T is normally associated with the direction of the most energetic parton.

In the three-jet case for instance, with $\vec{n} = (\cos\theta, \sin\theta, 0)$ and x_1 large enough (see eqs.II.2.1) it is quite easy to see that the maximizing solution occurs when $\theta = 0$.

W_T is then defined as the total transverse momentum perpendicular to the transverse thrust axis T :

$$W_T = \sum_k |\vec{p} \wedge \vec{n}|$$

that is

$$W_T = 2Q_T \quad \text{for a } 3-\text{jet event}$$

$$W_T = Q_T + |\vec{k_{T_1}}| + |\vec{k_{T_2}}| \quad \text{for a } 4-\text{jet event}$$

where $\vec{k_{T_1}}, \vec{k_{T_2}}$ are the transverse momentum of the emitted gluons.

We can now understand why W_T-distributions are calculable in IEA. If we recall that multigluon cross-sections are constructed in terms of that for one:

$$\frac{1}{\sigma}\frac{d\sigma}{dQ_T^2 d^2\mathbf{k}_{T_1} d^2\mathbf{k}_{T_2}} = \frac{1}{2\pi}\left[\frac{1}{\sigma_0}\frac{d\sigma^{(1)}}{dk_{T_1}^2}\right]\left[\frac{1}{\sigma_0}\frac{d\sigma^{(1)}}{dk_{T_2}^2}\right] \delta^{(2)}(\mathbf{k}_{T_1} + \mathbf{k}_{T_2} - \mathbf{Q}_T)$$

then we can suitably change variables (as outlined in the last section in the calculation of the D-distribution) to obtain the IEA-expression for $1/\sigma_0 d\sigma/dW$ from which we can easily compute the mean transverse momentum:

$$\langle W \rangle = \frac{\int \frac{1}{\sigma_0}\frac{d\sigma}{dW} W}{\int \frac{1}{\sigma_0}\frac{d\sigma}{dW}}$$

However, it should be emphasized that the above expression for $\langle W \rangle$ is not yet free of singularities, which occur when the emitted gluons are soft and/or collinear with the parent fermions. These singularities are of course regularized by similar divergences in the virtual graphs. Analytical cancellations of such singularities are performed in some detail in the next chapter (§V.2.1)

IV.4 Comparison with a recent calculation.

As it has been emphasized already in the introduction of this thesis, studies of transverse momentum distributions in semi-hard processes (that is when Q_T is not only large but very much less than Q : $\Lambda_{QCD} \ll Q_T \ll Q$) are of great interest, particularly as the applicability of perturbative QCD in such kinematic regimes is under question. In fact, the growing coupling $\alpha_s(Q_T)$ and the presence of the new scale which gives rise to large terms of order:

$$\frac{1}{Q_T^2}\,\alpha_s^n(Q_T^2)\,\ln^m\!\left(\frac{Q^2}{Q_T^2}\right) \qquad , \qquad m \leq 2n-1$$

force the simple perturbative expansion to break down. Multigluon emissions become increasingly important, requiring all orders in perturbation theory to be considered.

One of the major theoretical advances of recent years has been the development of techniques to sum these large logarithms to all orders. As outlined in §II.1, such resummation was first attempted by Dokshitzer, Dyakonov and Troyan (DDT) in the leading double logarithmic approximation (DLLA : m=2n-1) and subsequently modified and improved by Parisi and Petronzio. A consistent framework for going beyond DLLA has been indicated by Collins, Soper and Sterman (CSS) (see §II for references).

Recently, Altarelli, Ellis, Greco and Martinelli (AEGM) have studied transverse momentum distributions of lepton pair production in hadron-hadron collisions, in connection with the W and Z^0 production experiments [ref.II.4,9]. They re-examined the QCD predictions for the Q_T-distribution of the lepton pair, incorporating in a systematic way the theoretical information accumulated in recent years, in particular the analyses of CSS. Their final expression not only sums the multigluon emissions to DLLA at small Q_T, but at large Q_T reproduces the $O(\alpha_s)$ perturbative result coming from the one gluon emission.

As we shall see in some detail in the next section, however systematic and sophisticated their approach is, their calculation is not free of theoretical ambiguities and a number of important questions remain unanswered. The purpose of this part of chapter IV is to investigate these problems and to assess the accuracy of their calculation, in the less convoluted problem of multijet production in e^+e^- annihilation (that we have been studing so far).

If we recall that all resummation methods imply an ansatz for 1, 2, 3 ... gluon emission, and note that the single gluon result is usually included more-or-less exactly (being the basis of these) then we turn to the two gluon cross-section. We shall consequently detail the ansatz of AEGM for this and compare it with exact $O(\alpha_s^2)$ result as well as with the IEA result, both obtained in the last chapter [ref.IV.7].

IV.4.1 Review of AEGM's algorithm for transverse momentum distributions.

Their starting point is to separate the $O(\alpha_s)$ cross-section for $e^+e^- \rightarrow q\bar{q}g$ into two pieces (following the treatment of CSS).

$$\frac{1}{\sigma_0}\frac{d\sigma}{dQ_T^2} \quad = \quad X(Q_T^2) \quad + \quad Y(Q_T^2)$$

where the X term contains contributions which are singular as $Q_T \rightarrow 0$ and Y contains the remaining terms which are perfectly finite at $Q_T = 0$. Up to and including $O(\alpha_s)$, they write the following schematic expression for X:

$$X(Q_T^2) \quad = \quad 1\,\delta(Q_T^2) \quad + \quad \alpha_s A(Q_T^2) \quad + \quad \alpha_s B\delta(Q_T^2) \qquad \text{IV.4.1}$$

where each term comes from the diagrams shown in fig. II.2.3a, b and c respectively. The real-gluon term $A(Q_T^2)$ is singular as $Q_T \rightarrow 0$, that is in the limit that the emitted gluon becomes soft and/or collinear with one of the fermions. These singularities are regularized by the virtual contributions contained in the B term.

To distinguish between hard and soft/collinear gluons and to get a finite answer, the A term is decomposed into two pieces, using the '+ prescription' :

$$\begin{aligned} X(Q_T^2) &= 1\,\delta(Q_T^2) + \alpha_s\big[A_+(Q_T^2) + A_0\delta(Q_T^2)\big] + \alpha_s B\delta(Q_T^2) \\ &= \delta(Q_T^2)\big[1 + \alpha_s(A_0 + B)\big] + \alpha_s A_+(Q_T^2) \end{aligned} \qquad \text{IV.4.2}$$

or, in their notation:

$$X(Q_T^2) = \delta(Q_T^2)[1 + \alpha_s F] + S(Q_T^2)$$

with

$$S(Q_T^2) = \frac{\alpha_s}{2\pi} C_F \left[2\Big(\frac{\ln(Q^2/Q_T^2)}{Q_T^2}\Big)_+ - \Big(\frac{3}{Q_T^2}\Big)_+ \right] \qquad \text{IV.4.3}$$

The resummation of the large, soft/collinear terms : $1/Q_T^2 \ln Q^2/Q_T^2$, $1/Q_T^2$ is performed in the impact parameter space [ref.II.6,18]. The b-transform of $X(Q_T^2)$ is given by:

$$X(b^2) = 1 + F + S(b^2)$$

$$S(b^2) = \int_0^{A_T^2} \frac{dQ_T^2}{Q_T^2} \frac{\alpha_s(Q_T^2)}{2\pi} C_F \left[J_0(bQ_T) - 1 \right] \left[2\frac{\ln Q^2}{Q_T^2} - 3 \right]$$

where A_T^2 is the kinematic limit for the transverse momentum squared. The summation in b-space of all orders in α_s is performed by replacing the $O(\alpha_s)$ result of $1 + S(b^2)$ by $\exp S(b^2)$. Thus X is written as:

$$X(b^2) = (1 + F)\exp S(b^2)$$

Finally, the differential Q_T-distribution is recovered by Fourier transforming back to Q_T space:

$$\frac{1}{\sigma_0}\frac{d\sigma}{dQ_T^2} = \int \frac{d^2\mathbf{b}}{4\pi} e^{-i\mathbf{b}\cdot\mathbf{Q}_T} \big[(1 + F)\exp S(b^2)\big] + Y(Q_T^2) \qquad \text{IV.4.4}$$

Recall that the Y term represents the hard, single gluon contribution from which the terms singular in the $Q_T \to 0$ limit have been subtracted. These singular terms are in fact included in the first term, in the exponential. The latter represents the so-called Sudakov form factor and its appearance reflects the resummation of the soft, multigluon emissions.

IV.4.2 Theoretical Uncertainties in the AEGM formalism.

a.] As the soft gluon resummation was performed at DLLA, it is natural to ask what is the effect of the neglected subleading terms [ref.IV.8].

b.] As a complete two-loop calculation has not yet been performed, it was not possible for AEGM to include the $O(\alpha_s^2)$ in an entirely consistent way; thus, the effect of the neglected higher order terms needs to be examined [ref.IV.9].

c.] As AEGM followed the analyses of CSS and exponentiated only part of the first order contribution, it would be interesting to compare their results with the ones obtained in the naive IEA, where the whole $O(\alpha_s)$ is exponentiated.

d.] Finally, as AEGM point out, there remains an ambiguity in the choice of the scale of the running coupling, which cannot be removed without a complete knowledge of the $O(\alpha_s^2)$ terms. However, in the light of the remarks made in §III.4.c, this problem can be further investigated in the IEA framework, where the several proposed choices can be critically compared.

IV.4.3 $e^+e^- \rightarrow$ 4jets using AEGM's algorithm.

To throw some light on these questions, we now calculate the tranverse momentum distribution for a four-jet event in e^+e^- annihilation using the AEGM algorithm outlined in §IV.4.1 and compare the result with the 'exact' $O(\alpha_s^2)$ answer as well as with the simple IEA result, both obtained in the last chapter. To get the AEGM four-jet contribution, we first expand eq. IV.4.4 to second order and identify the AEGM two-gluon term. If we recall their decomposition of real and virtual graphs (cf. eqs.IV.4.1 and 2) and the origin of every term in their final expression (eq.IV.4.4), it is then easy to see that such a term is only contained in the expansion of the exponential: $\exp S(b^2)$, and we only need to consider the term:

$$\frac{1}{\sigma_0}\frac{d\sigma^{AEGM}}{dQ_T^2} = \int \frac{d^2\mathbf{b}}{4\pi} e^{-i\mathbf{b}\cdot\mathbf{Q_T}} S^2(b^2)$$

As $S(b^2)$ depends only on the moduli of the momenta and not their direction (eq.IV.4.3), we can trivially perform the angular integration in the above expression to get:

$$\frac{1}{\sigma_0}\frac{d\sigma^{AEGM}}{dQ_T^2} = \frac{1}{2}\int bdbJ_0(Q_Tb)\int dp^2\Big[J_0(bp)-1\Big]\frac{\alpha_s(p^2)}{2\pi}C_F\left[2\frac{\ln(Q^2/p^2)}{p^2}-\frac{3}{p^2}\right]\times$$

$$\times\int dq^2\Big[J_0(bq)-1\Big]\frac{\alpha_s(q^2)}{2\pi}C_F\left[2\frac{\ln Q^2/q^2}{q^2}-\frac{3}{q^2}\right]$$

Clearly, the -1 arises from the virtual gluon graphs which regularize the infrared singularities as $p, q \to 0$. As four-jet events can only originate from two real real gluons, these virtual contributions need not be taken into account, so that we are left with:

$$\frac{1}{\sigma_0}\frac{d\sigma^{AEGM}}{dQ_T^2} = \frac{1}{2}\int dp^2\,dq^2\left[\frac{C_F}{2\pi}\right]^2\alpha_s(p^2)\alpha_s(q^2)\left[2\frac{\ln(Q^2/p^2)}{p^2}-\frac{3}{p^2}\right]\times$$

$$\times\left[2\frac{\ln(Q^2/q^2)}{q^2}-\frac{3}{q^2}\right]\int b\,db\,J_0(Q_Tb)J_0(pb)J_0(qb) \qquad \text{IV.4.5}$$

where we have interchanged the order of b, p and q integrations.

Moreover, in order to ensure a finite answer and four distinct jets in the final state, we have to integrate eq.IV.4.5 *only* over those regions of phase space where the four outgoing partons are well defined and well separated from each other. Given the form of the AEGM-equation and noting its structural similarities with the IEA-equation III.2.2, we can identify p and q with the transverse momenta k_{T_1} and k_{T_2} of the two gluons and impose IEA-type jet-resolving cuts on them, namely:

$$p, q \geq k_0 \qquad \text{and} \qquad \theta_0 \leq \theta(p, q) \leq \pi - \theta_0$$

(see §III.3.3 for details).

Finally, note that the integration of the three Bessel functions gives rise to the $W_3(p,q,Q_T)$-function of eq.III.2.4, which, recall, is only defined if the vectors of length p, q and Q_T can form a closed triangle:

$$(p+q)^2 \quad \geq \quad Q_T^2 \quad \geq \quad (p-q)^2$$

IV.4.4 Comparison of AEGM with IEA. Discussion.

As has been already noted in the last section, the AEGM expression for the transverse momentum distribution of a four-jet event is *not* very different in form from the corresponding IEA result. Moreover, numerical predictions based on eqs.III.2.2 and IV.4.5 and using the same values for the various parameters (choice of cuts, running of α_s) differ by just a fraction of one percent. This implies that, despite their systematic and sophisticated approach, AEGM do *not* treat multigluon emissions much better than the naive IEA does, so that their analysis can be seen *only* as a plausible theoretical approximation to the (much awaited) 'complete and explicit treatment of the soft gluon effects' [ref.II.4].

In the last chapter, we introduced the IEA formalism as another approximate framework, particularly useful for calculating transverse momentum distributions in the multijet case, and we showed that there was a non-trivial kinematic region in which IEA agreed very well with the exact fixed-order results. In this chapter, we indicated that these approximations are not very different from each other, as they were seen to be in remarkable structural and numerical agreement. However, despite these similarities, the two approximations display a number of theoretical differences, which are highlighted below:

a.] As the whole of the $O(\alpha_s)$ one gluon cross-section is naively exponentiated in IEA, some of the subleading terms are included, whereas AEGM neglect these terms on the grounds that their effect can roughly be reproduced by a corresponding change in the value of Λ_{QCD}.

b.] This uncertainty in the value of Λ_{QCD} cannot be removed until second and higher order terms are calculated. However, as it will be detailed in the next chapter, IEA can be used to study the effect of these terms, particularly as it allows multigluon contributions to be easily calculated (see eq.III.2.1) and has virtual corrections already built in.

c.] Finally, as far as the above mentioned ambiguity in choosing the argument of the running coupling is concerned, note that, while AEGM prefer the simple choice of Q^2 or Q_T^2 and emphasize the need for a complete $O(\alpha_s^2)$ calculation to resolve the issue, IEA allows several choices to be considered and compared. In fact, because of the way the Q_T-distribution is generated by multigluon emissions, gluon transverse momenta can be used in the argument of α_s, and that has already been seen in chapter III as equivalent to including often dominant corrections to all orders.

IV.5 SUMMARY OF CHAPTER IV.

In this chapter, we put the IEA model to more tests. First of all, we investigated its agreement with the exact QCD results by making comparisons both with an Abelian QCD and a Planar Abelian QCD theory. We concluded that the agreement of IEA (which is effectively planar and Abelian) with the full, non-Abelian answer was due to a colour-suppression of the non-planar graphs and a (suggested) kinematic-suppression of the non-Abelian ones.

Then, we outlined how the IEA formalism can be used to calculate distributions in other variables that have been proposed to describe the multijet structure of the final hadronic state (such as the D-variable and the total transverse momentum W_T). In particular, we described the IEA calculation of the D-distribution in some detail and compared its predictions with the exact ones obtained using a Monte Carlo generation of events according to the full QCD matrix elements. The comparison echoed the conclusion of chapter III: There is a non-trivial kinematic region in which IEA is a realistic approximation to the exact theory.

Finally, we contrasted the simple IEA approach for calculating transverse momentum distributions with the more systematic and complete algorithm of Altarelli *et. al.* and found that they were in a remarkable structural as well as numerical agreement. This agreement was then seen as another attractive feature of the IEA model, on top of those emphasized in §II.3.4 (recall, IEA not only sums the - almost independent - multigluon emissions at small Q_T, but also reproduces the $O(\alpha_s)$ result at large Q_T). The use of this model to study higher order corrections to multijet cross-sections is the subject of the next chapter.

CHAPTER V $e^+e^- \rightarrow$ 3 JETS

V.1 INTRODUCTION.

We now turn to three-jet events in e^+e^- annihilation to $O(\alpha_s^2)$ in the Independent Emission Approximation (I E A) by considering the two-gluon cross-section in those regions of phase space, where the four final-state particles define only three distinct jets. The corresponding soft and collinear singularities are regularised by taking into account the contributions of the virtual graphs to the same order in α_s.

The above cancellation of singularities between real and virtual graphs is shown explicitly and the analytic behaviour of the cross-section in the soft limit is investigated in detail (§V.2). In the light of these analytic studies, we arrange that the two contributions are combined under the same integral (cf eq.III.2.3) and the relevant numerical integration is performed to a high level of accuracy (§V.3). Finally successful comparisons with existing calculations are also made and the theoretical questions formulated in the beginning of this work (§II.1.1) are given reliable answers.

V.2 THREE JETS IN I E A.

In I E A, the $O(\alpha_s^2)$ cross-section for two gluon emission is given in terms of $O(\alpha_s)$ cross-section for single gluon emission:

$$\frac{1}{\sigma_0}\frac{d\sigma^{(2)}}{d^2\mathbf{Q}_T\, d^2\mathbf{k}_{T_1}\, d^2\mathbf{k}_{T_2}} = \frac{1}{2!}\frac{1}{\sigma_0}\frac{d\sigma^{(1)}}{d^2\mathbf{k}_{T_1}}\frac{1}{\sigma_0}\frac{d\sigma^{(1)}}{d^2\mathbf{k}_{T_2}}\delta^{(2)}(\mathbf{k}_{T_1}+\mathbf{k}_{T_2}+\mathbf{Q}_T) \quad \text{V.2.1}$$

Since the cross-sections depend only on the magnitude k_T^2 and not on the direction of $\mathbf{k}_T$, we can deduce: (eq.III.1.3 and 4)

$$\frac{1}{\sigma_0}\frac{d\sigma^{(2)}}{dQ_T^2} = \frac{1}{2\pi}\int dk_{T_1}^2 \frac{1}{\sigma_0}\frac{d\sigma^{(1)}}{dk_{T_1}^2} \int dk_{T_2}^2 \frac{1}{\sigma_0}\frac{d\sigma^{(1)}}{dk_{T_2}^2}\times$$

$$\times \frac{1}{\left[(Q_T+k_{T_1})^2-k_{T_2}^2\right]^{\frac{1}{2}}} \quad \frac{1}{\left[k_{T_2}^2-(Q_T-k_{T_1}^2)^2\right]^{\frac{1}{2}}} \quad \text{V.2.2}$$

We now want to integrate eq.V.2.2 over those regions of phase space, where the four final state particles define just three distinct jets. This will enable us to consider the 3-jet cross-section beyond the tree approximation (of Stirling *et. al.* [ref.II.10] for instance). Following our discussion of §III.2, this means that we have to consider configurations with:

(i) One hard - one soft gluon

(i.e. one of the gluons is 'energetic' enough ($k_{T_i} \geq k_0$, $i = 1,2$) to manifest itself as a jet, whereas the other one fails the cut ($k_{T_j} < k_0$, $j \neq i$).

(ii) Two collinear gluons

(i.e. two gluons that fail the angular cut introduced in §II.3)

These requirements for a three-jet final state, set the limits for the numerical integration in a way that is schematically described in figs.III.4.1 and V.2.1.

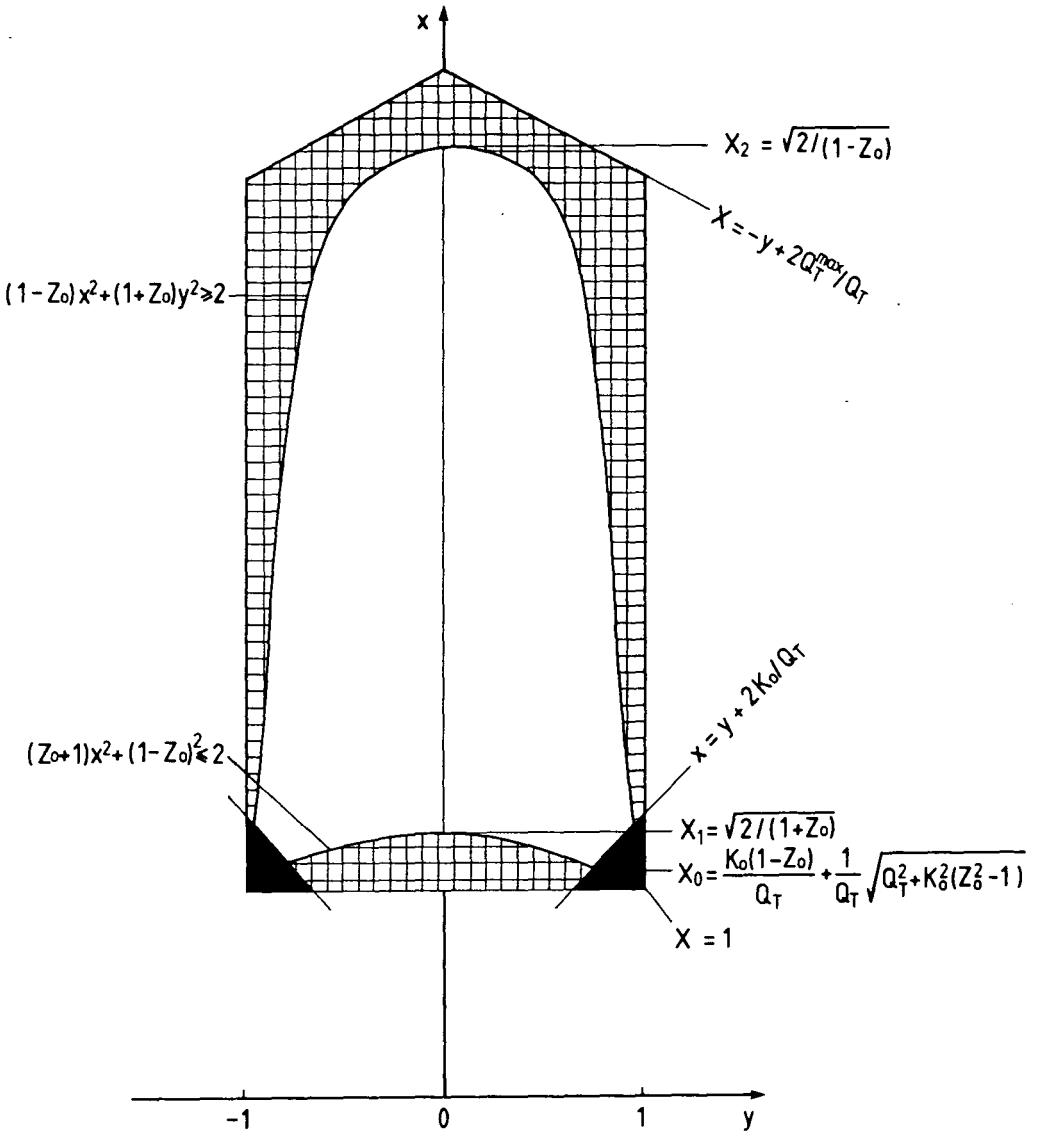

Figure V.2.1 Three-jet phase space.

The shaded area corresponds to the case where one of the gluons is hard ($k_{T_i} < k_0$ $i \neq j$) and the hatched area corresponds to two hard gluons but not sufficiently widely separated.

However, as has already been emphasized, perturbative QCD cross-sections diverge in those regions of phase space, where the final state particles are *not* well defined (i.e. either not energetic enough or not well separated from each other). To regularize these soft and collinear singularities, we have to include the contributions from the virtual graphs to the same order in α_s. The total answer is known to be finite by means of the K L N theorem [II.14].

In our case, this regularization has been performed in §III.2. The second term of eq.III.2.3 serves to compensate the soft singularity of the first term coming from the $1/k_{T_i}^2$ in $d\sigma^{(1)}/dk_{T_i}^2$ when either $k_{T_i} = 0$. (Recall that there are *no* collinear singularities in I E A).

The study of how this cancellation comes about, is the subject of the next section.

V.2.1 Cancellation of soft singularities.

We first recall the contribution of two real gluons expressed in terms of the dimensionless variables x and y introduced in §III.4:

$$I_R = \frac{4}{\pi Q_T^2} \int \frac{dx\,dy}{x(x+y)} \frac{f(k_{T_1})\,f(k_{T_2})}{(x^2-1)^{\frac{1}{2}}(1-y^2)^{\frac{1}{2}}} \qquad \text{V.2.3}$$

which is, of course, singular at $x = 1$ and $y = \pm 1$.

We shall now show, that these singularities are explicitly cancelled by the virtual gluon contribution:

$$I_V = -\frac{2}{Q_T^2} f(Q_T) \int \frac{dk_T}{k_T} f(k_T) \qquad \text{V.2.4}$$

(using the notation introduced in eq.III.4.2).

Without loss of generality, we consider the following simplified case:

a] We use the leading log formula for one-gluon cross-section:

$$f(k_T) = \frac{2\alpha_s C_F}{\pi} \ln\Big(\frac{Q}{2k_T}\Big) \qquad \text{V.2.5}$$

b] From fig.V.2.1 we can see that the region of the y-integration is given by the intervals [-1,-Y] and [Y,1]. However, the cancellation of the poles is not affected, if we extend the region to [-1,1]. Following the analysis of §III.3, we now choose to work in terms of the θ-variable introduced in eq. III.3.4, so that we have:

$$I_R = \frac{4}{\pi Q_T^2} \int_{x_{min}}^{x_{max}} \frac{dx}{x(x^2-1)} \int_{-\frac{\pi}{2}}^{\frac{\pi}{2}} d\theta \, f_1 f_2 \qquad \text{V.2.6}$$

where

$$f_1 = \frac{2\alpha_s C_F}{\pi} \left[\ln\left(\frac{Q}{Q_T}\right) - \ln\left(\frac{x^2-1}{x-\sin\theta}\right) \right] \qquad \text{V.2.7}$$

$$f_2 = \frac{2\alpha_s C_F}{\pi} \left[\ln\left(\frac{Q}{Q_T}\right) - \ln\left(\frac{x^2-2x\sin\theta+1}{x-\sin\theta}\right) \right] \qquad \text{V.2.8}$$

c] To regularise the pole at $x = 1$ in the real part of eq.V.2.3, we introduce an ϵ-cut, such that $x_{min} = 1 + \epsilon$. Similarly, the soft singularity in the virtual part is parametrised by a Δ-cut, which, on dimensional grounds can be written $\Delta = \mu Q_T$.

We now claim the following:

Given the ϵ-cut, we can choose an appropriate $\mu = \mu(\epsilon)$, such that the singularities cancel, on adding real and virtual contributions together!

Before we proceed, we note that, for the purpose of this cancellation, we can set $x = 1$ everywhere in eqs. V.2.6,7 and 8 except in the singular parts, so that we can write:

$$I_R = \frac{4}{\pi Q_T^2} \left[\frac{2\alpha_s c_F}{\pi}\right]^2 \int_{1+\epsilon} \frac{dx}{1(x-1)(1+1)} \times$$

$$\times \int_{-\frac{\pi}{2}}^{\frac{\pi}{2}} d\theta \left[\ln\left(\frac{Q}{Q_T}\right) - \ln\left(\frac{(1+1)(x-1)}{1-\sin\theta}\right) \right] \times$$

$$\times \left[\ln\left(\frac{Q}{Q_T}\right) - \ln\left(\frac{1-2\sin\theta+1}{1-\sin\theta}\right) \right] \qquad \text{V.2.9}$$

The original θ-integral can be written:

$$I_\theta = \left[\ln\left(\frac{Q}{Q_T}\right) - \ln 2\right]\left[\pi\left(\ln\left(\frac{Q}{Q_T}\right) - \ln 2 - \ln(x-1)\right) + \int_{-\frac{\pi}{2}}^{\frac{\pi}{2}} d\theta \ln(1-\sin\theta)\right]$$

evaluating the last integral in the above expression:

$$\int_{-\frac{\pi}{2}}^{\frac{\pi}{2}} d\theta \ln(1-\sin\theta) \quad = \quad -\pi \ln 2$$

we finally obtain the θ-integral:

$$I_\theta \quad = \quad \ln\left(\frac{Q}{2Q_T}\right) \quad \pi \quad \left[\ln\left(\frac{Q}{4Q_T}\right) - \ln(x-1)\right] \qquad \text{V.2.10}$$

Then, we look at the x-integral:

$$I_x \quad = \quad \pi\left[\ln\left(\frac{Q}{2Q_T}\right)\right] \quad \left[\ln\left(\frac{Q}{4Q_T}\right)\int_{1+\epsilon}\frac{dx}{x-1} - \int\frac{dx}{x-1}\ln(x-1)\right]$$

and we consider the contribution from the lower limit of the integration:

$$I_x \quad = \quad -\pi \ln\left(\frac{Q}{2Q_T}\right) \quad \left[\ln\left(\frac{Q}{4Q_T}\right)\ln\epsilon - \frac{1}{2}\ln^2\epsilon\right]$$

so that we obtain for the real gluon contribution:

$$I_R \quad = \quad \frac{2}{Q_T^2}\left[\frac{2\alpha_s C_F}{\pi}\right]^2 \quad \ln\left(\frac{Q}{2Q_T}\right) \quad \left[\frac{\ln^2\epsilon}{2} - \ln\epsilon\,\ln\left(\frac{Q}{4Q_T}\right)\right] \qquad \text{V.2.11}$$

We now turn to the virtual part, combining eqs.V.2.4 and 5:

$$I_V \quad = \quad -\frac{2}{Q_T^2}\left[\frac{2\alpha_s C_F}{\pi}\right]^2 \ln\left(\frac{Q}{2Q_T}\right) \quad \int_{\mu Q_T}^{Q_T^{max}} \frac{dk_T}{k_T}\left[\ln\left(\frac{Q}{2}\right) - \ln k_T\right]$$

and consider again the lower limit contribution:

$$I_V \;=\; -\frac{2}{Q_T^2}\left[\frac{2\alpha_s C_F}{\pi}\right]^2 \ln\left(\frac{Q}{2Q_T}\right)\;\left[\frac{\ln^2(\mu Q_T)}{2} - \ln\left(\frac{Q}{2}\right)\,\ln(\mu Q_T)\right] \qquad \text{V.2.12}$$

From eqs.V.2.11 and 12, it is then clear that the cancellation of the double logarithmic terms forces us to choose : $\mu = \lambda\epsilon$, with λ to be determined by the cancellation of the single logarithmic terms.

In fact, with some algebra, we obtain the following expression for the single logarithmic part of the final answer:

$$I_R + I_V \;=\; \left[-\ln\epsilon\,\ln\left(\frac{Q}{4Q_T}\right) - \ln\epsilon\,\ln(\lambda Q_T) + \ln\left(\frac{Q}{2}\right)\,\ln\epsilon\right]$$

which gives the equation that determines λ:

$$-\ln\left(\frac{Q}{4Q_T}\right) - \ln(\lambda Q_T) + \ln\left(\frac{Q}{2}\right) \;=\; 0$$

which can be easily solved, to give us:

$$\lambda \;=\; 2 \qquad \text{V.2.13}$$

Therefore we conclude that soft singularities are completely cancelled between real and virtual graphs, provided we choose the infrared regulator in the virtual part to be $\Delta = 2\epsilon Q_T$, ϵ being the soft regulator in the real part, which ensures the individual gluon k_T's are greater than $\epsilon Q_T/2$.

V.2.2 Numerical Integration.

We can now take advantage of this cancellation of soft singularities between real and virtual graphs to ensure maximum stability for our numerical integrations. In fact, we can arrange that both integrals have the same lower limit, so that they can be combined into one double integral. To do so, we first change variables in the virtual part:

Let

$$k_T \longrightarrow z_T$$

where

$$k_T = (z_T - 1)\,2Q_T \qquad \text{V.2.14}$$

So that we have for the lower limit

$$k_{T_{min}} = 2\epsilon Q_T \longrightarrow z_{T\,min} = 1 + \epsilon$$

and the virtual integral now reads:

$$I_V = -\frac{2}{Q_T^2} f(Q_T) \int_{z_{T\,min}}^{z_{T\,max}} \frac{dz_T}{(z_T - 1)} f\big(2Q_T(z_T - 1)\big)$$

which can be rewritten in the form of a double integral:

$$I_V = -\frac{2}{Q_T^2} f(Q_T) \int_{z_{T\,min}}^{z_{T\,max}} \frac{dz_T}{(z_T - 1)} \Big[\Big(\int_{-\frac{\pi}{2}}^{\theta_2} + \int_{\theta_3}^{\frac{\pi}{2}} \Big) \times$$

$$\times d\theta \Big(\frac{f(2Q_T(z_T - 1))}{\pi - \theta_3 - \theta_2} \Big) \Big]$$

and can be combined with the real gluon integrals:

$$I = I_R + I_V = \frac{4}{\pi Q_T^2} \int_{1+\epsilon}^{x_{max}} \frac{dx}{x-1} \left[\int_{-\frac{\pi}{2}}^{\theta_2} + \int_{\theta_3}^{\frac{\pi}{2}} \right] \times$$

$$\times d\theta \left[\frac{f_1 f_2}{x(x+1)} - \frac{\pi}{2} \frac{f(Q_T) f(2Q_T(x-1))}{\pi - \theta_3 - \theta_2} \right] \qquad \text{V.2.15}$$

where, recall, the integrals are finite as $\epsilon \to 0$.

Of course, due to the difference in the upper limits, there is a piece of the virtual integral left over, which has to be added to give us the final answer for the $O(\alpha_s^2)$ three-jet cross-section :

$$I_V^{REM} = -\frac{2}{Q_T^2} f(Q_T) \int_{(x_{max}-1)2Q_T}^{Q_T^{max}} \frac{dk_T}{k_T} f(k_T) \qquad \text{V.2.16}$$

so that

$$\frac{1}{\sigma_0} \frac{d\sigma}{dQ_T^2} = I_R + I_V + I_V^{REM}$$

V.2.3 ϵ-extrapolation.

The cancellation of the soft singularities between real and virtual parts (§V.2.1) guarantees a finite answer for the combined integral $I = I_R + I_V$ (§V.2.2). We now discuss how this finite value can be extracted reliably. To do this we study the behaviour of our integral as ϵ, the soft regulator, goes to zero, in some detail. Having seen (§V.2.1) how $\ln^2 \epsilon$ and $\ln \epsilon$ terms cancelled out between the two contributions, we now show that the finite terms which survive the cancellation are of the form

$$\delta \ln \delta \quad , \quad \delta \quad , \quad O(\delta^2) \quad , \ldots$$

where

$$\epsilon = \delta^2$$

We start from eq.V.2.15

$$I(\delta) = \frac{4}{\pi Q_T^2} \int_{1+\delta^2} \frac{dx}{x-1} \int d\theta \left[\frac{f(k_{T_1})\, f(k_{T_2})}{x(x+1)} - \right.$$

$$\left. - \frac{\pi}{2} \frac{f(Q_T)\, f\big(2Q_T(x-1)\big)}{\pi - \theta_3 - \theta_2} \right]$$

and recall it is I(0) we want to determine.

First we make use of the property that if

$$I(\delta) = \int_{g(\delta)} dx\, h(x)$$

then

$$\frac{dI(\delta)}{d\delta} = -\frac{dg(\delta)}{d\delta}\ h\big(x = g(\delta)\big)$$

to obtain

$$\frac{dI(\delta)}{d\delta} = \frac{4}{\pi Q_T^2} \frac{-2\delta}{\delta^2} \int d\theta \left[\frac{f(k_{T_1} f(k_{T_2})}{1(1+1)} - \frac{\pi}{2} \frac{f(Q_T) f(2Q_T\delta^2)}{\pi - \theta_3 - \theta_2} \right] \qquad \text{V.2.17}$$

where we have set $x = 1$, everywhere except in the singular parts.

We now recall (§III.4) that $\theta_3 - \theta_2$ is proportional to δ, so that we can write:

$$\theta_3 - \theta_2 = c\delta$$

and eq. V.2.17 now reads:

$$\frac{dI(\delta)}{d\delta} = \frac{4}{\pi Q_T^2} - \frac{1}{\delta} \int d\theta \left[f(k_{T_1}) f(k_{T_2}) - \pi \frac{f(Q_T) f(2Q_T\delta^2)}{\pi - c\delta} \right]$$

but for small δ

$$\left[1 - \frac{c\delta}{\pi}\right]^{-1} \simeq 1 + \frac{c\delta}{\pi}$$

so that

$$\frac{dI(\delta)}{d\delta} = \frac{4}{\pi Q_T^2}\left(-\frac{1}{\delta}\right)\left[\int d\theta\Big(f(k_{T_1})f(k_{T_2}) - f(Q_T)f(2Q_T\delta^2)\Big) - \right.$$

$$\left. -c\delta\int d\theta f(Q_T)f(2Q_T\delta^2)\right]$$

We now consider each of the terms on the right hand side in turn

(i) *Second term* To first order in δ, we can write:

$$S' = \frac{4}{\pi Q_T^2}\; cf(Q_T)f(2Q_T\delta^2)$$

If we now use the leading log formula (eq.V.2.5), we obtain:

$$S' = \frac{4}{4\pi Q_T^2}\; cf(Q_T)\;\frac{2\alpha_s C_F}{\pi}\ln\left[\frac{Q}{2(2Q_T\delta^2)}\right] ,$$

$$= \frac{4}{\pi Q_T^2}\; cf(Q_T)\;\frac{2\alpha_s C_F}{\pi}\left[\ln\Big(\frac{Q}{4Q_T}\Big) - 2\ln\delta\right]$$

which, upon integration over δ, gives a contribution of

$$S = \int S'(\delta)d\delta = \frac{4}{\pi Q_T^2}\; cf(Q_T)\;\frac{2\alpha_s C_F}{\pi}\times$$

$$\times\left[-2\delta\ln\delta + \delta\Big(2 + \ln(\frac{Q}{4Q_T})\Big) + \text{constants}\right]$$

which has the claimed form of

$$\text{constant} + A\delta + B\delta\ln\delta + O(\delta^2)\text{terms}$$

(ii) *First term* Here the θ-integration is not trivial, so a more complicated analysis is needed. However, we can still say something about this term. From eq.II.3.1 and eq.II.3.4 we have:

$$k_{T_1} = \frac{Q_T}{2}\Big[x + \frac{-1 + x\sin\theta}{x - \sin\theta}\Big] \qquad k_{T_2} = \frac{Q_T}{2}\Big[x - \frac{-1 + x\sin\theta}{x - \sin\theta}\Big]$$

and to first order approximation, in the limit $\delta \to 0 \quad (x = 1 + \delta^2)$ and

$\theta \to \pm\frac{\pi}{2} \quad (\sin\theta = \pm 1)$ we have

$$k_{T_1} = \frac{Q_T}{2}\Big[\frac{x^2 - 1}{x}\Big] \qquad k_{T_2} = \frac{Q_T}{2}\Big[\frac{x^2 + 1}{x}\Big]$$

that is

$$k_{T_1} = Q_T\delta^2 \quad \text{and} \quad k_{T_2} = Q_T$$

Therefore the first term reads:

$$F' = \frac{4}{\pi Q_T^2} \quad (-\frac{1}{\delta}) \quad \int d\theta\Big[f(Q_T\delta^2)f(Q_T) - f(Q_T)f(2Q_T\delta^2)\Big]$$

and it is easy to see that the $\ln\delta$-terms cancel out! The $1/\delta$ factor is cancelled by second order terms (so far ignored) and a better treatment of the θ-integral is needed for a complete analysis of this term.

So, although we have evidence for a $\delta\ln\delta + \delta + O(\delta^2)$ behaviour of our integral as δ approaches zero, we cannot determine the coefficients of every term. Instead, we follow an alternative route. We use the generic formula:

$$I(\delta) = I(0) + B\delta\ln\delta + A\delta$$

and fit numerical results obtained for different (but small) values of δ to estimate A, B and allow the physical I(0) to be extracted. This can be done in the following way:

Given the results of the numerical integration for three different values of δ, say δ_i , $i = 1,2,3$, we can set up the following system of linear equations:

$$I(\delta_i) = I(0) + A\delta_i + B\delta_i \ln \delta_i \quad , \quad i = 1,2,3.$$

and solve for A,B and I(0).

As a consistency check, we can now repeat the numerical calculation for different values of δ, say δ_j , $j \neq i$ and compare the result with the answer the analytic formula gives.

A few examples of these checks are shown in figs.V.2.2 and 3. Noting the spectacular agreement of the fit, even for really small values of δ we can trust the extrapolation procedure described above to follow our integral(eq.V.2.15) in the limit $\delta \to 0$, i.e. $x \to 1$.

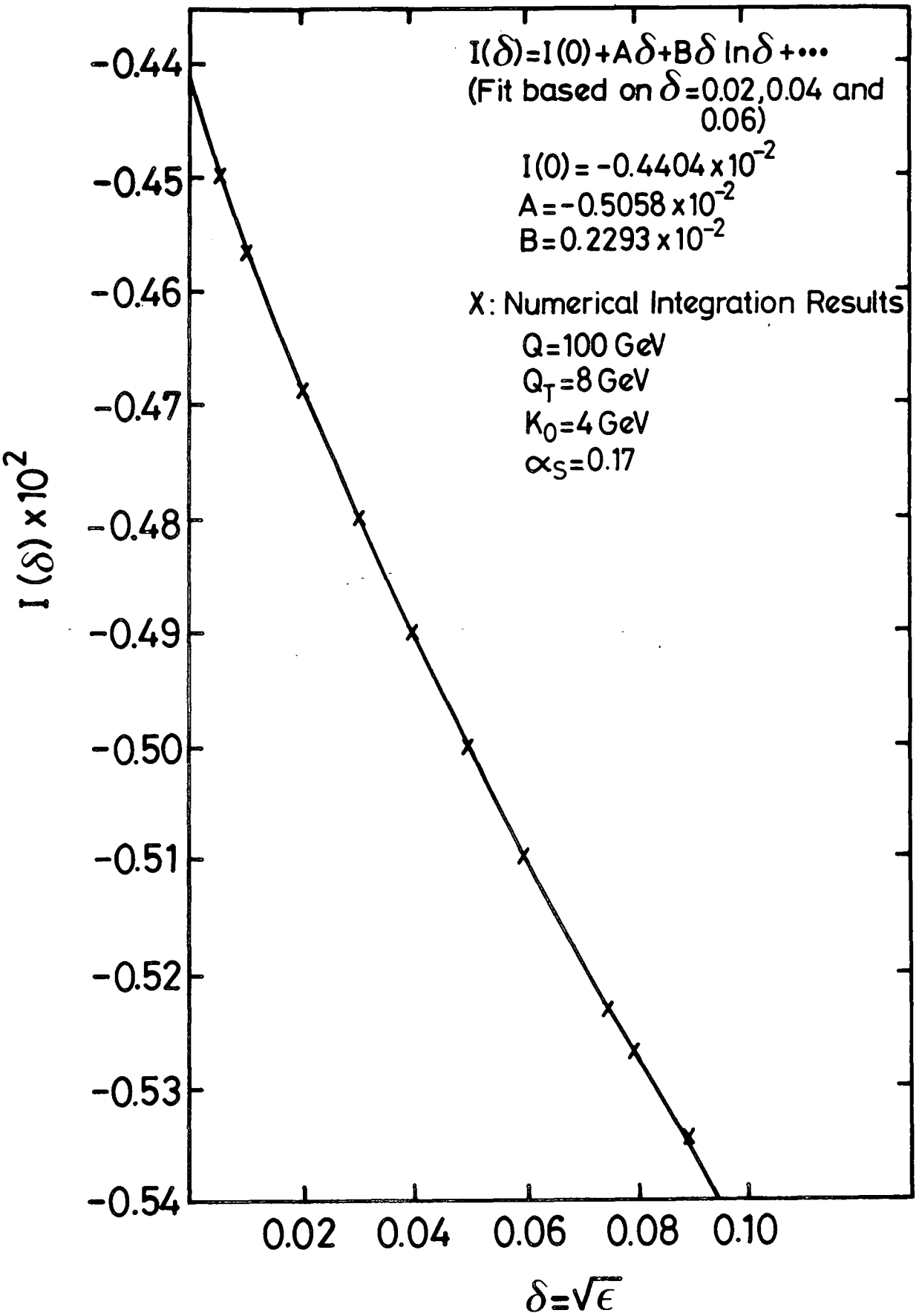

Figure V.2.2 : ϵ-extrapolation

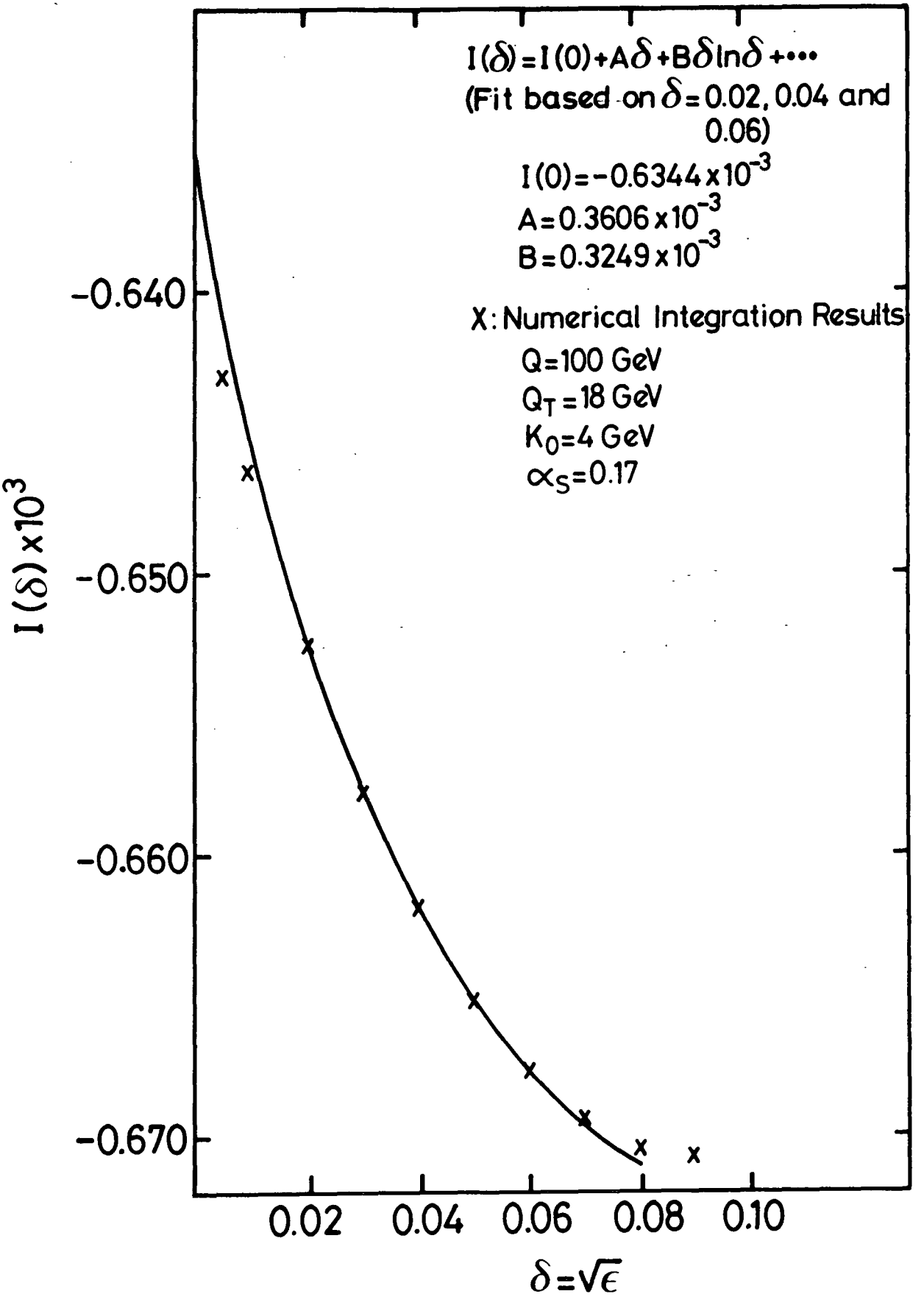

Figure V.2.3 : ϵ-extrapolation

V.3 RESULTS AND DISCUSSION.

As with the four jet case, we present our results for the quantity $d\sigma^{3jet}/\sigma_0 dQ_T^2$, where Q_T is defined with respect to the quantity with the largest thrust, so that we use eq.II.2.8 as input for the $O(\alpha_s)$ cross-section $d\sigma^{(1)}/\sigma_0 dQ_T^2$.

We recall the discussion of the four-jet results and make the following choices for the values of our parameters (see §III.5 for details).

a] Centre-of-mass energy : $Q = 100$ GeV

b] Running coupling constant $\alpha_s^2 = \alpha_s(k_{T_1})\alpha_s(k_{T_2})$

where

$$\alpha(\chi^2) = \frac{4\pi}{\beta_0\sqrt{ln^2\left[\frac{\chi^2}{\Lambda^2_{QCD}}+1\right]+\pi^2}}$$

with

$$\beta_0 = 11 - \frac{2N_f}{3}$$

$$N_f = 6$$

$$\Lambda_{QCD} = 0.2\text{Gev}$$

c] Jet defining cuts:

$$\cos\theta_0 = 0.9$$

$$k_0 = 3, 4 \text{ and } 7\,\text{GeV}$$

Echoing the conclusions of §III.5, we know there is a non-trivial kinematic region, namely $2k_0 \leq Q_T \leq 20\text{GeV}$, in which our model is most likely to give reliable results. In this region then, we compare the following cross-sections:(see figs. V.3.1, 2, 3, 4 and 5)

(i) $O(\alpha_s)$, tree-level, three-jet cross-section

(ii) $O(\alpha_s^2)$, three-jet cross-section (with virtual corrections included)

(iii) $O(\alpha_s^2)$, tree-level, four-jet cross-section.

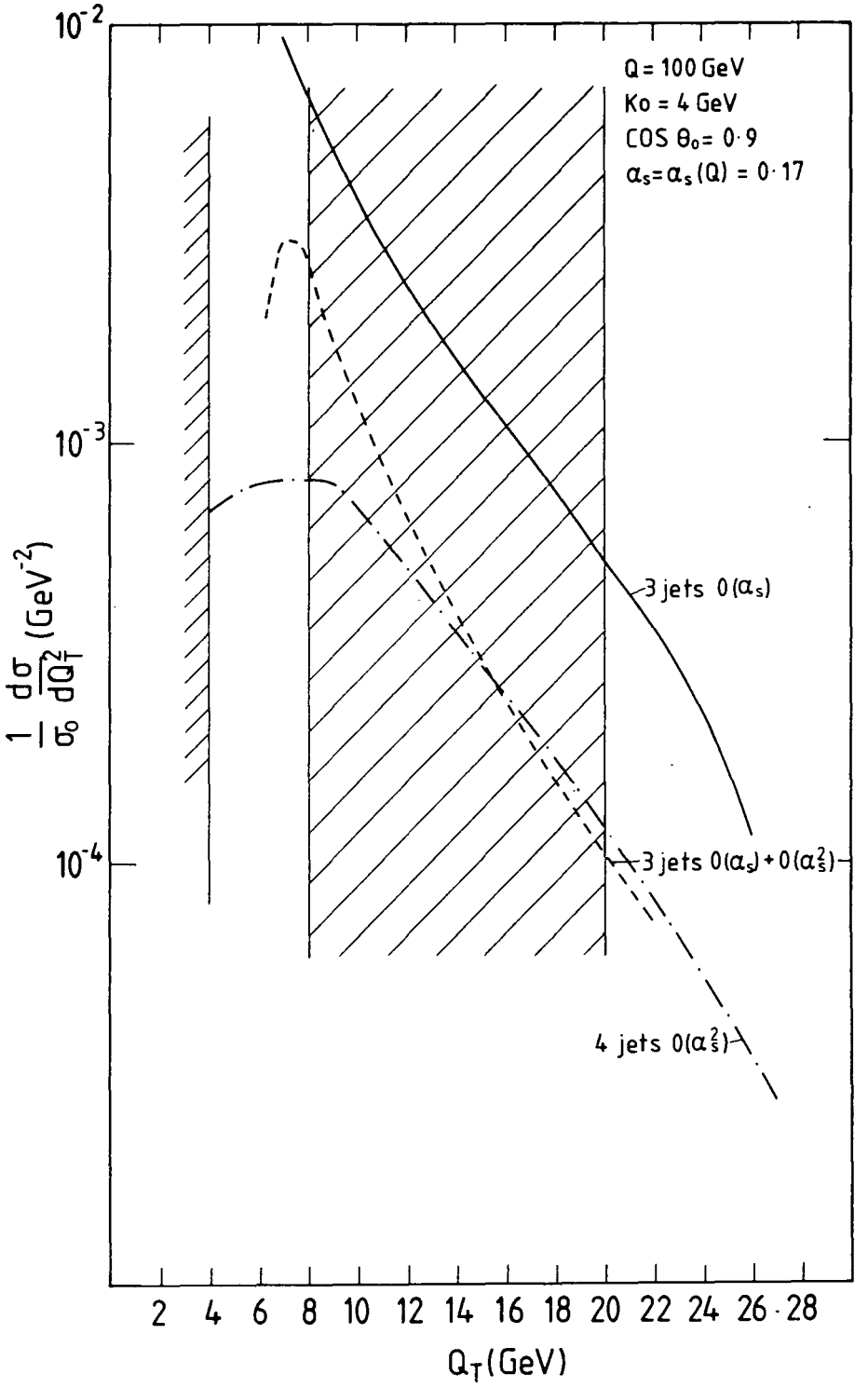

Figure V.3.1

Comparison of Q_T-distributions in e^+e^- annihilation.

(i) $O(\alpha_s)$, 3-jets (tree-level)

(ii) $O(\alpha_s^2)$, 3-jets with virtual corrections

(iii) $O(\alpha_s^2)$, 4-jets (tree-level)

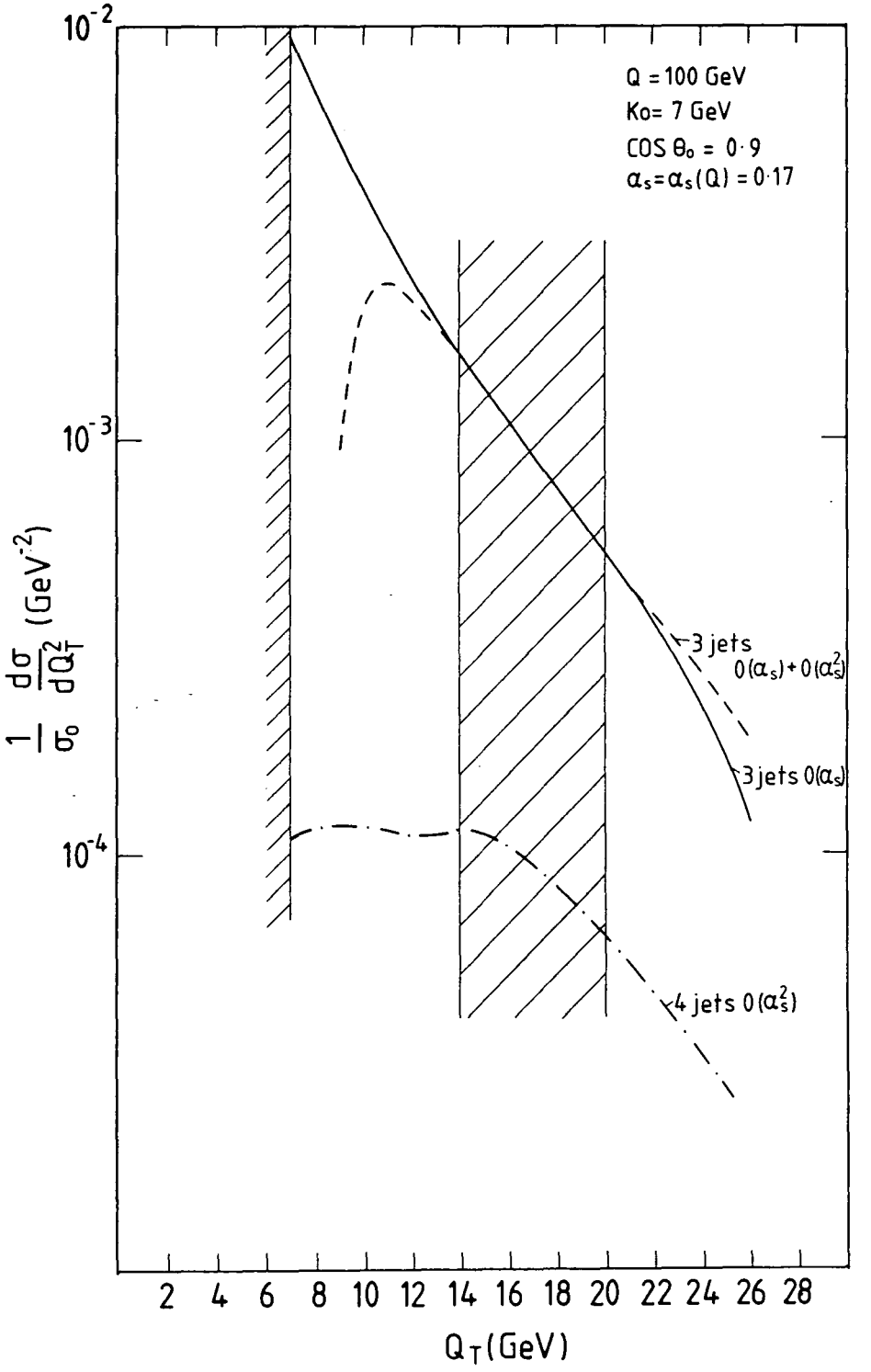

Figure V.3.2 : $e^+e^- \to$ 3 jets

Comparison of Q_T-distributions in e^+e^- annihilation.

(i) $O(\alpha_s)$, 3-jets (tree-level)

(ii) $O(\alpha_s^2)$, 3-jets with virtual corrections

(iii) $O(\alpha_s^2)$, 4-jets (tree-level)

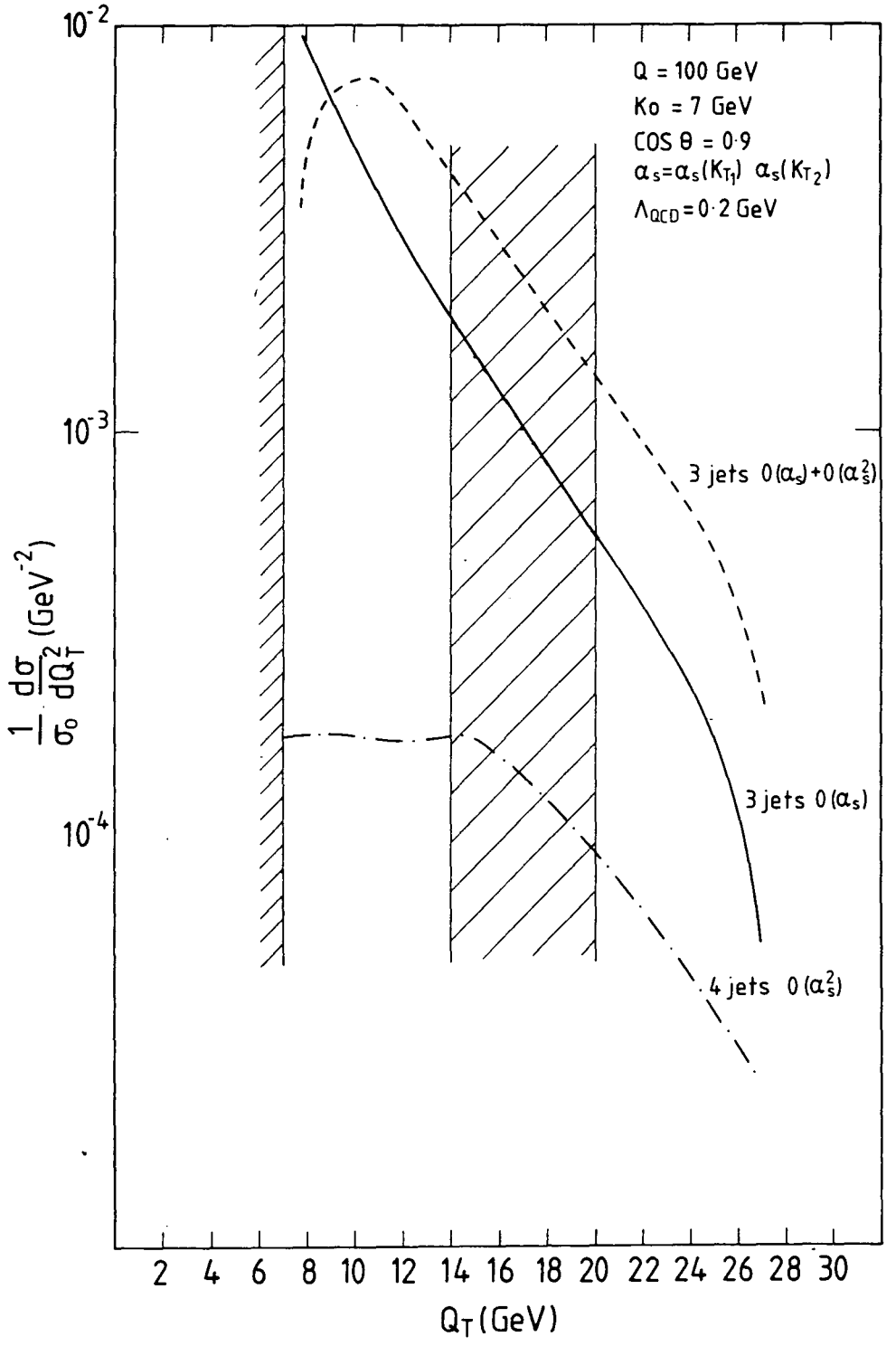

Figure V.3.3 : $e^+e^- \rightarrow$ 3 jets

Comparison of Q_T-distributions in e^+e^- annihilation.

(i) $O(\alpha_s)$, 3-jets (tree-level)

(ii) $O(\alpha_s^2)$, 3-jets with virtual corrections

(iii) $O(\alpha_s^2)$, 4-jets (tree-level)

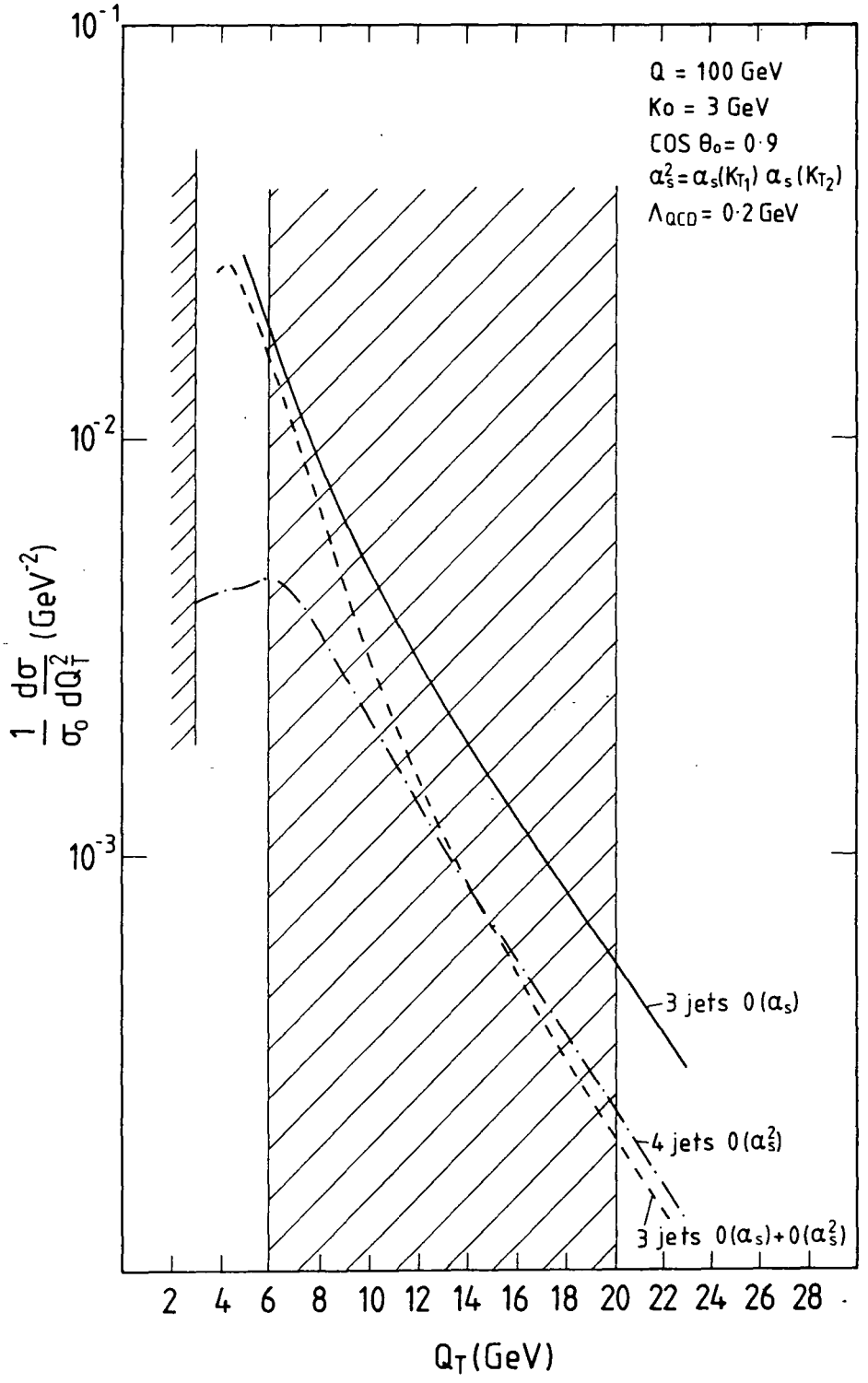

Figure V.3.4 : $e^+e^- \rightarrow$ 3 jets

Comparison of Q_T-distributions in e^+e^- annihilation.

(i) $O(\alpha_s)$, 3-jets (tree-level)

(ii) $O(\alpha_s^2)$, 3-jets with virtual corrections

(iii) $O(\alpha_s^2)$, 4-jets (tree-level)

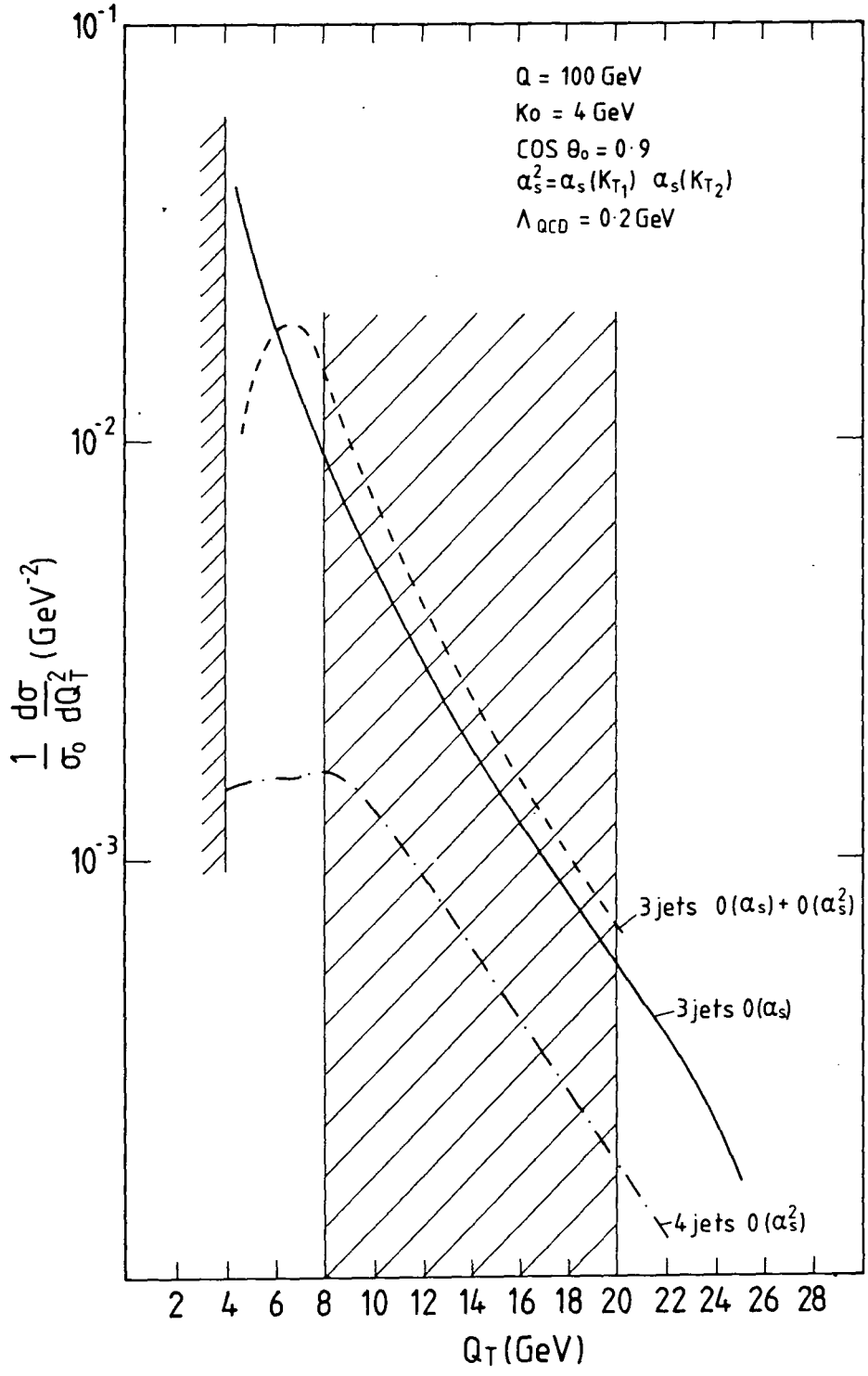

Figure V.3.5 : $e^+e^- \to$ 3 jets

Comparison of Q_T-distributions in e^+e^- annihilation.

(i) $O(\alpha_s)$, 3-jets (tree-level)

(ii) $O(\alpha_s^2)$, 3-jets with virtual corrections

(iii) $O(\alpha_s^2)$, 4-jets (tree-level)

As a result of such a comparison, a number of interesting remarks are in order:

1. Higher order corrections to tree-level results are indeed important. In particular, second order corrections to the three-jet cross-section are found to be large, especially for small values of the resolution parameters which are used to perform the cancellation of infrared and collinear singularities between second order real and virtual graphs.

2. As the size of the corrections depends on the values of these parameters which, recall, also serve as jet-defining cuts (as they govern the partial fractioning of the four-parton contributions into three- and four-jet hadronic states), the relative magnitude of the $O(\alpha_s^2)$ three- and four-jet cross-sections is *not* uniquely determined.

3. If we choose a relatively large value for the minimum transverse momentum cut (say: $k_T^0 = 7$ GeV), thus forcing the gluons to acquire rather large values for their transverse momenta, then we confirm the predictions of perturbative QCD. In this case, the coupling constant $\alpha_s(k_T)$ is small and the logarithms $\ln(k_T^2/Q^2)$ are under control so that perturbation theory is applicable. $O(\alpha_s^2)$-corrections to the tree-level $O(\alpha_s)$ three-jet cross-sections are indeed small and the $O(\alpha_s^2)$ four-jet cross-section is suppressed by another power of the (small) coupling constant.

4. On the other hand, for very small values of k_T^0 ($k_T^0 \leq 3$GeV), the $O(\alpha_s^2)$ corrections to the three-jet cross-section become large and negative, which signals the breakdown of perturbation theory for a cross-section with fixed number of jets. (Note that these large corrections, due to low mass partons, that is soft and collinear partons, push the four-jet cross-section *above* the three-jet one!)

5. Theoretically, cross-sections for fixed number of jets are applicable *only* for such values of the jet-defining cuts, which leave the effective expansion parameter small:

$$\frac{\alpha_s}{2\pi} \ln^2 x_T \quad \ll \quad 1$$

whereas experimentally, these cuts should *not* be smaller than the non-perturbative jet mass and jet opening angle given by the finite transverse momenta of the fragmentation process. a measure for the nonperturbative jet mass is the slim jet mass which at LEP energies (100 GeV) is expected to be 6 to 7 GeV [ref. III.7].

6. The above remarks are in agreement with similar conclusions deduced from recent calculations (using different sets of cuts such as the Sterman-Weinberg cuts and the invariant mass cut) [ref. V.1] which confirmed the dependence of the higher order corrections to the multijet cross-sections on the above cuts, needed to regularize the infrared and collinear divergences as well as to group the final-state partons into distinct jets. Moreover, these calculations have also emphasized the dependence of the cross-sections on the choice of the kinematical variables used to parametrize the shape of the oberved hadronic events (see §IV.3) as well as on the fragmentation mechanisms used to model the hadronization of the outgoing partons into hadronic jets.

7. Inevitably, these ambiguities concerning the size of higher-order corrections to multijet cross-sections heavily affect the determination of α_s or, equivalently, of the scale of the strong interactions Λ_{QCD} from analysing e^+e^- data, see §I.2.2 and [refs.I.17,V.1], as it is well known that the value of α_s cannot be readily extracted and compared with measurements from other processes (e.g. Deep Inelastic Scattering, Quarkonium Resonances) without the inclusion of the higher-order corrections [ref.III.12].

V.4 JET BROADENING.

In this chapter, we have been studying transverse momentum distributions for three-jet events in electron-positron annihilation using our approximation model IEA. Similar studies for four-jet events were described in chapter III. As has already been emphasized in §IV.3.4, one of the most characteristic predictions of QCD is that Q_T-distributions should broaden as the total energy Q^2 increases. (Broader Q_T-distributions are expected to be the result of the increasing gluon bremmstrahlung as the annihilation of the incoming particles is becoming more violent).

It is natural then to ask ourselves the question: 'Do we see such a behaviour of our Q_T-distributions in IEA?' A positive answer to this question will serve as another successfull test of the applicability of IEA to study multijet structures of hadronic final-states in e^+e^- annihilation.

As has been outlined in §IV.3.4, the jet-broadenig phenomenon is best parametrized in terms of mean values of transverse momenta which, in turn, are calculable in perturbative QCD:

$$\langle Q_T \rangle \quad = \quad \text{constant} + \eta \alpha_s Q + O(\alpha_s^2)$$

with η a dimensionless factor of order 1.

Using the simple LLA formula (eq.II.2.7) for instance, it is very easy to prove:

$$\langle Q_T \rangle \quad = \quad \frac{\int dQ_T Q_T \frac{d\sigma}{dQ_T}}{\int dQ_T \frac{d\sigma}{dQ_T}} \quad = \quad \frac{2C_F}{\pi} \alpha_s Q \quad \sim \quad 1 \alpha_s Q$$

The calculation of the full $O(\alpha_s^2)$ corrections, however, is more subtle as we have to consider not only four-parton final-states, but also loop-corrections to the three-parton process. On the other hand, second order corrections to the individual three- and four-jet transverse momentum distributions have been already calculated in the simple IEA model (§III.4 and IV.3).

Inevitably, the final expressions for the individual three- and four-jet distributions depend on the choice of the cuts needed both theoretically to define infrared- and collinear-safe cross-sections, and experimentally, to group the final state-particles into jets.

To eliminate this dependence on the jet-defining cuts and to get an estimate of the size of the total second-order corrections, we add the individual three- and four-jet distributions together (for the same values of the cuts) and consider the quantity:

$$\frac{1}{\sigma_0}\frac{d\sigma}{dQ_T^2} = \frac{1}{\sigma_0}\frac{d\sigma}{dQ_T^2}\Big]_{3jet}^{O(\alpha_s)+O(\alpha_s^2)} + \frac{1}{\sigma_0}\frac{d\sigma}{dQ_T^2}\Big]_{4jet}^{O(\alpha_s^2)}$$

for two different values of the total energy, namely for:

$$Q = 50, 100 GeV$$

Figure V.4.1 then verifies our claim that the $d\sigma/dQ_T^2$ distribution *does* get flatter as we increase the total energy Q. The above simple calculation serves as another check of the validity of the IEA model (rather than a rigorous proof of the jet-broadenig phenomenon).

This phenomenon (observed in both e^+e^- annihilation and hadron-hadron scattering) has been seen as a clear manifestation of the gauge nature of QCD. In a gauge theory, both soft and collinear gluon emissions are associated with large logarithms (up to two for each power of α_s) which make the effective expansion parameter to be $\alpha_s \ln^2$. This copiously-produced radiation gives rise to an increase of the relative transverse momentum [ref. IV.8b].

If we now recall that the terms $\alpha_s \ln(Q_T^2/Q^2)$ become problematic only in the region of small Q_T ($\Lambda \ll Q_T \ll Q$) where gluons are soft and/or collinear and the relevance of perturbative QCD is under question, then we can understand the importance of the jet-broadening phenomena and their studies as being directly related to the singularity structure of the underlying gauge theory.

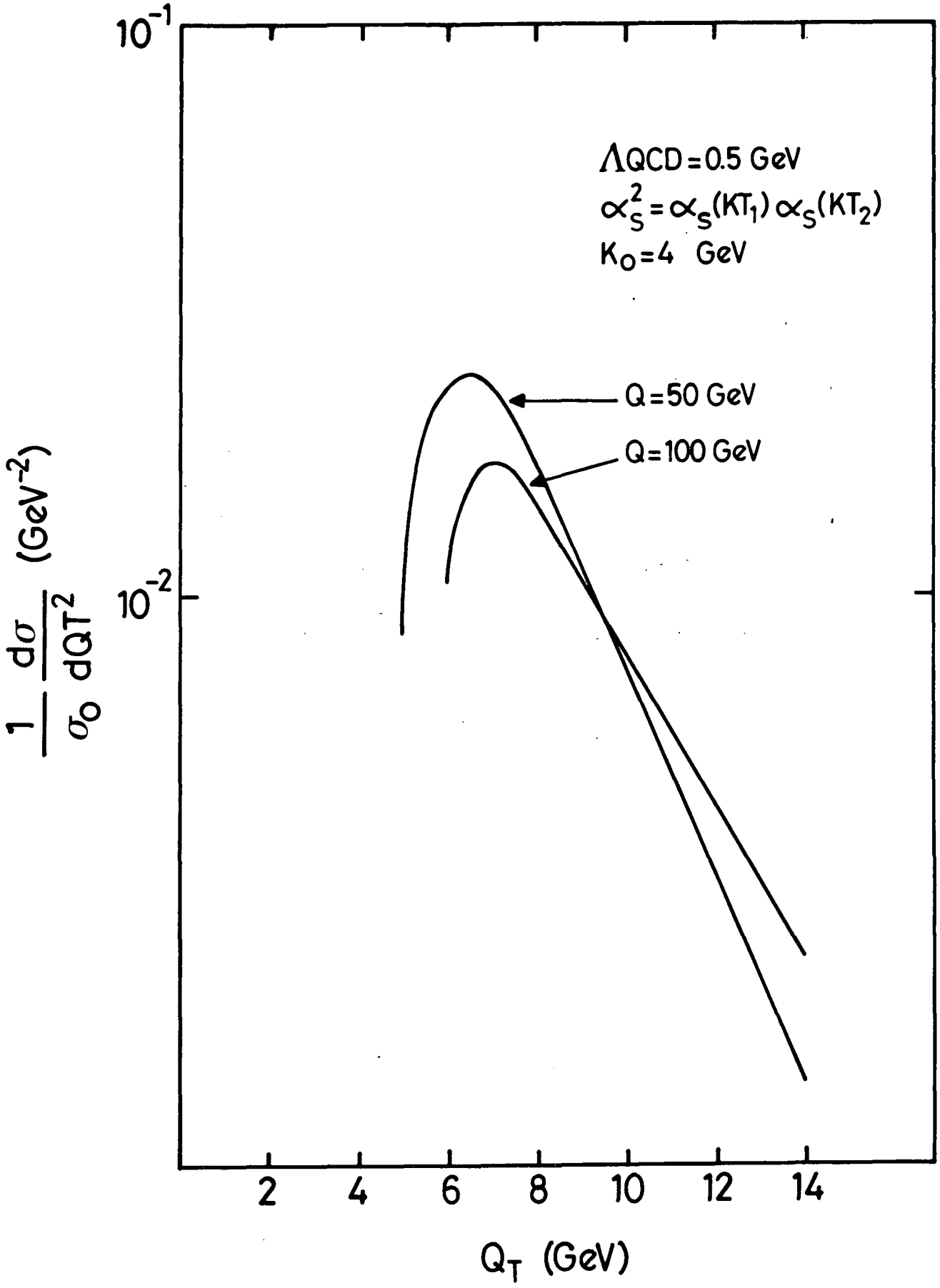

Figure V.3.1 : Jet broadening in e^+e^- annihilation

IV.5 SUMMARY OF CHAPTER V.

In this chapter, we used the IEA formalism to investigate the effect of higher corrections to tree-level results. In particular, we calculated the $O(\alpha_s^2)$ cross-section for three-jet events in e^+e^- annihilation by integrating the two-gluon contribution (eq.V.2.2) over those regions of phase space, where the four-final state particles define only three jets. Of course, to the same order in α_s, there were virtual contributions as well, which had to be taken into account. The individual real and virtual graphs exhibited the familiar soft and/or collinear singularities, but the total (physical) $O(\alpha_s^2)$ cross-section was seen to be finite, as the result of an exact cancellation of these singularities between real and virtual contributions. This cancellation was shown analytically and the two contributions were suitably combined under the same integral for maximal numerical stability.

This $O(\alpha_s^2)$ three-jet cross-section was then compared (in the kinematic region in which IEA was proved to be applicable and for various values of the 'jet-defining cuts' used to perform the above cancellation) with the tree-level cross-sections: $O(\alpha_s)$ for three-jet and $O(\alpha_s^2)$ for four-jets, to study the size of the higher order corrections as well as their dependence on the values of the jet-defining cuts. Our corresponding conclusions and their physical consequences were then discussed in some detail in §V.3, where they were also compared with similar results obtained from recent higher-order calculations of multijet cross-sections using differenet sets of cuts.

Finally, and as a consistency check, second order three- and four-jet cross-sections obtained for the same values of the cuts but at two different energies, were added together to confirm the well known phenomenon of broader tranverse momentum distributions at higher energies which has been seen as one of the most characteristic predictions of perturbative QCD.

CHAPTER VI SUMMARY AND FUTURE DEVELOPMENTS

VI.1 Summary of this Thesis

Studies of transverse momentum distributions in 'semi-hard' processes have recently attracted theoretical as well as experimental interest as it is realized that they are directly related to the singularity structure of the underlying theory. In chapter II we reviewed the progress that has been made in describing these processes in terms of perturbative QCD and we concentrated on some of the theoretical questions that remain unanswered (such as the importance of the - difficult to calculate - higher order corrections, the role of the - often neglected - nonleading terms and the uncertainties in determining the basic QCD prameters: α_s, Λ_{QCD}.

To shed some light on these questions, we set up a simply calculable model, based on the approximation that the gluons (responsible for these transverse momentum effects) are emitted independently (apart from transverse momentum conservation). This model, in which cross-sections for multigluon emissions were easily constructed in terms of that for a single gluon, was found to exhibit some useful features so that it could be used to study how Q_T-distributions are generated from multigluon emissions, as well as allow the individual multigluon cross-sections to be calculated.

To ascertain when and where such a model is a good approximation to the fixed order result, we looked in chapter III at two gluon emission in more detail. From this, we calculated the cross-section for four-jet production in electron-positron annihilation. To ensure that the four final-state particles were well defined and well separated in phase space, certain cuts had to be imposed on them. In particular, we required that each parton had a minimum transverse momentum k_0 and that there was a minimum angular separation θ_0 between each pair of them.

As it was then emphasized, these cuts were needed both theoretically, to regularize the singularities which arise when the emitted gluons are either 'soft' or 'collinear' with the emitting fermions, as well as experimentally, to group the final-states particles into distinct jets . Other sets of cuts that have been already proposed in the literature were reviewed and compared with the one we used.

Then, identical cuts were implemented for the full two-gluon result obtained by a Monte Carlo generation of events using the 'exact' matrix elements. The comparison of the two results helped to identify the kinematic region in which our model is most likely to be reliable, and determined the choice of the various parameters for maximal agreement. It was in fact found that, for realistic values of the above jet-defining parameters, there was a non trivial kinematic region in which our model agreed remarkably well with the 'full' result.

Then, in chapter IV, we set about testing this agreement more fully. First came a comparison with an 'exact' Abelian QCD theory: Because the assumption of independently emitted gluons required that the gluons did *not* interact with each other, no triple-gluon graphs were included in our analysis of multi-jet cross-sections. Remembering that the gluon self-coupling is one of the most characteristic manifestations of the non-Abelian nature of QCD, that meant that our approximation was that of an essentially Abelian theory. That encouraged us to compare our results with the exact ones obtained in an Abelian QCD theory, hoping for an improved agreement between the two answers. However, that was not the case, and that led us to investigate the colour structure of our model in some detail. This investigation (which also involved comparisons with different subsets of Feynman diagrams, such as a 'planar Abelian QCD' theory) helped us to conclude that the agreement of our IEA model (which was effectively planar and Abelian) with the full non-Abelian results was due to the colour-suppression of the non-planar graphs and a kinematical-suppression of the non-Abelian ones.

The use of IEA to study other processes (not very different from Bthe Q_T-distribution of a multijet event) was elaborated in the rest of chapter IV. Its ability to calculate distributions in other variables that have been proposed to describe the multijet structure of hadronic final-states in electron-positron annihilation (such as the D-variable and the total transverse momentum W_T of the event) served as further successful tests of its potential to be used as a tool to attack some of the (still unanswered) theoretical questions formulated in the introduction.

Moreover, a critical review of recent theoretical developments in understanding the low-Q_T regime (where the applicability of QCD is under question due to the growing coupling constant α_s and the presence of large logarithms of the type: $\ln(Q_T/Q)$) by taking into account effects of multigluon emissions to all orders α_s , and in particular a comparison of the naive IEA with a systematic calculation which summarized the large amount of information accumulated in these studies, confirmed all the above claims. IEA predictions for multijet cross-sections were found not to be very different from those obtained using these sophisticated algorithms.

All these tests encouraged us to use the IEA formalism to investigate the effect of higher order corrections to the tree-level results. In chapter V in particular, we calculated the $O(\alpha_s^2)$ cross-section for three-jet production in e^+e^- annihilation by considering the two-gluon cross-section in those regions of phase space, where the four-final state particles defined only three distinct jets. The corresponding soft and collinear singularities were regularized analytically by taking into account the contributions of the virtual graphs to the same order in α_s. This $O(\alpha_s^2)$ three-jet cross-section was then compared (in the kinematic region in which IEA is applicable) with the tree-level cross-sections: $O(\alpha_s)$ for three-jets and $O(\alpha_s^2)$ for four-jets.

The comparison of these results confirmed the importance of the higher order corrections, as these were found to be large, especially for small values of the jet-defining cuts used to perform the cancellation of the infrared and collinear divergences between second order real and virtual graphs. Theoretical as well as experinental limits to the values of the cuts were also discussed. As a consistency check, we added the second-order cross-sections for three- and four-jets to get the total $O(\alpha_s^2)$ Q_T-distribution, which then was seen to flatten with increasing energy Q, thus reproducing the well-known phenomenon of 'jet-broadening' at higher energies.

Our results of chapter V were seen to be in agreement with similar conclusions obtained from recent calculations of higher-order multijet cross-sections (using different sets of cuts) which emphasized the dependence of the cross-sections not only on the values of the jet-defining cuts, but also on the choice of the kinematical variables used to describe the shape of the observed hadronic events. This highlights the ambiguities in extracting α_s, or euiavalently Λ_{QCD}, from the ratio of (n+1) to n jet cross-section and underlines the need for more theoretical work on these matters.

I V.1.1 Jets, QCD and IEA at LEP

With the approaching starting up of LEP, perturbative QCD studies of multijet structures in electron-positron annihilation are of great phenomenological relevance. The high energy scales of LEP would allow kinematical reconstruction of multijet (n $\geq$ 4) final-states with much improved statistics that would provide new quantitative tests of QCD (measurements of α_s, tests of its non-Abelian nature etc). The simplified IEA framework could then prove practical useful for simple, yet accurate calculations of the individual multijet cross-sections (or at least their transverse momentum disrtibutions), with their higher order virtual corrections included (needed for a quantitative understading of multijets, but yet well-nigh impossible to compute exactly).

VI.2 Status of the Standard Model

In this thesis, we have studied transverse momentum distributions of multijet structures in e^+e^- annihilation using perturbative QCD terms. QCD is a non-Abelian Gauge Field theory based on a local $SU(3)_c$ symmetry, which we believe successfully describes the strong interactions between the coloured quarks and gluons, at least when large energy/momentum scales are involved. In these cases, the QCD's strong interaction gauge coupling constant is rather small (as a consequence of the property of Asymptotic Freedom) and that allows us to calculate high-energy QCD effects perturbatively in this small coupling. QCD predictions in such high energy kinematic regimes have been successfully tested in a number of experimental situations (Deep Inelastic Scattering, Jets in e^+e^- annihilation etc). On the other hand, the non-perturbative aspects of QCD, apparently related to the quark confinement problem, are still not very well understood. The lack of a complete understanding of the hadronization mechanism that converts quarks into hadrons, the difficulties in quantitative descriptions of hadron spectroscopy and the remaining problems at the perturbative level (missing of higher orders in QCD matrix elements, uncertainties in fixing Λ_{QCD}etc) are all due to insufficient theoretical understanding [ref.VI.1].

By and large, we can regard QCD as *the* theory of strong interactions in the same way that the Glashow, Salam and Weinberg mobel is thought to be the SU(2)xU(1) (unified) theory of electroweak interactions [ref. I.1]. Together they constitute the so-called Standard Model of Particle Physics which has been enormously successful in explaining all data at presently available energies. Recent searches for deviations from the standard model cross-sections greater than the experimental errors have all been negative [ref. I. 17]. Despite all this experimental confirmation, the Standard Model is *not* free from theoretical uncertainties, as several oustanding problems are left unresolved:

1. *The Generation Problem*

   This is the problem of understanding the apparent proliferation of flavours of elementary particles (at least six quarks and six leptons), their arbitrary masses, the relative strengths of their charged weak interactions (normally parametrized by the Cabbibo-Kobayashi-Maskawa mixing matrix [ref. VI.2]), and their grouping into 'families'. (see Table I.2.2) Why should this pattern hold? How many generations are there? Are these particles really elementary?

2. *The Mass Problem*

   Particles (quarks, leptons and gauge bosons) in the Standard Model can only acquire masses when the SU(2)xU(1) electroweak gauge symmetry is spontaneously broken. This is achieved through the vacuum expectation value of a Higgs field which represents a spin-zero particle with mass $M_H = O(10^{0\pm1})M_W$. However theoretically necessary, there is as yet *no* experimental evidence for any such particle. But the problem does not end here, as it has been emphasized that, due to large radiative corrections, it is extremely difficult to formulate a consistent theory containing a light elementary boson. (The hierarchy problem).

3. *The Unification Problem*

   Although strong, electromagnetic and weak interactions have all similar structures based on Gauge Theories, they are in fact described by distinct SU(3), SU(2) and U(1) gauge groups with different coupling constants. Is there any way to embed them into a (appropriately large) single gauge group with a universal coupling? Why are these the only forces we see and how does gravity fit into the picture?

VI.3 Physics at LEP (and beyond it)

Given the history of successes in Elementary Particle Physics, it has been suggested that the Standerd Model is just a very good low energy approximation to a deeper underlying theory which can account for most of the above ambiguities and resolve some of the theoretical problems outlined in the last section. In fact, as we discuss see below, several ideas have already been put forward, many of which have a relatively low mass scale ($\leq$ 1 TeV). As the new generation of accelerators (LEP, SLC and SSC) is expected to push the limits of our experimental knowledge to that sort of energy levels, it is worth a quick review of these ideas [ref. V.3].

One approach to the generation problem is to postulate that the apparently elementary quarks and leptons are actually composite objects containing more fundamental particles called preons, bound together by new superstrong interactions [ref. VI.4]. Recent negative experimental searches for substructure have set the limit on the compositeness scale parameter to be of the order of a TeV.

A very attractive proposal to attack the mass problem and to stabilize the Higgs mass is to postulate a complete set of 'supersymmetric' partners for the known particles, which cancel out the excessive corrections to the Higgs mass [ref.VI.5]. To do this job, the (yet to be observed experimentally) supersymmetric particles must have masses of $\leq$ 1 TeV. It should also be noted that, if supersymmetry is made local (that is, if we allow supersymmetry transformations to be different at different points in space) in the same way that gauge symmetries were made local in §I.1.B.2, then gravity must be included and a supergravity theory is constructed.

The most favoured approach to the unification problem has been that of grand unification: the, so far dinstinct, strong, weak and electromagnetic interactions are combined into a simple guage group with a single gauge coupling. However, in order to accommodate the great differences between the strong and elecroweak coupling, this unification can take place only at very high energies of $\sim 10^{15}$ Gev. Grand Unified Theories (GUT's) have had some successes (predictions of θ_W , m_b) [ref. VI.6], but none of their dramatic predictions (proton decay, magnetic monopoles, neutrino masses) have been observed as yet.

The last two ideas can be combined into one scheme when we go beyond the four dimensions of space-time in which the Standard Model is usually formulated [ref. VI.7]. In fact, ten-dimensional supergravity has been seen as a natural starting point for unifying all matter and forces. Most recently, such a possibility of a single unifying Theory of Everything (TOE) has been seriously boosted with the advent of Superstring Theories. These theories, in which the elementary particles are pictured as one-dimensional objects (strings) rather than points as in conventional Quantum Field Theories, display a number of attractive features (GUT's and gravity are included, finiteness) that have made them candidate TOE's, despite the many theoretical problems and the difficulties in testing them experimentally [ref.VI.10]. However, certain possible low-energy signatures of the superstring have been suggested (extra gauge boson Z^0 and new scalar quarks) and will be tested at the new accelerators.

In summary, while there is a lot of 'Standard Physics' to be confirmed at LEP and the new machines (precision tests, detection of the t-quark, Higgs searches, neutrino counting) and several theoretical propositions of 'New Physics' are 'expected' to be tested there (composite quark and leptons, new heavy leptons and bosons, supersymmetric particles etc), one can never exclude the possibility of seeing completely new and unexpected phenomena!

APPENDIX A : Colour Factors

We calculate the colour factors of the diagrams shown in Figure IV.2.4.

$$\beta_1 = T^a_{ij}\,T^a_{jk}\,T^b_{kl}\,T^b_{li} = C_F\,\delta_{ik}\,C_F\,\delta_{ki} = C_F^2 N$$

$$\beta_2 = T^a_{ij}\,T^b_{jk}\,T^b_{kl}\,T^a_{li} = T^a_{ij}\,C_F\,\delta_{jl}\,T^a_{li} = C_F^2 N$$

$$\beta_3 = T^a_{ij}\,T^b_{jk}\,T^a_{kl}\,T^b_{li}$$

$$= T^a_{ij}\,T^b_{jk}\left[T^b_{kl}\,T^a_{li} + i f_{abc}\,T^c_{ki}\right] = C_F^2 N + i f_{abc}\,T^a_{ij}\,T^b_{jk}\,T^c_{ki}$$

where

$$f_{abc}\,T^a_{ij}\,T^b_{jk}\,T^c_{ki} = f_{abc}\,T^a_{ij}\left[T^c_{jk}\,T^b_{ki} + i f_{bcd}\,T^d_{ji}\right]$$

$$= f_{acb}\,T^a_{ij}\,T^b_{jk}\,T^c_{ki} + i f_{abc}\,f_{dbc}\,T^a_{ij}\,T^d_{ji}$$

$$= -f_{abc}\,T^a_{ij}\,T^b_{jk}\,T^c_{ki} + i C_A\,T^a_{ij}\,T^a_{ji}$$

so that

$$2\,f_{abc}\,T^a_{ij}\,T^b_{jk}T^c_{ki} = i C_A C_F N$$

and

$$\beta_3 = C_F N(C_F - C_A/2)$$

$$\beta_4 = T^a_{ij}\,f_{abc}\,f_{dcb}\,T^d_{ji} = -C_A\,T^a_{ij}\,T^a_{ji} = -C_A C_F N$$

$$\beta_5 = i\,T^a_{ij}\,T^b_{jk}\,T^c_{ki}\,f_{abc} = -C_A C_F N$$

APPENDIX B : $\mathbf{D = \frac{27}{4}\frac{x_1^2 x_T^2 x_k^2}{x_1 x_2 x_3 x_4}}$

Let x_1 represent the energy fraction (thrust) of the most energetic fermion, with respect to which we measure the transverse momentum fraction x_T. We also define x_k to be the gluon momentum fraction out of the plane defined by x_1 and x_T. Then, the four-momentum fractions for the quark, the antiquark and the two gluons can be written as:

$$\begin{aligned} x_q &= (x_1 \ , \ -x_1, 0, 0) \\ x_{\bar{q}} &= (x_2 \ , \ x_L, x_T, 0) \\ x_{g_1} &= (x_3 \ , \ x_A, x_\lambda, x_k) \\ x_{g_2} &= (x_4 \ , \ x_1 - x_L - x_A, -x_T - x_\lambda, -x_k) \end{aligned}$$

where x_L, x_A and $x_F = x_1 - x_L - x_A$ are the longitutidal momenta of the antiquark and the two gluons, respectively.

Longitudinal and transverse montum conservation are already embodied in eq.1, but energy conservation and the masslessness of our particles impose the constraints:

$$\begin{aligned} x_4 &= 2 - x_1 - x_2 - x_3 \\ x_2^2 - x_L^2 - x_T^2 &= 0 \\ x_3^2 - x_A^2 - x_\lambda^2 - x_k^2 &= 0 \\ x_4^2 - x_F^2 - (x_T + x_\lambda)^2 - x_k^2 &= 0 \end{aligned}$$

so that only x_1, x_2, x_3, x_T and x_k can be seen as independent variables. We shall show now how the D variable (introduced in Chapter IV) can be nicely expressed in terms of these.

Given the energy-momentum fractions, the components of the 3x3 tensor θ^{ij} are easily computed acording to:

$$\theta^{ij} = \frac{\sum_\alpha \frac{x_{p\alpha}^i x_{p\alpha}^j}{x_\alpha}}{\sum_\alpha x_\alpha}$$

where the α-sum runs over all final state particles and x_α and $x^i_{p_\alpha}$ are the energy fraction and the three-momentum fractions (respectively) of the α^{th}-particle.

Then, D, defined in terms of the product of the eigenvalues of the θ^{ij} tensor (see eq. what), can be expressed in terms of the above energy-momentum fractions:

$$D = \left[\theta_{11}\theta_{22}\theta_{33} + 2\theta_{12}\theta_{13}\theta_{23} - \theta_{12}^2\theta_{33} - \theta_{13}^2\theta_{22} - \theta_{23}^2\theta_{11}\right]$$

that is

$$8D/27 = \left[\frac{x_1^2}{x_1} + \frac{x_L^2}{x_2} + \frac{x_A^2}{x_3} + \frac{x_F^2}{x_4}\right]\left[\frac{x_T^2}{x_2} + \frac{x_\lambda^2}{x_3} + \frac{(x_T+x_\lambda)^2}{x_4}\right]\left[x_k^2(\frac{1}{x_3} + \frac{1}{x_4})\right]$$

$$+2\left[\frac{x_L x_T}{x_2} + \frac{x_A x_\lambda}{x_3} - \frac{(x_T+x_\lambda)x_F}{x_4}\right]\left[x_k(\frac{x_A}{x_3} - \frac{x_F}{x_4})\right]\left[x_k(\frac{x_\lambda}{x_3} + \frac{x_T+x_\lambda}{x_4})\right]$$

$$-\left[\frac{x_L x_T}{x_2} + \frac{x_A x_\lambda}{x_3} - \frac{(x_T+x_\lambda)x_F}{x_4}\right]^2\left[x_k^2(\frac{1}{x_3} + \frac{1}{x_4})\right]$$

$$-\left[x_k(\frac{x_A}{x_3} - \frac{x_F}{x_4})\right]^2\left[\frac{x_T^2}{x_2} + \frac{x_\lambda^2}{x_3} + \frac{(x_T+x_\lambda)^2}{x_4}\right]$$

$$-\left[x_k(\frac{x_\lambda}{x_3} + \frac{x_T+x_\lambda}{x_4})\right]^2\left[\frac{x_1^2}{x_1} + \frac{x_L^2}{x_2} + \frac{x_A^2}{x_3} + \frac{x_F^2}{x_4}\right]$$

From the last expression, we can already see that D is proportional to x_k^2, the square of the momentum fraction out of the plane. To proceed, we decompose it into two parts: part one is made of the first and the last terms, whereas the rest constitute part two. It is then rather straightforward to show that in each part, there is a complete cancellation of terms proportional to x_λ^2 and x_λ, which simplifies consuderably the expression for D:

$$\frac{8D}{27x_k^2} = \frac{x_T^2(x_3+x_4+x_2)}{x_2x_3x_4}\left[\frac{x_1^2}{x_1} + \frac{x_L^2}{x_2} + \frac{x_A^2}{x_3} + \frac{x_F^2}{x_4}\right]$$

$$+\frac{x_T^2}{x_2^2x_3^3x_4^3}\Big[x_3^2(x_Lx_4-x_Fx_2)(x_2x_Ax_4-x_4x_Lx_4+x_Fx_4x_2-x_3x_Lx_)+$$

$$+x_2x_3(x_4x_A-x_3x_F)(x_3x_Lx_4-x_4x_Ax_4+x_3x_4x_F-x_2x_4x_A)\Big]$$

In the last equation we identify the following terms:

$$x_F^2 \quad \text{with} \quad \text{coefficient} \quad \frac{x_T^2}{x_2x_3x_4}$$

$$x_A^2 \quad \ldots \quad \ldots \quad \frac{x_T^2}{x_2x_3x_4}$$

$$x_Ax_F \quad \ldots \quad \ldots \quad \frac{2x_T^2}{x_2x_3x_4}$$

$$x_A \quad \ldots \quad \ldots \quad \frac{2x_T^2x_L}{x_2x_3x_4}$$

$$x_F \quad \ldots \quad \ldots \quad \frac{2x_T^2x_L}{x_2x_3x_4}$$

remaining terms:

$$\frac{x_T^2(x_3+x_4+x_2)}{x_2x_3x_4}\Big[\frac{x_1^2}{x_1}+\frac{x_L^2}{x_2}\Big]+\frac{x_T^2}{x_2^2x_3x_4}\Big[-x_L^2(x_4+x_3)\Big]$$

Factorizing and collecting them together again, we make use of the fact that $x_A+x_F=x_1-x_L$ to cancel x_L^2 and x_L terms to obtain:

$$\frac{8D}{27x_k^2} \quad = \quad \frac{x_T^2}{x_2x_3x_4}\Big[x_1^2+(x_2+x_3+x_4)x_1\Big]$$

That is:

$$D=\frac{27}{4}\frac{x_1^2x_T^2x_k^2}{x_1x_2x_3x_4}$$

REFERENCES

Introduction

[I.1] For an Introduction to the Ideas of Particle Physics see:

a. Close, F. M.Marten and C.Sutton, *The Particle Explosion*, Oxford University Press, Oxford, 1987

b. Dodd, J.E. *The Ideas of Particle Physics*,Cambridge University Press, Cambridge, 1984

c. Gottfried, K. and V.F.Weisskopf, *Concepts of Particle Physics*, Vol.1 and 2, Oxford University Press, Oxford, 1984

d. Pickering, A. *Constructing Quarks*, Edinburgh University Press, Edinburgh, 1984

More about the Physics of this introductory chapter can be found in any of the 'standard' textbooks on Elementary Particle Physics and Gauge Field Theories:

a. Aitchison, I.J.R. and A.J.G.Hey, *Gauge Theories in Particle Physics*, Adam Hilger, Bristol, 1982

b. Cheng,T.P. and L.F.Li, *Gauge Theory of Elementary Particle Physics*, Oxford University Press, Oxford, 1984

c. Halzen, F. and A.D.Martin, *Quarks and Leptons*, John Wiley & Sons, N.Y., 1984

d. Huang,K. *Quarks, Leptons and Gauge Fields*, World Scientific, 1982

e. Okun,L.B. *Leptons and Quarks*, North-Holland, Amsterdam, 1982

f. Perkins, D.H. *Introduction to High Energy Physics*, Addison-Wesley, Reading, Massachusetts, 1982

g. Quigg,C. *Gauge Theoties of Strong, Weak and Electromagnetic Interactions*, Benjamin, Reading, Massachusetts, 1983

The list of references of this introductory chapter consists mostly of review articles, lecture notes, conference talks and proceedings, where references to the original papers as well as more technical details can be found.

[I.2] M.Gell-Mann and Y.Ne'eman, *The Eightfold Way*, Benjamin, New York, 1964

Use of Group Theory in Particle Physics :

b. H.Georgi, *Lie Algebras in Particle Physics*, Benjamin, Menlo Park, California, 1982

[I.3] J.J.J.Kokkedee, *The Quark Model*, Benjamin, Reading, Massachusetts, 1969

[I.4] Thorough developments of the Quark-Parton Model and Phenomenological Applications:

a. F.E.Close, 'The Quark Parton Model', Rep. Prog. Phys. **42** (1979) 1285; *An Introduction to Quarks and Partons*, Academic Press, London, 1979

b. E.Leader and E.Predazzi, *An Introduction to Gauge Theories and the New Physics*, Cambridge University Press, Cambridge, 1982

[I.5] The path to Maxwell's equations:

W.K.H.Panofsky and M.Phillips, *Classical Electricity and Magnetism*, Addison-Wesley, Reading, Massachusetts, 1962

[I.6] Electomagnetism as a Gauge Theory:

a. E.S.Abers and B.W.Lee, Phys. Rep. **9C** (1973) 1

b. I.J.R.Aithcison and A.J.G.Hey *op.cit.*

[I.7] Non-Abelian Gauge Theories: B

a. E.S.Abers and B.W.Lee *op.cit.*

b. C.Itzykson and J.-B.Zuber, *Quantum Field Theory*, McGraw-Hill, New York, 1980

c. P.Ramond, *Field Theory: A Modern Primer*, Benjamin, Menlo Park, California, 1981

d. Past, Present and Future of Gauge Theories are evoked in the 1979 Nobel lectures by S.L.Glashow, S.Weinberg and A.Salam in Rev. Mod. Phys. **52** (1980) 515, 525 and 539

[I.8] For a general introduction see: K.Wilson, Sci. Am. **214** (1979) 140

For a more technical introduction: S.Coleman, 'Dilatations', in *Properties of the Fundamental Interactions*, Vol. 9A, 1971 International School of

Physics 'E.Majorana', Erice, edited by A.Zichichi, Editrice Compositore, Bologna, 1973

[I.9] Applications of RGE to Gauge Theories and the property of Asymptotic Freedom are reviewed by: D.J.Gross, in *Methods in Field Theory*, 1975 Les Houches Lectures, edited by R.Balian and J.Zinn-Justin, North-Holland, Amsterdam, 1976

For recent monographs:

b. P.Pascual and R.Tarrach, *QCD: Renormalization for the Practitioner*, Lecture Notes in physics 194, Springer Verlag, 1984

c. J.C.Collins, *Renormalization*, Cambridge University Press, Cambridge, 1984

[I.10] O.W.Greenberg, Phys. Rev. Lett. **13** 598

[I.11] Reviews of QCD:

Discussion of Asymptotic Freedom:

a. H.D.Politzer, Phys. Rep. **14C** (1974) 129;

b. E.Reya, Phys. Rep. **69** (1981) 195

General structure of the theory:

c. W.J.Marciano and H.Pagels, Phys. Rep. **36C** (1978) 137; and for a popularization: 'QCD', Nature **279** (1979) 479

International Conferences:

d. 'Quantum Chromodynamics', Proc. of the *X G.I.F.T. International Seminar on Theoretical Physics* Jaca, Huesca (Spain) 1979, ed by J.L.Alonso and R.Tarrach, Springer-Verlag, Berlin, 1980

e. 'Perturbative Quantum Chromodynamics', *AIP Conference Proceedings* Vol.74, Tallahassee, 1981, eds. D.W.Duke and J.F.Owens, American Institute of Physics, New York, 1981

Evolution of Parton Distributions and Corrections to the Quark Parton Model:

f. Y.L.Dokshitzer, D.I.Dyakonov and S.I.Troyan, Phys.Rep.**58** (1980) 269

g. G.Altarelli, Phys. Rep. **81** (1982) 1

Phenomenological Applications:

h. G.G.Ross, in *Gauge Theories and Experiments at High Energies*, Proc. 21st Scottish Universities Summer School in Physics, St.Andrews, 1980, eds K.G.Bowler and D.G.Sutherland

i. M.R.Pennington, Rep. Prog. Phys. **46** (1983) 393
Chiral Dynamics and the QCD Vacuum:

j. F.J.Yndurain, *Quantum Chromodynamics*, Springer-Verlag, N.Y., 1983

[I.12] General review of Confinement Theories:
M.Bander, Phys. Rep. **75** (1981) 75

[I.13] E.Witten, Nucl. Phys. **160** (1979) 57; Physics Today, (1980) 38

[I.14] N.S.Craigie,*The Theory and Detection of Monopoles in Gauge Theories*, World Scientific, Singapore, (1985)

[I.15] S.Coleman, 'The Uses of Instantons', in *The Whys of Subnuclear Physics*, 1977 Erice School, edited by A.Zichichi, Plenum, New York and London, 1979

[I.16] J.B.Kogut, Rev. Mod. Phys. **51** (1979) 659; **55** (1983) 775

b. M.Creutz, *Quarks, Gluons and Lattices*, Cambridge University Press, Cambridge, 1983

c. A.Hasenfratz and P.Hasenfratz, Florida State University-preprint, FSU-SCRI-85-2 (1985)

[I.17] Recent review of e^+e^- Physics:
B.Naroska, Phys. Rep. **148** (1987) 67

[I.18] For more details on the Physics of this section see any of the textbooks of ref. [I.1]

[I.19] First proposal of three-jet events: J.Ellis, M.K.Gaillard and G.G.Ross, Nucl. Phys. **B111** (1976) 253
Experimental discovery of the gluon:

b. P.Söding, in the *Proceedings of the International Conference on High Energy Physics*, CERN, Geneva, 1979
Recent reviews on the Physics of Jets:

c. S.D.Ellis, 'Jets in QCD: A Theorist's Perspective', lectures presented at the *11th SLAC Summer Institute on Particle Physics*, July, 1983

d. F.Barreiro, 'Jets in e^+e^- Annihilation and QCD', DESY-preprint, 85-088 (1985)

[I.10] For reviews on Jet Fragmentation and Hadronization see:

a. T.D.Gottshalk, CALT-68-1075 (1983); CERN-TH-3810 (1983)

b. D.H.Saxon, RAL-85-077 (1985); RAL-86-057 (1986)

c. B.R.Webber, Cambridge preprint, 86/3 (1986)

Transverse Momentum Distributions

[II.1] See refs. [1.17,19d] and references therein

[II.2] For a recent review see: *Proceedings of the Drell Yan Workshop*, Fermilab, 1982 and in particular the contributions by J.C.Collins et. al., M.Greco and R.Odorico.

[II.3] F.Halzen and F.Herzog, 'QCD Collider Physics', review talk at the *XV Symposium on Multiparticle Dynamics*, Lund, Sweden, 1984;

b. A.Nicolaidis, Phys. Rev. **D33** (1986) 2572

c. S.D.Ellis, R.Kleiss and W.J.Stirling, 'Jet activity in $W^{\pm}, Z^0$ events-a Theoretical Analysis',CERN-TH 4185/85 (1985), talk presented at the *5th Topical Workshop on Proton-Antiproton Collider Physics*, Saint-Vincent, Aosta Valley, Mar.1985;

d. Z.Kunszt and W.J.Stirling, Durham DPT/87/16 preprint, (1987)

[II.4] G.Altarelli, R.K.Ellis, M.Greco and G.Martinelli, Nucl. Phys. **B246** (1984) 12

[II.5] Y.L.Dokshitzer, D.I.Dyakonov and S.I.Troyan, Phys. Lett. **78B** (1978) 290 and **79B** (1978) 269. For a review see: Phys. Rep. **58** (1980) 269

[II.6] G.Parisi and R.Petronzio, Nucl. Phys. **B154** (1979) 427

b. G.Curci, M.Greco and Y.Srivastava, Phys. Rev. Lett. **43** (1979) 834; Nucl. Phys. **B159** (1979) 451

[II.7] F.Halzen, A.D.Martin and D.M.Scott, Phys. Rev. **D25** (1982) 754; Phys. Lett. **112B** (1982) 160; see also: A.D.Martin, 'Production of Z and W Bosons at the $p\bar{p}$ Colliders', talk presented at the *Forward Collider Physics Topical Conference*, Madison, Wisconsin, USA, Dec. 1981

[II.8] J.C.Collins, Phys. Rev. **D22** (1980) 1478

J.C.Collins and D.E.Soper, Nucl. Phys. **B193** (1981) 381; **B194** (1982) 445; **B197** (1982) 446;

J.C.Collins, D.E.Soper and G.Sterman, in [II.2] and Nucl. Phys. **B250** (1985) 199

[II.9] Altarelli et. al. in [II.4]

For Phenomenological implications see:

b. G.Altarelli, R.K. Ellis and G. Martinelli, Phys. Lett. **151B** (1985) 457; Z. Phys. **C27** (1985) 617

c. E.B.Kiritsis and S.Katsanevas, CALT-68-1236 (1985)

[II.10] S.D.Ellis, R.Kleiss and W.J.Stirling, Phys. Lett. **154** (1985) 435

b. For recent experimental reports see: UA1 Collab., Phys. Lett. **193B** (1987) 389; UA2 Collab., Phys. Lett. **194B** (1987) 158

[II.11] Ref.[I.19] and any of the textbooks of ref. [I.1]

[II.12] M.R.Pennington, J. Math. Phys. **25** (1984) 1548

[II.13] see [II.12] and P.Hoyer et.al. Nucl. Phys. **B161** (1979) 349

[II.14] T.Kinoshita, J. Math. Phys. **3** (1962) 650;

b. T.D.Lee and M.Nauenberg, Phys. Rev. **133** (1964) 1549

[II.15] M.R.Pennington in [I.11]

[II.16] J.C.Collins *et. at* in [II.8];

b. M.Ciafaloni, Phys. Lett. **95B** (1980) 113

c. G.Sterman, Nucl. Phys. **B281** (1987) 310

d. K.Tesima, OITS 360 (1987), talk given at the *SSC Workshop at Univ. of Madison*, Wisconsin, May.1987

[II.17] S.D.Ellis and W.J.Stirling, Phys. Rev. **D23** (1981) 214;

b. S.D.Ellis, N.Fleishon and W.J.Stirling, Phys. Rev. **D24** (1981) 1386

[II.18] P.E.L.Rakow and B.R.Webber, Nucl. Phys. **B187** (1981) 254;

b. J.C.Collins, 'Sudakov Form Factors', Argonne National Lab. preprint ANL-HEP-84-36 (1984)

[III.1] M.R.Pennington, Nucl. Phys. **B204** (1982) 189

[III.2] See for instance the Jet-reviews in [I.17,19,20]

[III.3] See the PETRA report in [I.17] and the UA1 and UA2 reports in [II.10b]

[III.4] G.Sterman and S.Weinberg, Phys. Rev. Lett. **39** (1977) 1436

[III.5] L.Clavelli, Phys. Lett. 85B (1979)

b. L.Clavelli and H.P.Nilles, Phys. Rev. **D21** (1980) 1242

[III.6] K.Fabricius, G.Kramer, G.Schierholz and I.Schmitt, Phys. Lett. **97B** (1980) 431; Z. Phys. **C11** (1981) 315

b. G .Kramer and B.Lampe, DESY-preprints 86-103, 119 (1986)

[III.7] F.Gutbord, G.Kramer and G.Schierholz, Z. Phys. **C21** (1984) 235

[III.8] See UA1 and UA2 reports in [II.10b]

[III.9] For a review see: G.Altarelli, Phys. Rep. **81** (1982) 1

[III.10] M.R.Pennington, G.G.Ross and R.G.Roberts, Phys. Lett. **120B** (1985) 275

[III.11] R.M.Barnett, D.Schlatter and L.Trentadue, Phys. Rev. Lett. **46** (1981) 1659

b. Y.Gabellini and J.L.Meunier, Univ. of Nice preprint NTH-81/10 (1981)

c. G.Parisi and R.Petronzio, Phys. Lett. **94B** (1980) 51

[III.12] For reviews on determinations of α_s and Λ_{QCD} see:

a. D.W.Duke and R.G.Roberts, Phys. Rep. **120** (1985) 275

b. R.Y.Zhu, Caltech-preprint CALT-68-1306 (1986)

[III.13] Y.Michopoulos, N.Brown and M.R.Pennington, Durham-preprint DPT-87-xx (1987) (submitted to Nucl. Phys.)

[III.14] D.Danckaert, P.D.Cansmaecker, R.Gasrtmans, W.Troost and T.T.Wu, Phys. Lett. **114B** (1982) 203

IEA in Practice

[IV.1] See also W.Bartel et al., JADE collaboration, Phys. Lett. **119B** (1982) 239

[IV.2] For a recent review see: S.Brant, 'Jet analysis in e^+e^- annihilation experiments', talk presented at the *International Workshop on Advanced Methods in Nuclear Scattering Data*, Berlin 1985, Siegen preprint Si-85-09 (1985), to be published in the series of *Lecture Notes in Physics* by Springer Verlag

[IV.3] R.K.Ellis, D.A. Ross and A.E.Terrano, Nucl. Phys. **B178** (1981) 421

b. G.Parisi, Phys. Lett. **74B** (1978) 65

c. G.C.Fox and S.Wolfram, Phys. Rev. Lett. **41** (1978) 1581; Nucl. Phys. **B149** (1979) 413; Phys. Lett. **82B** (1979) 134

[IV.4] N.Brown, private communication

[IV.5] R.K.Ellis and B.R.Webber, 'QCD Jet Broadening in Hadron-Hadron Collisions', Fermilab-Conf-86/151-T (1986), to be published in the Proc. of the *1986 Summer Study on the Design and Utilization of the SSC*, Snowmass, Colorado, 1986

b. P.E.L.Rakow and B.R.Webber, Nucl.Phys. **B191** (1981) 63

[IV.6] See refs. [I.17,19d] and

b. Ch.Berger *et al.*, PLUTO Collab., Z.Phys. **C22** (1984) 103

[IV.7] For more details on this section see: [III.14]

[IV.8] P.Chiappetta and M.Greco, Nucl. Phys. **B199** (1982) 77; **B221** (1983) 269; Phys. Lett. **135B** (1984) 187

b. L.Trentadue, Phys. Lett. **151B** (1985) 171; CERN-TH-4524 (1986)

[IV.9] R.K.Ellis, G.Martinelli and R.Petronzio, Phys. Lett. **104B** 45; Nucl. Phys. **B211** (1983) 106

b. C.T.H.Davies, W.J.Stirling, Nucl. Phys. **B244** (1984) 337

c. C.T.H.Davies, B.R.Webber and W.J.Stirling, Nucl. Phys. **B256** (1985) 413

d. J.Kodaira and L.Trentadue, Phys. Lett. **112B** (1982) 66; **123B** (1983) 335

$e^+e^- \to$ 3jets

[V.1] See refs. [III.6,7], [IV.3a]. For more details on $O(\alpha_s^2)$ calculations:

b. A.Ali et.al. Nucl. Phys. **B167** (1980) 454

c. D.A.Ross, Nucl. Phys. **B188** (1981) 109

d. J.A.M. Vermaseren, K.J.F.Gaemers and S.J.Oldham, Nucl. Phys. **B197** (1981) 301

e. Z.Kunszt, Phys. Lett. **99B** (1981) 429; **107B** (1981) 123

f. T.D.Gottschalk, Phys. Lett. **109B** (1982) 331; **150B** (1985) 451

g. G.Kramer and B.Lampe, DESY preprints 87-043 (1987); 86-119, 86-103 and 86-038 (1986)

h. F.Gutbrod et. al. DESY-preprint 87-047 (1987)

i. G.Schuler, PhD thesis, University of Mainz, DESY Internal Report T-87-01 (1987)

For use of Fragmentation Models in these multijet calculations see [I.16] and [I.19] and references therein

For experimental results see [I.16] and [I.18] and:

j. S.Bethke, DESY preprint 86-115 (1986)

k. R.Barlow, DESY preprint 87-009 (1987)

Summary and Future Developments

[VI.1] Status of QCD:

a. J.C.Collins, 'The Status of Perturbative QCD', talk given at DPF Conference Eugene, OR, USA, 1985

b. A.H.Muller, 'QCD and Jets', talk givan at the *1985 International Symposium on Lepton and Photon Interactions at High Energies*, Kyoto, Japan, 1985, eds. M.Konuma and K.Takahasi,1986

c. A.Ali et al., in *Physics at LEP*, CERN report 86-02, vol.2 (1986); DESY preprint 86-139 (1986)

[VI.2] For reviews on quark mixing, generation of quark masses and CP-violation in the Standard Model see:

a. L.L.Chau, Phys. Rep. **95C** (1983) 1

b. A.J.Buras, Max-Planck Institute preprints MPI-PAE PTh 46/84 (1984) and 64/85 (1985)

c. L.Wolfenstein, Com. Nucl. Part. Phys. **14** (1985) 135

[VI.3] J.Ellis and R.Peccei, *Physics at LEP*, CERN report 86-02 vols. 1 and 2 (1986)

b. A.Böhm and W.Hoogland, (eds.) *EFCA Workshop on LEP 200* Aachen, W.Germany, 1986, CERN-Report 87-02 (1987)

c. S.C.Loken, (ed.) *XXIII Int. Conf. on HEP, Berkeley, California, 1986*, World Scientific, Singapore, 1987

[VI.4] L.Lyons, Prog. Part. Nucl. Phys. **10** (1983) 227

b. M.E.Peskin, 'Substructure at the TeV Scale', talk at the *1985 Int. Lepton-Photon Symposium*, Kyoto, Japan, 1985

[VI.5] C.H.Llewllyn Smith, Oxford Univ. preprint 87/84 (1984), lectures given at the Scottish Universities Summer School,1984

b. H.P.Nilles, Phys. Rep. **110C** (1984) 1

c. H.E.Haber and G.L.Kane, Phys. Rep. **117C** (1985) 75

d. J.Ellis, 'Supersymmetry and Supergravity', talk at the *1985 International Lepton-Photon Symposium*, kyoto, Japan, 1985

e. D.V.Nanopoulos and A.Lahanas, Phys. Rep. **145C** (1987) 1

[VI.6] P.Langacker, Phys. Rep. **72C** (1981) 185; and talk at the *1985 International Lepton-Photon Symposium*, Kyoto, Japan, 1985

b. R.Slansky, Phys. Rep. **79C** (1981) 1

c. J.Ellis, 'Phenomenology of Unified Gauge Theories', CERN-report TH-3174 (1981)

d. G.G.Ross, *Grand Unified Theories*, Benjiamin, Menlo Park, CAlifornia, 1985

[VI.7] M.Duff, CERN report TH-4288 (1985) talk given at the *Int. Europhysics Conf. on HEP* Bari, Italy, 1985

[VI.8] J.Ellis, 'Superphysics', lectures in the *1986 CERN School of Physics*, Sweden, 1986, CERN report 87-02 (1987); and for a popularization: Nature, **323** (1986) 595